STUDIES IN

ASTRONOMICAL NARROW BAND

SPECTROPOLARIMETRY

Thesis
submitted to the
University of Glasgow
for the Degree of
Ph.D.
by
IAN S. McLEAN

Department of Astronomy,
University of Glasgow.

August, 1974.

To my wife,

Maureen,

and our parents.

CONTENTS

PART I

(Instrumentation)

1. INTRODUCTION

2. INSTRUMENTAL REQUIREMENTS FOR LINE PROFILE POLARIMETRY

3. AN AUTOMATIC TWIN Hβ-SPECTROPOLARIMETER

The twin Hβ-spectropolarimeter at the Cassegrain focus of the
2.5 m (98-inch) Isaac Newton Telescope at the Royal Greenwich
Observatory, Herstmonceux, Sussex.

P R E F A C E

The aims of the work reported in this thesis have been the design, development and application of a narrow band polarimeter capable of measuring small polarizational effects across spectral line profiles. These aims have been met in full. An automatic photoelectric spectropolarimeter has been constructed to record the Hβ line profile with 3 - 10 Å resolution or and to allow narrow band polarization measurements to be made simultaneously at any two discrete wavelengths near Hβ. This instrument has been applied successfully to the measurement of a polarization effect in the Hβ line of blue sky light, to the investigation of intrinsic linear and circular polarization of magnetic and other Ap stars and to the study of intrinsic polarization of Be stars. A reduced polarization has been discovered in the Hβ emission lines of the shell stars γ Cas and ζ Tau, giving a new independent and direct confirmation of the intrinsic nature of the polarization of these stars. Variability has been observed in these effects and the hint of further polarization structure is reported and discussed. The thesis falls naturally into two parts - Instrumentation (Part I) and Applications (Part II).

Chapter 1 contains an introduction to astronomical optical polarimetry, outlining the important possibilities associated with polarization measurements across spectral line profiles and mentions recent advances in narrow band polarimetry.

Chapter 2 discusses the instrumental requirements for the study and describes the approach adopted for an Hβ scanning spectropolarimeter.

In Chapter 3 details of the optical and electronic arrangement of the

new polarimeter are given, together with a few preliminary results of stellar observations.

Chapter 4 contains an account of the investigations to which the polarimeter has so far been applied and in Chapter 5 the achievements of the polarimetric method used are summed up and the importance of polarization measurements with high spectral resolution are emphasized.

The original work of the thesis is contained in Chapters 2, 3 and 4, thereby including the instrumentation development, the new observations and their interpretation.

It is a pleasure to acknowledge Professor P. A. Sweet for the facilities in his department. Thanks are due to all the members of the Astronomy Department for interesting discussions and, in particular, Mr. W. Edgar, who constructed the polarimeter, for his invaluable advice concerning various aspects of its mechanical design. I am very grateful to Mr. T. H. A. Wyllie for numerous discussions and assistance with some of the observations and I am especially indebted to Mrs. M. I. Morris for her exceedingly careful reproduction of the diagrams and typing of the thesis.

The research topic was suggested by Dr. David Clarke, whose ingenuity and enthusiasm has been a source of great encouragement throughout. It is a pleasure to acknowledge his guidance and assistance. Finally, I would like to thank my wife for her patience and support and for transcribing much of the manuscript from rough notes during an injury to my right hand.

This work was undertaken while the author was in receipt of a Science Research Council Postgraduate Studentship.

IAN S. McLEAN.

POLARIMETRIC UNITS AND DEFINITIONS

A glossary of the most important symbols used in the text is given at the end of the thesis. Summarised here for convenience are the definitions, units and notation needed for the description of the polarization state of light.

Stokes Parameters: I, Q, U, V.

I represents total intensity; $I = I_p + I_u$, where p and u refer to the polarized and unpolarized intensity components of the light.

Q and U represent the two components of the linear polarization, and V the component of circular polarization.

Co-ordinate Systems:

When the Stokes parameters are referred to an arbitrary, right-handed Cartesian co-ordinate system (x, y, z), with positive z-axis along the direction of propagation, this is denoted by attaching the suffices x and y to the normalised Stokes parameters.

Normalised Stokes Parameters:

$$p_x = Q/I = p \cos 2\phi$$
$$p_y = U/I = p \sin 2\phi$$
$$q = V/I .$$

where $p = (p_x^2 + p_y^2)^{\frac{1}{2}}$ and $\phi = \frac{1}{2} \arctan \frac{p_y}{p_x}$; p is the degree of linear polarization, ϕ is the position angle of the linear polarization measured counterclockwise from the x-axis and q is the degree of circular polarization.

When the normalised Stokes parameters are specifically referred to the astronomical equatorial co-ordinate system, the notation adopted is,

$$p_1 = p \cos 2\Theta$$

$$p_2 = p \sin 2\Theta$$

$$q$$

Here, $\Theta = 0^\circ$ means that the electric vector is preferentially directed N or S (parallel to the 1-axis), while $\Theta = 45^\circ$ implies a polarization directed NE or SW.

By definition, positive (right-handed) circular polarization occurs when the electric vector maximum has increasing Θ with time (i.e. a counter-clockwise rotation of the electric vector to an observer facing the source). This notation was adopted following IAU Colloquium No. 23, Tucson, Arizona, 1972. According to the "snap-shot" picture of the electric vector in a beam of elliptically polarized light, given by Clarke and Grainger (1971), the above definition corresponds to a left-handed helix in space.

Units:

The degree of linear polarization p, and the degree of circular polarization q, are generally expressed as decimal fractions or in percentage notation.

For example, $p \simeq 0.60$ or 60 per cent, is common in the terrestrial blue sky, while the precision of the stellar polarimetry reported in this thesis is typically about ± 0.0002 or ± 0.02 per cent; by "precision" is meant the standard error (σ) of the mean measured value of p or q.

When the precision is very high ($\sim \pm 0.01$ per cent or better) or the values of p or q very small, even the percentage notation becomes cumbersome. One solution, in common use, is to multiply the fractional polarization by 10^4 and express, for example, $\sigma(q) = \pm 0.00010$ ($\equiv \pm 0.010$ per cent), simply as ± 1.0. These units are only referred to in Section 4.4 and in Table 3.2.

PART I

(Instrumentation)

1. INTRODUCTION

1.1 Astronomical Polarimetry

In the opening chapter of the book "Planets, Stars and Nebulae studied with photopolarimetry," based on the proceedings of an IAU Colloquium in Tucson, Arizona in 1972, the editor, Tom Gehrels, remarks that "now may be the last chance to produce a single volume containing all polarimetry; the field is expanding so rapidly." Indeed, although the polarization state of light has been a thoroughly respectable astrophysical observable for many years, a casual glance at the astronomical literature of the last half decade reveals a remarkable upsurge of interest in instrumentation, new observations and theoretical studies suggesting novel situations where polarized light might be generated.

A chronology for the principal events in polarimetry can be found in the text already referred to (Gehrels, 1974), while a brief compilation of mechanisms that produce linear and circular polarization, with the emphasis on those of current astronomical interest, has been given by Angel (1974).

Outlined below is a review of the major developments (until 1970) in the study of those phenomena treated observationally in this thesis, viz., scattering of light in the terrestrial atmosphere, the intrinsic polarization of starlight, and polarization associated with Zeeman splitting of spectral lines by a magnetic field.

Probably the earliest recorded application of polarimetry to astronomy was by Arago in 1809. He found that the light from the sunlit sky is partially polarized, established the fact that the polarization maximum in the sky is located at about 90° from the Sun and discovered the existence of a point of zero polarization (the neutral point of Arago) at a position

$20^{\circ} - 25^{\circ}$ above the antisolar direction. Arago also observed the polarization of two comets and of the Moon. An explanation of the polarization of the blue sky was given by Lord Rayleigh (Strutt 1871) in terms of scattering by particles of size much smaller than the wavelength of light. However, his simple theory, while explaining several of the observed features of the colour and polarization of the blue sky, failed to account for the location of the neutral points and for the fact that the maximum value of the degree of polarization does not reach 100 per cent. The development of the theory of scattering by spherical particles of arbitrary size (Mie, 1908) and, much later, the introduction of new theoretical techniques by Chandrasekhar (1950), Sobolev (1963) and others, for the calculation of radiative transfer in relatively realistic model planetary atmospheres, has now provided an explanation for the observed deviations from the Rayleigh theory. A good review entitled "Polarization in the Environment" has been given by Coulson (1974).

All of the scattering mechanisms operating in the terrestrial atmosphere have been considered to be elastic processes, that is processes in which no change in the wavelength of the scattered light occurs. Recently, Brinkmann (1968) has proposed the existence of an inelastic component of sky light, produced by rotational Raman scattering from air molecules, in order to explain the observation that Fraunhofer lines in the spectrum of blue sky are "filled-in" relative to those in direct sunlight (Grainger and Ring, 1962a). Noxon and Goody (1965) observed that the degree of polarization decreased across the Fraunhofer lines in the blue sky spectrum and associated this with the filling-in effect. Results of a further study of this phenomenon, for the Hβ line only, is one of the applications to be discussed in this thesis.

Among the first astronomers to attempt polarimetry of stars and stellar-like objects was Öhman who observed, photographically, polarization in the Hγ line of β Lyr (Öhman 1934) and in the light from the Andromeda galaxy (M31) (Öhman 1942). This latter result probably foreshadowed the historical discovery that starlight could become polarized by passage through the interstellar medium, however, perhaps the most important event in stellar polarimetry occurred in 1946. In that year, Chandrasekhar published the solution of the equation of radiative transfer for a pure electron-scattering, plane-parallel stellar atmosphere and predicted that the emergent continuum radiation would be polarized as a function of position on the observable disc. For a spherically symmetric star, no net polarization results. For a binary system, however, in which a hot early-type star is partially eclipsed by a cooler companion, polarized light produced by electron-scattering from the visible part of the hot star, diluted by light from the cooler companion, might be observable during eclipse. Somewhat inconclusive evidence for this effect was reported for the eclipsing binary U Sge by Janssen (1946) on the basis of photographic measurements. It was apparent that the polarization effect was too small to be convincingly detected by photographic polarimeters. Fortunately, commercially available photoelectric sensors (in particular, the photomultiplier) were coming into regular use in astronomy about the same time and photoelectric polarization observations by Hall and Hiltner of the eclipsing binary CQ Cep showed a constant polarization, also present in many field stars with a similar parallax. Further independent studies by Hall (1949) and Hiltner (1949) led to the discovery that the light from the majority of distant stars, irrespective of spectral type, was linearly polarized. The amount of polarization was strongly correlated to the colour excess of the star, indicating an interstellar origin. Subsequently, there developed a

period of intense activity of observing interstellar polarization mostly for the purpose of determining the direction of the galactic magnetic field, assumed to be responsible for aligning elongated interstellar grains and thereby causing polarization of starlight by forward scattering. The photoelectric polarimeters involved were capable of a precision of about $\pm$ 0.001, that is, 0.1 per cent of total intensity (see, for instance, Hall and Mikesell 1950, Hiltner 1951, Behr 1956 and Fessenkov 1959).

Until 1959, all measurements were made on so called white light and observers paid little attention to the wavelength dependence of stellar (or planetary) polarization. Behr (1959a) found between 3700 Å and 5200 Å a small decrease towards shorter wavelengths for four stars and no such effect for two other stars. Independently of Behr, measurements were made by Gehrels and Teska (1960) using discrete broad band colour filters and a double-beam Wollaston polarimeter with a Lyot depolarizer, leading to the discovery of strong wavelength dependence of polarization for stars, planets and blue sky. Broad band spectropolarimetry of stars has since been extended by many workers, and much more insight into the nature of the interstellar material has been obtained.

The first indirect evidence for intrinsic polarization of starlight came some 13 years after Chandrasekhar's prediction, with observations that the degree of polarization of some stars changed with time, the changes usually being correlated with variations in light (for example, Behr 1959). More recently, it has been shown that almost all stars that show emission lines in their spectrum, exhibit a peculiar wavelength dependence of polarization, distinct from that of the interstellar medium, implying intrinsic effects (Serkowski 1968, Coyne and Kruszewski 1969). Polarization produced by scattering in a circumstellar shell of material is one mechanism proposed to account for the observed wavelength dependence.

Although Hale (1908) discovered the existence of strong magnetic fields in sunspots by means of polarization measurements of the Zeeman effect in lines in their spectra, it was almost forty years later before the magnetic fields of peculiar A-type stars were discovered by Babcock (1947). Until recently, these were the only stars known to possess magnetic fields. The discovery of strong circular polarization in the light from white dwarf stars (Kemp and Swedlund 1970, Kemp, Swedlund, Landstreet and Angel 1970) associated with intense magnetic fields has stimulated considerable interest in searching for intrinsic polarization, both linear and circular, in the light from other magnetic and suspected magnetic objects and, indeed, for interstellar circular polarization. Narrow band photoelectric polarimetry with sufficiently high resolution to investigate spectral lines, can be used to detect stellar magnetic fields, by observing the residual intrinsic polarization of the line produced by Zeeman splitting, even when this splitting cannot be spectrally resolved.

With the high precisions now being attained in polarimetry (typically 0·01 per cent or better) we have come, at last, full circle, since it is now difficult to study interstellar polarization without considering the possibility that intrinsic effects may be present in the stars being used as light sources! This is especially true of stars of spectral class O, B and A and all others not on the main sequence.

1.2 Intrinsic Stellar Polarization - Stellar Line Profiles

Besides the well-known polarization associated with the Zeeman splitting, other polarizational effects have also been predicted to occur within stellar line profiles. However, there is only marginal observational evidence to give qualitative support to such theories.

The first work in this field would seem to be that of Öhman (1934) who noted that one wing of the Hγ line of β Lyr exhibited some polarization that depended on the phase of this eclipsing binary. Other more recent observations are those of Tamburini and Thiessen (1961), who claimed that the equivalent widths of the Balmer lines of some early-type stars depended on the selected direction of vibration for observation. Both of these observations were performed photographically. Clarke and Grainger (1966) have also reported a large polarization effect across the Hβ line in γ UMa, which was apparently confirmed, though photographically, by Dervis (1970) who attributed it to the transverse Zeeman effect.

On the theoretical side, following Chandrasekhar's (1946) famous paper predicting polarizational effects at the limbs of early-type stars, Öhman (1946) suggested that the effects might be detected in such stars that also present Doppler broadened absorption features as a result of rapid rotation. Öhman's simple theory consisted of subdividing the observed stellar disc into three parts parallel to the rotation axis and corresponding to the red wing, line centre and blue wing of the spectral feature. By averaging the components of the polarized flux in each sector, he formed the net polarization which, in a favourable case resulted in a differential variation of 0·8 per cent in the degree of polarization across the line. The azimuth of vibration would be expected to rotate through 90° going from either wing to the line centre. Since Chandrasekhar's work involved the solution of the radiative transfer equation for a non-rotating, plane-parallel, pure-scattering (i.e. grey) atmosphere, it is important to reconsider his findings in the light of more recent research.

Harrington and Collins (1968) calculated the net degree of polarization of the continuum flux to be expected from a rapidly rotating, pure-scattering,

plane-parallel atmosphere. They found that up to 1·7 per cent net polarization might be obtained in this manner, however, since they assumed a grey atmosphere no wavelength dependence or spectral-type dependence could be estimated. Harrington (1969) also demonstrated that larger polarizations might result if the gradient of the source function was steep enough and that such extinctions may arise in the atmospheres of Mira variables, already known to exhibit intrinsic polarization (Serkowski 1966).

Intrinsic polarization arising in rotationally distorted non-grey plane-parallel atmospheres from Thomson scattering by free electrons was first tackled by Collins (1970). His results, applied explicitly to early-type stars, indicate almost no net polarization (about 0·1 per cent) in the visible but up to 2 or 3 per cent in the far ultra-violet.

Serkowski (1970) has pointed out that the only rapidly rotating early-type stars observed to show measurable polarization in broad bands are those that have extended atmospheres or envelopes, as evidenced by the presence of emission lines. Models of the complexity of those of Collins are not yet available for extended atmospheres. However, Cassinelli and Haisch (1974) have recently investigated the simpler problem of polarization by pure electron-scattering (grey) atmospheres that are geometrically extended, using the numerical results of Cassinelli and Hummer (1971). In the latter paper, the transfer equation for scattering according to the Rayleigh law was solved for spherical, rotating atmospheres with different density distributions. At the limb of an extended atmosphere (i.e. at a line of sight having tangential optical depth unity) the degree of polarization of the continuum flux is very large, approximately 50 per cent, compared with only 11 per cent at the limb of a plane-parallel model. The inclusion of an absorptive opacity (non-grey atmosphere) is ignored by these workers on the

grounds that the extremely low electron densities present in stars with extended atmospheres implies that scattering is the dominant form of opacity.

To determine the net polarization Cassinelli and Haisch (1974) integrated the polarized flux over the apparent projected areas of two models, viz., a disc model and a Roche model (rigid rotator). A net degree of polarization as high as 6 per cent was found for a disc envelope and 2 per cent for a Roche atmospheric model.

There are two important points for narrow band polarimetry. First, the net polarization of the continuum radiation of the underlying star could be affected by unpolarized emission from the outer layers of the envelope. Secondly, the high polarization near the limb of the envelope may be reflected in the structure of rotationally broadened line profiles, that is, we have the Öhman effect. At first sight, it appears that the magnitude of any differential polarization present in a Doppler broadened profile will be greatly enhanced. Unfortunately, the situation is complicated by the fact that in an extended atmosphere the limb darkening is very severe, so that the actual contribution of the outermost regions of the projected disc may be quite small. In fact, using the data given by Cassinelli and Hummer (1971) then, at the "limb" of the extended atmosphere, the radiation is polarized tangentially to the disc, with degree of polarization of about 50 per cent but the intensity is only 0·002 of that at the centre of the disc. Comparing this to 11 per cent polarization and a limb darkening factor of 0·3, for a typical plane-parallel model, then it appears that Öhman's calculations may be an overestimate by more than an order of magnitude. Nevertheless, with polarimetric precisions of the order of $\pm$ 0·01 per cent, and severely geometrically distorted rotating stars or binary systems, the effect should still be observable.

In an investigation of the effect of thermal Doppler broadening by an electron-scattering atmosphere, Sen and Lee (1961) have shown that small amounts of polarization are likely to be present and to vary across both emission and absorption lines. Strong polarization effects in certain solar metallic emission lines arising from, for example, resonant scattering in prominences and the coronal plasma, have been discussed by Tandberg-Hanssen (1974). Both these effects may be manifest in the Balmer lines in early-type stars and luminous giant stars due to the severe departures from local thermodynamic equilibrium (LTE) encountered in their atmospheres.

For the case of magnetic and suspected magnetic stars, the polarization of their line profiles is associated with the Zeeman effect. The circular polarization produced in the wings of stellar line profiles, by the longitudinal Zeeman effect, offers the possibility of detecting magnetic fields too weak to give a measurable displacement of the σ components of the Zeeman triplet, by observation of the line profile alone. This effect has been extensively used for many years in solar observations, very high precisions (1 - 10 gauss) being obtained mostly through the use of photoelectric electro-optic (Pockels cell) polarimeters (see, for example, the review by Beckers (1970)).

In Babcock's classic work on stellar magnetic fields (Babcock 1960), the measurements were performed photographically and the fields deduced from the mean wavelength separation of opposite circularly polarized lines in the stellar spectra. This technique is limited to the investigation of sharp-lined stars, that is stars which are intrinsically slow rotators or those which are seen pole-on. Babcock (1958), in his catalogue of magnetic stars, has listed over 60 stars, mostly Ap and Am, in which the lines are too broad or the fields too weak to yield a measurable splitting. Therefore, for

these and weak-field stars of other spectral types, information on their
magnetic fields can only be determined by polarimetry.

Although the metallic lines have the largest Landé g-factors and the
lowest ratio of line width to Zeeman splitting, and hence the largest dif-
ferential polarization, observations of such lines require very high spec-
tral resolution (0·2 Å or better). This resolution often implies the use of
a spectrometer at the coudé focus, thereby increasing the difficulties of
instrumental polarization because of the oblique reflections in the mirror
system (Clarke 1973), and necessitates the use of a large collector because
of the low throughput. An alternative approach is to observe very strong
lines, such as the Balmer lines. Narrow band interference filters with pass-
bands of 3 - 10 Å enable most of the wings of, for example, the Hβ line to
be observed for polarization in stars of various spectral types. In this
case, the throughput is high but the numerical value of the fractional cir-
cular polarization ($q = V/I$), on one line wing, is quite small, typically
$q \sim 0 \cdot 033$ per cent per kilogauss. Observationally, the antisymmetric
nature of q across the profile effectively doubles this polarization and
the measurement efficiency is improved if both wings of the line are obser-
ved simultaneously.

Intrinsic linear polarization associated with magnetic stars has been
sought for many years, (Thiessen 1961, Hiltner and Mook 1967, Serkowski
and Chojnacki 1969). However, most of these observations were made through
broad band filters,rather than across spectral lines, where one would expect
the effect to show because of the Zeeman splitting. A quantitative analysis
of the transverse Zeeman effect in stellar atmospheres is much more compli-
cated than for the longitudinal effect (Stenflo 1971). In the simple case of
an unresolved triplet in an optically thin absorbing layer the degree of

linear polarization due to a transverse field is given by

$$p \sim (\Delta\lambda)^2 \cdot (d^2 I(\lambda)/d\lambda^2)$$

where $I(\lambda)$ is the line shape and $\Delta\lambda$ the Zeeman splitting. This gives three unresolved /peaks, a central (π) component polarized parallel to the field direction and peaks with the azimuth of the direction of vibration rotated by 90° on the wings (σ components). However, the magnitude of the polarization is small, $p \sim (\Delta\lambda/\Gamma)^2 \sim q^2$ (where Γ is the half-intensity width of the spectral line), at least for atmospheres in local thermodynamic equilibrium (LTE) (Borra 1973), but the rotation of the azimuth of vibration should aid in detecting the effect.

Further references and more detailed discussions are deferred to the relevant section of Chapter 4 which contains an account of the observational aspects of the thesis.

1.3 Narrow Band Spectropolarimetry - Recent Advances

Outlined in this section are the most recent developments in astronomical narrow band spectropolarimetry to July, 1974. It is most encouraging to note that a rapid increase in interest in this subject has occurred during the course of this research (1971-1974). Even now the field has been barely opened.

In the binary X-ray sources, synchrotron emission by matter falling into the magnetic field of a neutron-star secondary (or other highly collapsed object) is one proposal for the origin of the X-rays (Foreman, Jones and Liller 1972), while an alternative mechanism proposed by Bachall, Kulsrud and Rosenbluth (1973) is that X-rays come from the interaction of two magnetic stars which are not co-rotating. Kemp and Wolstencroft (1973a) report the discovery of large variable magnetic fields in HD77581, associated with

Vela XR-1, and θ^2 Orionis proposed as the optical counterpart of 2U 0525-06. Analogous results were reported later for HD153919 (2U 1700-37), (Kemp and Wolstencroft, 1973b). Detection was by means of the Zeeman effect in Hβ, as measured by circular polarization on the line wings. Similar measurements on the wings of Hα, together with profile scans, in HD77581 and HD153919 by Angel, McGraw and Stockman (1973) did not indicate significant Zeeman splitting.

The electro-optic method of measuring magnetic fields, developed by Babcock (1953) for solar magnetic measurements has been adapted by Severny (1970) and Angel and Landstreet (1970) for the measurement of stellar fields. Detection is by circular polarization in the wings of sharp metallic lines. Severny (1970) reports a survey of eight stars with standard errors between 12 and 50 gauss and claims positive detection of magnetic fields of ~ 40 gauss in Sirius and ~ 200 gauss in γ Cyg and β Ori. Borra and Landstreet (1973) and Borra, Landstreet and Vaughan (1973) have surveyed 23 stars, mostly later than A0; they detected a field in γ Cyg on several occasions but in no other stars in their sample. A few of these stars were observed independently of these workers by the writer and the results are described later. A new technique, involving the use of a television camera with a solar spectrograph, to search for magnetic fields in bright stars, has been employed recently by Auman et al. (1971).

About fifty white dwarf stars have been observed by Angel and Landstreet for circular polarization in the wings of the Balmer lines (Angel and Landstreet, 1970a, b; Landstreet and Angel 1971). A discussion of these and other measurements is given by Landstreet (1974) and both positive and negative results reported.

Intrinsic linear polarization of Hβ and the continuum has been discovered for three magnetic Ap stars, HD215441, 53 Cam and α^2 CVn (Kemp and Wolstencroft 1973c, 1974). The degree of linear polarization is larger than expected from simple LTE theory of the transverse Zeeman effect (Borra, 1973), being of the same order as the degree of circular polarization q, that is, typically 0·1 per cent or more. In a broad blue band (Δλ ~ 1400 Å) centred on Hβ, the azimuth of vibration of the polarization of 53 Cam rotates through 360° over one magnetic period and there appears to be a similar behaviour within the Hβ line. The results are compatible with the oblique-rotator model of magnetic stars. To account for the size of the observed component, a non-LTE process involving resonant scattering in a magnetic field (Hanle effect) has been proposed by Finn and Kemp (1974). By introducing the decentred dipole configuration of the magnetic field geometry, first proposed by Landstreet (1970), the observed features of the polarization variability can be reproduced.

On the basis of theoretical Zeeman-analysed line profiles, Borra (1972, 1974) has shown that a decentred dipole model can alter the interpretation of the orientation of the magnetic axes in Ap stars. It can also account for the discrepancy sometimes observed between photographic and photoelectric measurements of magnetic fields, due to a tendency to overemphasize the cores of the spectral lines in the former method.

These recent successes have revealed the importance of linear and circular polarimetry, with high spectral resolution, of magnetic and suspected magnetic stars. Unfortunately, the most interesting objects for study are fainter than fifth magnitude, therefore a large collecting aperture (≳ 2 m) is essential to yield viable integration times.

Capps, Coyne and Dyck (1973) have observed the wavelength dependence of the polarization of the Be-shell star ζ Tau in the wavelength range 3000 Å to 2·2μm, by using a series of medium bandwidth filters. Their results support the suggestion by Coyne and Kruszewski (1969) that the polarization is produced in a flattened disc about the star. Zellner and Serkowski (1972) report unpublished narrow band linear polarization observations of ζ Tau across Hβ which indicate that the emission is less polarized than the neighbouring continuum. One of the major achievements of the polarimeter described in this thesis has been the discovery of a strong and variable depolarization of the Hβ emission feature in the Be-shell star γ Cas (Clarke and McLean, 1974b). Confirmation is also given of the effect in ζ Tau. These results give a clear indication of the intrinsic nature of the polarization of emission line shell stars. In contrast, high precision measurements at Hβ of the supergiant α Cyg, which shows Hα emission, reveal no polarization effects. Variability peculiar to the Hβ emission feature of γ Cas has been established conclusively because the spectropolarimeter (Clarke and McLean, 1974a) can record the stellar line profile and monitor the polarization at two passbands simultaneously. The report of a similar depolarization effect at Hα in ζ Tau has been made recently by Coyne (1974, personal communication).

Finally, it is interesting to note that narrow band polarimetry has recently been applied to the study of interstellar absorption bands, viz., the 4430 Å band. The presence of differential polarization across the 4430Å band would indicate absorption by impurity atoms distributed uniformly over the surface or throughout the volume of the grains. Negative results are reported by A'Hearn (1972) and Martin et al. (1973, 1974), however a small but definite polarization anomaly across the band has been reported by Kemp and Wolstencroft (1974, preprint) for three stars.

In the subsequent chapters the design and development of the Hβ-spectro-polarimeter is presented together with the results of the observations made concerning the three topics mentioned in the introduction.

2. INSTRUMENTAL REQUIREMENTS FOR LINE PROFILE POLARIMETRY

2.1 Introduction

Any spectropolarimeter can be conceptually regarded as a combination of an optical part and an electronic part. The optical part contains elements which modulate the state of polarization of the light in a known way, at each wavelength interval isolated, to produce intensity variations which are then measured by the electronic part. Included in the electronic part must be a photodetector and all the electronics necessary to retrieve the information contained in the detector output. It is also convenient to include in the electronic part any automatic control of the optical components, since that control must be synchronised with the signal-handling electronics. The optical section can be further sub-divided into a part for achieving spectral isolation and a part for performing polarimetry. In making the combination of all these parts several criteria must be met simultaneously.

When astronomical polarimetric observations are limited by signal noise generated by the passage of the starlight through the Earth's atmosphere, then the noise can be removed very effectively by using a double-beam polarizing prism and two detectors (see, e.g., Hiltner 1951, Gehrels and Teska 1960; Serkowski and Chojnacki 1969). With such a two-channel system, spectropolarimetry can be performed by using filters, having no polarizing effects, prior to the double-beam polarizer, so that each resolved component contains the identical spectral passband.

If spectropolarimetry is contemplated at medium-to-high spectral resolution or with a scanning monochromator, then the application of double-beam techniques with prior spectral isolator loses its attraction. Both prism and grating monochromators have polarizing properties and would introduce parasitic polarization that must be calibrated out. Grating monochromators

are particularly troublesome in that their strong polarizances are very de-
pendent on wavelength. Perhaps the only type of scanning monochromator that
might be applied successfully prior to a double-beam polarimeter is the
Fabry-Pérot interferometer. However, such a device is reserved for achiev-
ing very narrow spectral passbands, and the noise on the measurements is
likely to result from photon shot noise rather than from effects of the
atmosphere; in this case, provision of the second channel results only in
a $\sqrt{2}$ advantage over a single channel.

For a monochromator giving rise to polarizing effects, it is obviously
better to place it after the polarimetric system so that it receives a con-
stant direction of vibration. In such a position, the polarizing effects
do not disturb the polarimetry, but they may control the signal level accor-
ding to the orientation of the monochromator. Obviously the orientation
which gives the best transmittance should be sought, but it may be wave-
length dependent. However, it is now difficult to consider using double-beam
polarimetry because of the awkwardness of directing the two resolved com-
ponents into the same entrance aperture of the spectral isolator and recoup-
ing them for separate detection after the exit aperture. Except for simple
devices such as filters, one would not normally think of employing two sepa-
rate monochromators for each beam. Again, as mentioned above, at high spec-
tral resolution, we are likely to be limited by photon shot noise, and the
loss of the second channel is perhaps of marginal importance.

The considerations above suggest that medium-to-high resolution polari-
metric studies might be performed simply by using a single-channel polari-
metric system whose spectral passband is controlled by a following mono-
chromator.

In order to perform polarimetric observations of, for example, a

stellar Hβ line profile, a typical spectral resolution of about 2.5 Å at Hβ is required. (However, one should also allow some scope for broader passbands of 10. Å to 200 Å to be used). This kind of value does not readily go hand in hand with photoelectric spectrometry in that for conventional medium-sized angular dispersive instruments, it is difficult to ensure acceptance of the complete seeing disc by the entrance aperture without losing the potential resolving power. Since such spectrometers are also physically large in proportion to the size of the collecting aperture of small telescopes (0.5 - 1.0 m) they may cause problems of mounting and flexure. Yet it is well known that for the brighter stars sufficient energy can be collected by small aperture telescopes to allow photoelectric recording of stellar spectra at a resolving power of 2×10^3 ($\lambda \sim 5000$ Å) with good photometric accuracy (1 per cent) in quite acceptable observation times.

The next two sections review briefly the photometric accuracies and integration times expected and the approach adopted to the problem of the matching of telescope/spectrometer systems. Section 4 discusses relevant properties of narrow band interference filters and the last two sections elaborate on the polarimetric methods used.

2.2 Photoelectric Photometry

Ideally, the precision of any photometric measurement should be limited only by quantum noise, i.e. by the fluctuations in the photoelectron production rate. The number of photoelectrons produced in t seconds by a photocathode of quantum efficiency q illuminated by the light collected by a telescope of aperture D cm from a star of magnitude m is given by

$$N(m) = \frac{\pi}{4hc} \lambda \, \Delta\lambda \, F_\lambda \, \tau \, q \, D^2 \, t \, (2.512)^{-m}$$

where the wavelength λ and the spectral interval $\Delta\lambda$ are expressed in microns (μm); τ is the total transmittance of unpolarized light by the Earth's atmosphere, the telescope and instrument optics; F_λ is the absolute flux density for a star of magnitude 0.00 (AOV), expressed in watts cm^{-2} μm^{-1} and is given by Johnson (1966) for various filter passbands, while h is Planck's constant (6.626 x 10^{-34} Ws^2) and c is the speed of light (2.998 x 10^{14} μms^{-1})..

For a wavelength of 0.4861 μm (Hβ), a passband of 0.00025 μm (2.5 Å), an aperture of 50 cm and taking m = 0, τ = 0.05, q = 0.10 and F_λ = 7.2 x 10^{-12} W cm^{-2} μm^{-1} for the B spectral band (λ = 0.44 μm) then

$$N(0) \approx 4 \times 10^4 .t \quad counts.$$

Since the number of counted photoelectrons is approximately subject to Poisson statistics the mean error of this number is $\sqrt{N}$ i.e. the photometric accuracy expressed as a percentage is 100 $(N)^{-\frac{1}{2}}$. In a one second integration time in the above example the photometric accuracy is 0.5 per cent.

This order of precision is extremely difficult to obtain, except under excellent atmospheric conditions if an absolute photometric measurement is required, i.e. if no means of compensating for atmospheric effects is provided in the photometer. Polarimetric precision, however, can be orders of magnitude higher than photometric precision, because only relative photometry is needed, and thus the effects of atmospheric scintillation, seeing and extinction can be eliminated or greatly minimised. For many astronomical objects the observed polarization is very small, making such high polarimetric precision obligatory.

If in a one second integration time atmospheric effects set a limit of 1 per cent on the precision of absolute photometry then, for the site, telescope and wavelength passband given in the example above, the stellar magni-

TABLE 2.1a : Approximate Count Rates Expected from a star of magnitude $m = 0\overset{m}{\cdot}0$ as a Function of $\Delta\lambda(\mu)$ and $D(cm)$. $N = 6\cdot9 \times 10^4.\Delta\lambda.D^2.t.(2\cdot512)^{-m}$. with the values of λ, F_λ, τ and q given in the text.

$\Delta\lambda$ \ D	50 cm	91 cm	250 cm
1 Å	$1\cdot7 \times 10^4$ s^{-1}	$5\cdot7 \times 10^4$	$4\cdot3 \times 10^5$
2·5	$4\cdot3 \times 10^4$	$1\cdot4 \times 10^5$	$1\cdot1 \times 10^6$
10	$1\cdot7 \times 10^5$	$5\cdot7 \times 10^5$	$4\cdot3 \times 10^6$
25	$4\cdot3 \times 10^5$	$1\cdot4 \times 10^6$	$1\cdot1 \times 10^7$
60	$1\cdot0 \times 10^6$	$3\cdot4 \times 10^6$	$2\cdot6 \times 10^7$
100	$1\cdot7 \times 10^6$	$5\cdot7 \times 10^6$	$4\cdot3 \times 10^7$
Flux Gain	1	$3\cdot3$ ($1\overset{m}{\cdot}3$)	25 ($3\overset{m}{\cdot}5$)

TABLE 2.1b : Integration Times (t) as a Function of m and Photon Noise Limited Error ε ($\equiv N^{-\frac{1}{2}}$) for $\Delta\lambda = 2\cdot5$ Å and $D = 50$ cm. $\varepsilon^2 t = 1\cdot4452 \times 10^{-5}.(2\cdot512)^m / \Delta\lambda(\mu).D^2$.

ε \ m	1 %	0·5 %	0·1 %	0·05 %	0·01 %	0·005 %
0	0·23 s	0·92	23·2	92·8 s	$2\cdot32 \times 10^3$	$9\cdot28 \times 10^3$
1	0·58	2·32	58·0	$\begin{cases} 2\cdot32 \times 10^2 \\ 3\cdot9 \text{ min} \end{cases}$	$5\cdot8 \times 10^3$	$2\cdot32 \times 10^4$
2	1·46	5·84	$1\cdot46 \times 10^2$	$\begin{cases} 5\cdot84 \times 10^2 \\ 9\cdot7 \text{ min} \end{cases}$	$1\cdot46 \times 10^4$	$5\cdot84 \times 10^4$
3	3·68	14·6	$3\cdot68 \times 10^2$	$\begin{cases} 1\cdot47 \times 10^3 \\ 24\cdot5 \text{ min} \end{cases}$	$3\cdot68 \times 10^4$	$1\cdot47 \times 10^5$
4	9·23	36·8	$9\cdot23 \times 10^2$	$\begin{cases} 3\cdot69 \times 10^3 \\ 61\cdot5 \text{ min} \end{cases}$	$9\cdot23 \times 10^4$	$3\cdot69 \times 10^5$
5	23·2	92·8	$2\cdot32 \times 10^3$	$\begin{cases} 9\cdot28 \times 10^3 \\ 154\cdot7 \text{ min} \end{cases}$	$2\cdot32 \times 10^5$	$9\cdot28 \times 10^5$

For $\Delta\lambda = 10$ Å, $t \to t/4$; for $D = 250$ cm, $t \to t/25$ or for both conditions, $t \to t/100$.

tude at which this source of error equals the photon noise error is obtained
from

$$N(m) \approx 4 \times 10^4 \cdot t \cdot (2 \cdot 512)^{-m}$$

with $N(m) = 10^4$ and $t = 1$, i.e. $m \simeq 1 \cdot 5$. For fainter stars the dominant
source of error is photon shot noise but the integration time required to
obtain an accuracy of 0.5 per cent in the photometric signal is only 100 s
for a star of magnitude 5·0. (The values of transmittance and quantum
efficiency were chosen to give count rates that were roughly consistent
with those obtained with our polarimeter attached to telescopes of apertures
51 cm, 91 cm and 250 cm). Tables 2.1a, 2.1b are included to give some idea
of the count rates expected for various passbands and the integration times
required to obtain certain photometric precisions under photon limited con-
ditions. These times are easily related (Section 2.5) to the mean error
associated with the measurement of an individual Stokes parameter under
those same conditions. Of course, in practice, the observed count rates
must be employed to estimate the measurement precision or predict the total
integration time.

Although the resolution and photometric accuracy can in principle be
achieved it is necessary to take into consideration the enforced operating
conditions and the problem of maximising the amount of light reaching the
detector.

2.3 Matching of Telescope/Spectrometer Systems

When considering the transfer of light from one optical system to
another it is important to know the luminosité (throughput) of each system
(see e.g. James and Sternberg 1969, Jacquinot 1954, Meaburn 1970). The
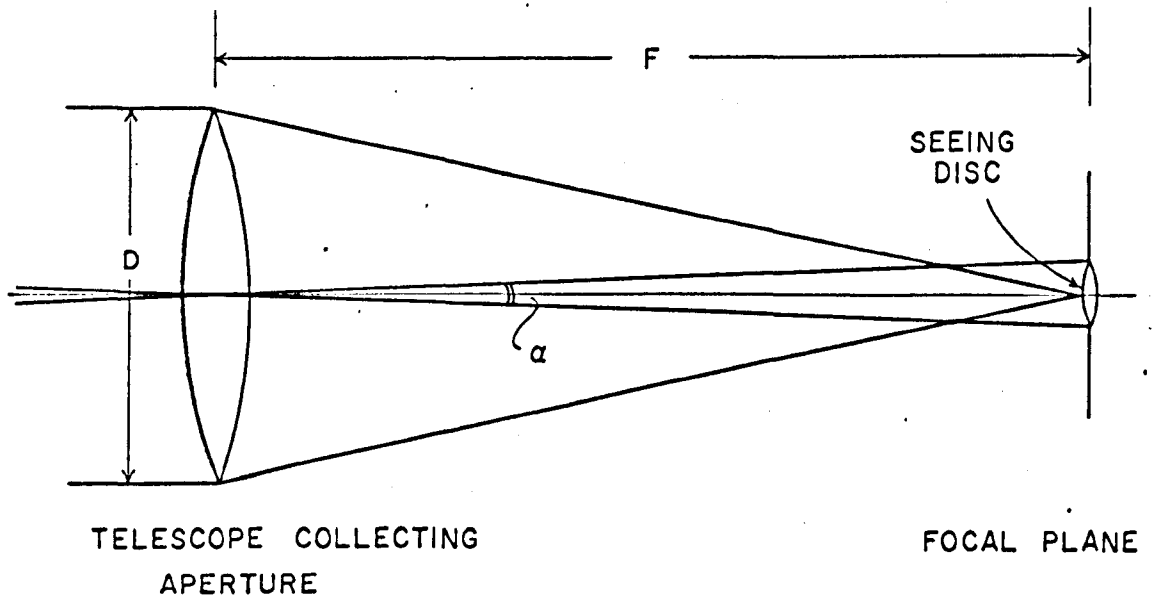luminosité of a system is usually defined by the relation

$$L = \varepsilon A \Omega$$

Fig. 2.1 Effective luminosité (throughput) of a telescope of aperture D, with angular diameter of seeing disc, in the focal plane, α.

$$L = \frac{\pi D^2}{4} \cdot \frac{\pi (F\alpha)^2}{4} \cdot \frac{1}{F^2} = \frac{\pi^2 D^2 \alpha^2}{16} \text{ cm}^2. \text{ sterad}$$

where ε = transmission coefficient (ε is often ignored, at least until the term AΩ has been evaluated), A = acceptance area and Ω = acceptance solid angle. The most efficient transfer is achieved when the subsequent system has a luminosité that at least matches that of the initial system. For the case of a telescope and spectrometer, all the light collected from a star can only be passed into the spectrometer if its entrance aperture is sufficiently large to accept the whole of the star's seeing disc. One can consider the problem by thinking of the telescope aperture in combination with the seeing disc as providing an effective luminosité (see Fig. 2.1), which may be written as

$$L = \frac{\pi^2}{16} D^2 \alpha^2 \text{ cm}^2 \text{ sterad.}$$

D is the diameter of the telescope aperture (cm) and α is the angular diameter of the seeing disc (radian). It is then a simple matter to compare this expression with those for the luminosités of several types of spectrometer systems derived for given working resolving powers and with circular entrance and exit apertures. For convenience these expressions are listed in Table 2.2.

From Fig. 2.2 such comparisons show clearly that, for example, for a telescope of aperture 50 cm with a 10 arc sec seeing disc, at an operating wavelength of λ = 5,000 Å and a resolution of 1 Å, prism spectrometers are wholly inadequate, while a physically large grating spectrometer is required to just obtain an optical match under these conditions. On the other hand the problem is overcome by use of a Fabry-Pérot-type system and at the same time a more compact instrument is achieved.

Now the interference filter can be considered as being a special form of the Fabry-Pérot with enhanced luminosité. Eather and Reasoner (1969)

TABLE 2.2   Luminosité expressions for several spectrometer systems

achieving resolving power, R, with circular entrance apertures.

Spectrometer System	Luminosité (Circular Apertures)
Prism: base length t; height h; bh = area of refracting face. $(\frac{\partial \mu}{\partial \lambda})$ = dispersion of prism material.	$L_P = \frac{\pi}{16} \cdot \frac{t^2 h}{b} \cdot (\frac{\partial \mu}{\partial \lambda})^2 \cdot \frac{\lambda^2}{R^2}$
Grating: grating area A_g; order of interference m; d^{-1} = number of lines/cm.	$L_G = \frac{\pi}{4} \cdot \frac{m^2 A_g}{d^2 \cos i} \cdot \frac{\lambda^2}{R^2}$
Fabry-Pérot: useful plate area A_{FP}	$L_{FP} = 2\pi A_{FP} \cdot \frac{1}{R}$
Interference Filter: (cf. Fabry-Pérot) useful area of filter = A_{IF} μ^* is an effective refractive index (see text).	$L_{IF} = 2\pi A_{IF} \cdot \frac{\mu^{*2}}{R}$

It is assumed that two neighbouring wavelengths λ and $\lambda + d\lambda$ are just re-
solved, in the focal plane of the camera lens, when their linear separation
is equal to the width of the image of the entrance aperture.
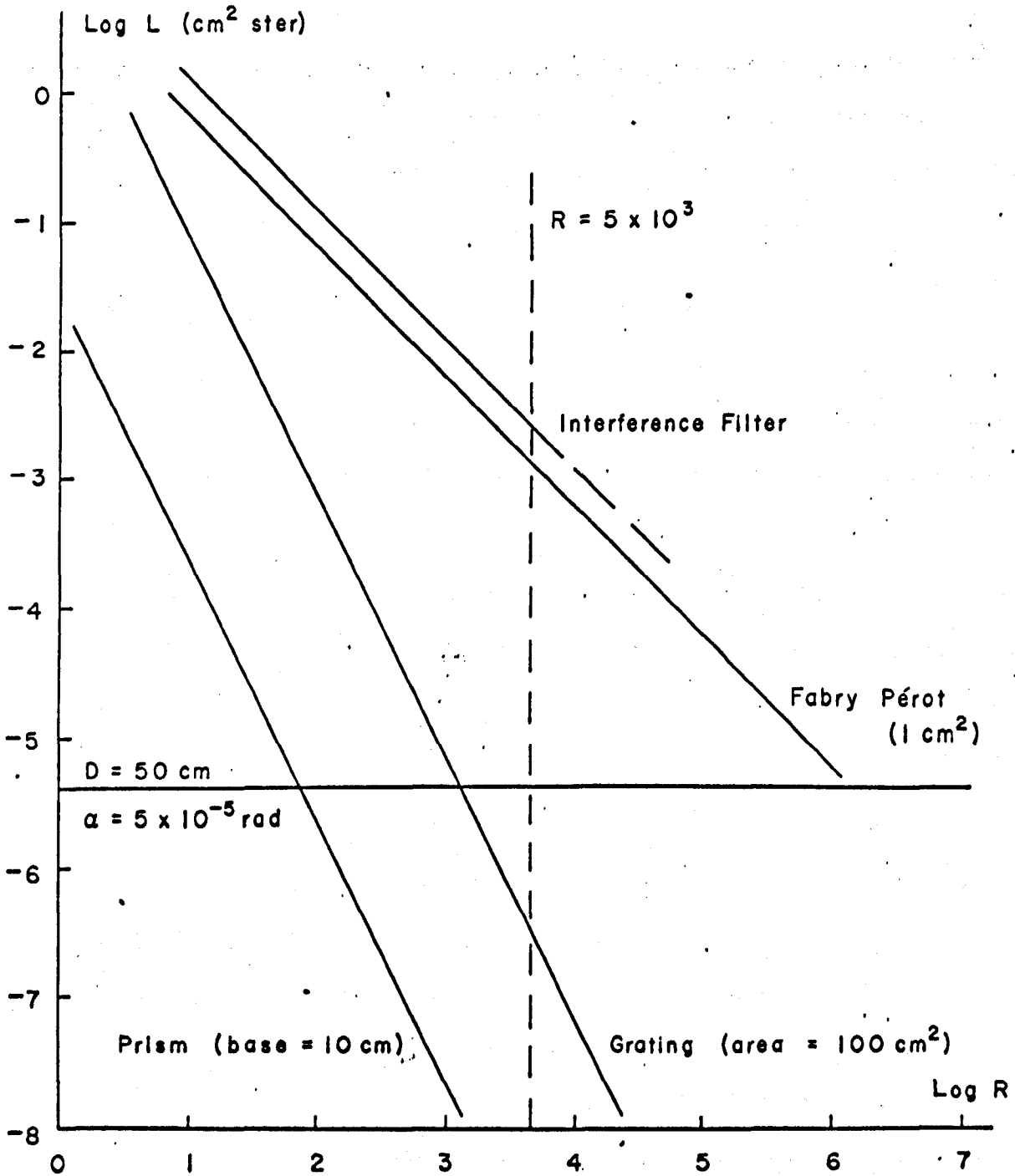
Fig. 2.2   Variation of luminosité (L) with resolving power (R) for the
spectrometer systems given in Table 2.2 assuming the following
typical dimensions: $\lambda = 5 \times 10^{-5}$ cm,

   Prism: b = h, t = 10 cm, $\partial\mu/\partial\lambda = 600$ cm^{-1}.
   Grating: i = 0, m = 2, d^{-1} = 3,000 lines/cm, A$_g$ = 100 cm^2.
   Fabry-Pérot: A$_{FP}$ = 1 cm^2.
   Interference Filter: A$_{IF}$ = 1 cm^2, $\mu^* = 1.4$

The horizontal line indicates the effective luminosité of a
telescope (D = 50. cm, α = 10 arc sec).

have shown that by tilting it to alter the position of its wavelength pass-band, it has application as a scanning monochromator. Tilt-tuning of the passband is common in filter photometry. It can be shown that, to a good approximation, the relationship between the wavelength (λ) passed by the filter and the angle of tilt (β) can be represented by

$$\lambda = \lambda_o \left\{ 1 - C\beta^2 \right\}$$

where λ_o is the wavelength of peak transmission at normal incidence and C is a parameter related to the design of the particular filter. By tilting through an angle of 15° from normal incidence a scan range of ~ 70 Å is obtained.

Small 25 mm diameter interference filters with fullwidth passbands at half maximum transmittance (FWHM) of ~ 2 Å - 10 Å are readily available commercially at reasonable cost; (the 2.5 Å, and both 10 Å filters used in this study were manufactured by Thin Film Products, Infrared Ind. Incorp., Cambridge, Mass.).

Because of its simplicity, with small size and low weight, while accepting easily the angular spread of a star's seeing disc, a tilting-filter scanning monochromator was investigated for incorporation in a Line Profile Spectropolarimeter. Apart from a low resolution study by de Vaucouleurs (1967) of red-shifts in the H and K lines of galaxies but which also included occasional star scans, this simple method has not been applied previously to stellar observations and is a completely ~~original~~ new technique for obtaining polarization measurements across any restricted spectral feature.

The advantages and disadvantages of the method and the relevant theory are discussed in the next section.

2.4 Tilt-scanning of Narrow Band Interference Filters

The mathematical expression of the theory of interference in thin films is often rather involved but is well treated in some detail in, for example, works by Heavens (1960) and MacLeod (1969). Applications of interference filters in non-scanning circumstances are described in papers by Cruvelier (1967) and Meaburn (1970), while treatments of the tilt-scanning theory and applications to extended sources, e.g. aurorae, are given by Eather and Reasoner (1969) and Pidgeon and Smith (1964).

Briefly, the interference filter is a special case of the Fabry-Pérot étalon. Empirically, Pidgeon and Smith have shown that the angle-scanning behaviour in a collimated beam may be characterised by a monolayer of refractive index μ^* intermediate between the high and low refractive indices of the component layers. Therefore in the Fabry-Pérot equation

$$2 \mu t \cos \phi = n\lambda \ ,$$

μ is replaced by μ^*, resulting in an increase in throughput (luminosité) by a factor μ^{*2}. As a function of external angle of incidence β the fractional peak-wavelength shift is easily derived to be

$$\frac{\lambda_o - \lambda}{\lambda_o} = 1 - \cos \phi$$

but $\sin \phi = \sin \beta / \mu^*$ therefore

$$\frac{\lambda_o - \lambda}{\lambda_o} = 1 - (1 - \frac{\sin^2 \beta}{\mu^{*2}})^{\frac{1}{2}}$$

$$\text{i.e.} \ \ \lambda = \lambda_o (1 - \frac{\sin^2 \beta}{\mu^{*2}})^{\frac{1}{2}} \ ,$$

where $\lambda_o = 2 \mu^* t/n$ and is the wavelength of peak transmission at normal incidence ($\beta = 0$). Clearly the shift is towards shorter wavelengths. Pidgeon and Smith have shown that the approximate form of this equation

$$\lambda = \lambda_o \left(1 - \frac{\sin^2 \beta}{2\mu^{*2}}\right)$$

is valid to an accuracy of about 3 per cent in the fractional wavelength shift for values of β up to 40°. For scans of less than about 15° it is in practice feasible to put $\sin \beta = \beta$ to obtain the relation

$$\lambda = \lambda_o \left(1 - C\beta^2\right)$$

where $C = 1/2\mu^{*2}$. This relation was verified experimentally in the laboratory for $\beta \leqslant 20^o$.

The transmission coefficient at normal incidence is given by the Airy Relation,

$$\tau(\lambda) = \left(1 + F \sin^2 \frac{\delta}{2}\right)^{-1}$$

where $F = 4R/(1 - R^2)$, R being the reflectivity, at normal incidence, of the reflecting stack consisting of a large number of quarter-wave dielectric layers of alternate high and low refractive indices. The phase difference between successive emerging beams is $\delta = (4\pi\mu^* t . \cos \emptyset)/\lambda$.

For high order filters at normal incidence, the passband, that is the bandwidth at the half transmission point (FWHM), is given by

$$(\Delta\lambda)_o = 2\lambda_o/(\pi n F^{\frac{1}{2}})$$

where n is the order of interference. The terms passband and halfwidth are used interchangeably to denote the FWHM of the filter profile.

Since the reflection coating is essentially a dielectric surface it will obey Fresnel's laws of reflection. Thus the reflectivity and hence the transmission coefficient and passband, will be different for beams polarized parallel and perpendicular to the plane of incidence. Also, phase shifts are introduced on reflection such that the wavelength of peak transmission

not only changes but its <u>rate</u> of change is different according to the direction of vibration of the incident light. Therefore, as β increases, the passband develops into a doublet, the shorter wavelength transmitting the light polarized perpendicular to the plane of incidence. This is not serious for tilts less than 15 to 20 degrees but can be avoided in a polarimeter when the filter follows a fixed polarizer.

Although the maximum acceptance angle for an interference filter used in a convergent beam is increased by a factor $\sim \mu^*$ over that for a normal Fabry-Pérot étalon, resolution will be lost even at normal incidence. (For the filters used by Pidgeon and Smith the bandwidth increased by about 14 per cent for an incident cone angle of $20°$).

To sum up, the advantage of the high throughput of an interference filter over prism and grating spectrometers has already been referred to. The shift to shorter wavelengths of the position of the filter passband with tilt is nonlinear, but calibration to a linear wavelength scale is easily effected. Although the filter passband (FWHM) increases with tilt, i.e. the scan is recorded with a varying instrumental profile, the distortion by this effect on the profiles of broad features is small (see the Hβ scans in Chapter 3); the broadening of the passband with tilt is accompanied by a decrease of transmittance, thus offsetting serious signal level changes when scanning a continuum. With unpolarized incident light, the passband develops into a doublet as the filter is tilted, the component corresponding to the direction of vibration perpendicular to the plane of incidence transmitting the longer wavelength. Further, the halfwidth increases at a slightly different rate for each of the two directions of vibration, the perpendicular component having the slower broadening rate. Such effects are negligible over the small angles of tilt necessary to

record the majority of line profiles but, in any case, the relative orientation of the polarizer and tilt axis has been chosen so that the most favourable component is selected.

2.5 Measurement of Polarized Light

A broad classification of polarimetric methods has been given by Clarke and Grainger (1971) and a comparison of various types of polarimeters for optical astronomy has been compiled recently by Serkowski (1974).

It has already been emphasised that narrow band polarization measurements made with medium-sized collectors are limited in accuracy by photon counting statistics except for the brightest stars. Under photon limited circumstances the improvement in the measurement precision allowed by a double-beam ratio technique is $\sqrt{2}$ over that of a single beam method. However, some kind of mode must be implemented to reduce the influence of atmospheric effects if advantage is to be taken of higher count rates, when telescopes of larger collecting apertures are used. Employing tilt-scanning narrow band filters in each beam of a two beam polarimeter in which each beam is used as a single beam polarimeter, offsets the $\sqrt{2}$ factor of the double-beam ratio polarimeter exactly since, in the identical <u>total</u> observation time the same precision of polarimetry can be obtained at two spectral points simultaneously rather than sequentially.

Several single beam systems that achieve compensation for scintillation, seeing and atmospheric extinction are in use and all of these employ AC techniques, that is, rapid modulation of the Stokes parameters. For example, the photoelastic modulators of Mollenauer et al. (1969), Kemp et al. (1970); the electro-optic modulators of Angel and Landstreet (1970) and the Dollfus modulator improved by Tinbergen (1972). Compensation is achieved by alternating between the observables faster than any time varying atmospheric

effects (i.e. at frequencies of 10 Hz to 50 kHz). With the use of modern phase sensitive (lock-in) detectors and high speed synchronous counting systems these polarimeters are indeed capable of very high precision. However, these systems are quite expensive to construct initially, especially if two spectral regions are to be observed, using a double-beam analyser, due to the doubling of the electronics. Further, with the exception of the Dollfus-type modulator, all of these instruments are intrinsically non-achromatic.

An alternative method of obtaining partial compensation has been suggested by Clarke and Ibbett (1968). In this technique separate intensity measurements are made at discrete positions of a phase plate (which could be achromatic) and the counts integrated into separate channels. Frequency components higher than 1 Hz in the noise are easily averaged over a period of a few seconds and the effect of longer term, quasi-periodic transparency drifts and secular changes in extinction are minimised by cyclic chopping of the set positions of the phase plate and channelling of the output signal. For three set positions of the phase plate, the first cycle is completed in typically less than 10 seconds. This is a hybrid method which bears similarities to a very slow AC mode and to a fast DC mode using pulse counting.

The method just outlined has the rather attractive feature of being inexpensive since the necessary electronics is reduced to simple scalers, one for each channel. Clarke has shown the method to be capable of smoothing scintillation, except at very low altitudes, and also capable of reducing systematic errors due to signal level changes arising from slowly varying haze and thin cirrus cloud (meteorological phenomena). However, the technique has not been applied to the measurement of stellar polarization, at least not to the very high precision required to detect differential linear

THE PRISM IS MADE FROM TWO PIECES OF A BIREFRINGENT MATERIAL (CALCITE), SEE CLARKE AND GRAINGER (1971).

BEAM 2

Polarizing Axes (parallel to edges of prism)

BEAM 1

45°

Double-Beam Polarizing Prism
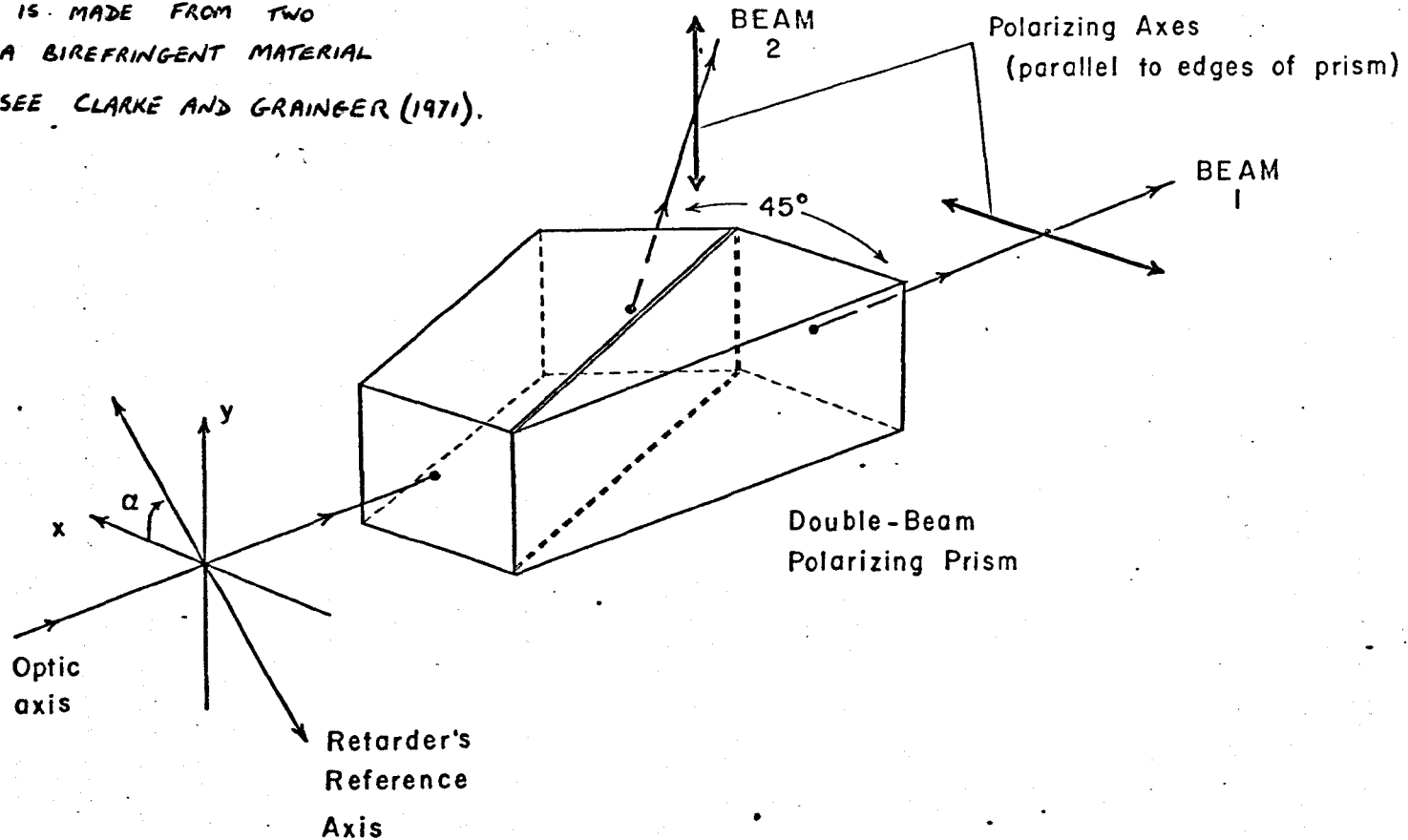
y

α

x

Optic axis

Retarder's Reference Axis

Fig. 2.3 Double-beam polarizing prism giving a 45° separation of the orthogonally polarized components. The polarizing axis of Beam 1 is used to define the x-axis of a right-handed Cartesian coordinate system with positive z-axis along the direction of propagation of the incoming light.

and circular polarization effects, across stellar line profiles.

Because of the simplicity, low cost, reasonable smoothing of atmospheric effects, the possibility of monitoring two wavelength passbands and, with suitable choice of the set positions of the phase plate, easy presentation of the Stokes parameters, Clarke's method has been adopted.

For the prototype instrument a mica half-wave plate was used prior to the fixed double-beam linear polarizer illustrated schematically in Fig. 2.3. A simple half-wave plate, for wavelength λ, is useful over a range of approximately 300 $\overset{o}{A}$ about λ without serious error arising from departure from a retardation of π. The operation of this combination as a narrow band linear polarimeter is easily described by the Stokes vector representation of partially polarized light and the Mueller matrix calculus; introductions to these mathematical formulations and further references may be found in the following books, Clarke and Grainger (1971), Shurcliff (1962) and Van de Hulst (1957).

When coherence properties are not of importance, the intensity and state of polarization of a light beam can be completely described by a set of 4 scalars, all of dimension intensity. These are called the Stokes parameters, denoted by I, Q, U and V. I represents total intensity, Q and U the two components of the linear polarization, and V the circular polarization. Q and U are related to the linear polarization intensity $I_p = pI$, where p = the degree of linear polarization, and the position angle or azimuth (Θ) of the major axis of the polarization ellipse by: $Q = I_p \cos 2\Theta$, $U = I_p \sin 2\Theta$ (see Polarimetric Units and Definitions). The fact that radiation cannot be more than 100 per cent polarized is expressed by $I \geq \sqrt{Q^2 + U^2 + V^2}$. In astronomy, the angle Θ is conventionally measured counterclockwise from the direction of the northern celestial pole in the

equatorial co-ordinate system. The effect of an optical component on the light beam is represented by a linear transformation of the Stokes parameters. If the Stokes parameters are written as a 4-vector, the optical component is represented by a 4 x 4 matrix:

$$
\begin{bmatrix} I \\ Q \\ U \\ V \end{bmatrix}_{out} = \begin{bmatrix} m_{11} & m_{12} & m_{13} & m_{14} \\ m_{21} & m_{22} & m_{23} & m_{24} \\ m_{31} & m_{32} & m_{33} & m_{34} \\ m_{41} & m_{42} & m_{43} & m_{44} \end{bmatrix} \cdot \begin{bmatrix} I \\ Q \\ U \\ V \end{bmatrix}_{in}
$$

Various useful Mueller matrices are summarised in Appendix I.

A natural Cartesian co-ordinate system for describing the new polarimeter is already provided by the double-beam polarizer (see diagram). The matrix of an ideal half-wave plate with its reference axis at an angle α with respect to the positive x-axis is given by

$$
\begin{bmatrix} R \end{bmatrix} = \begin{bmatrix} 1 & 0 & 0 & 0 \\ 0 & C & S & 0 \\ 0 & S & -C & 0 \\ 0 & 0 & 0 & -1 \end{bmatrix}
$$

where $C = \cos 4\alpha$ and $S = \sin 4\alpha$.

The half-wave plate/ideal linear polarizer combination is given by the product matrix $\begin{bmatrix} M \end{bmatrix}$ where,

$$
\begin{bmatrix} M \end{bmatrix} = \begin{bmatrix} P \end{bmatrix}\begin{bmatrix} R \end{bmatrix} = \frac{1}{2} \begin{bmatrix} 1 & \pm1 & 0 & 0 \\ \pm1 & 1 & 0 & 0 \\ 0 & 0 & 0 & 0 \\ 0 & 0 & 0 & 0 \end{bmatrix} \begin{bmatrix} 1 & 0 & 0 & 0 \\ 0 & C & S & 0 \\ 0 & S & -C & 0 \\ 0 & 0 & 0 & -1 \end{bmatrix}
$$

i.e.

$$\left[M \right] = \begin{bmatrix} 1 & \pm C & \pm S & 0 \\ \pm 1 & C & S & 0 \\ 0 & 0 & 0 & 0 \\ 0 & 0 & 0 & 0 \end{bmatrix} \qquad \left\{ \begin{array}{l} + \mathbin{/\!/} \text{x-axis} \\ - \mathbin{/\!/} \text{y-axis} \end{array} \right.$$

The emergent Stokes vector therefore has the form,

$$\begin{bmatrix} I' \\ Q' \\ U' \\ V' \end{bmatrix} = \frac{1}{2} \begin{bmatrix} I \pm Q \cos 4\alpha \pm U \sin 4\alpha \\ \pm I + Q \cos 4\alpha + U \sin 4\alpha \\ 0 \\ 0 \end{bmatrix}$$

thus, the output light is completely (i.e. 100 per cent) linearly polarized along the mutually orthogonal axes of the double-beam analyser, independent of α, while the intensity I' can clearly be modulated according to known values of α to obtain Q and U. Note that the V parameter is not involved.

In terms of the measured signal (number of counts) the final expression is

$$N (\alpha) = \frac{1}{2} G (I \pm Q \cos 4\alpha \pm U \sin 4\alpha) \qquad (1)$$

where the + sign refers to Beam 1 and the - sign to Beam 2 (the beam deviated by 45°) of the analyser. G/2 is the instrument's response to unpolarized light of unit intensity.

Although there are only two unknowns of polarimetric interest in the above equation, viz., the normalised Stokes parameters Q/I and U/I, at least three measurements must be made in order to eliminate the factor GI/2. Various possible values of α can be combined to reclaim Q/I, U/I. In fact, for the work presented in this thesis two methods have been tried, viz., Fessenkov's method and the Stokes Parameter Method. Both methods are outlined below with reasons for preferring the latter.

FESSENKOV'S METHOD

Intensity measurements are required at angular settings of the half-wave plate separated by $30°$ or its equivalent (e.g. $120°$). If N_1, N_2 and N_3 correspond to the set of intensity measurements, taken in equal time intervals, then the degree of polarization is given by (see Clarke and Grainger, 1971),

$$p = 2 \frac{\{N_1(N_1 - N_2) + N_2(N_2 - N_3) + N_3(N_3 - N_1)\}^{\frac{1}{2}}}{N_1 + N_2 + N_3}$$

and the position angle (or azimuth) of the direction of vibration relative to the angular position of the first intensity measurement is given by

$$\tan 2\theta = \frac{\sqrt{3}\,(N_3 - N_2)}{2N_1 - N_2 - N_3} .$$

When the degree of polarization is small then $N_1 \simeq N_2 \simeq N_3 = N_0$ say, the error in the degree of polarization can then be written as,

$$\Delta p = \sqrt{\frac{2}{3}} \frac{\Delta N_0}{N_0} .$$

For photon limited intensities, $\Delta N_0 = \sqrt{N_0}$, or in terms of the <u>total</u> integration time t and mean count rate $n*$, $N_0 \simeq \frac{1}{3}n*t \equiv \frac{1}{3}N$, where N = total count,

$$\therefore \Delta p = \sqrt{\frac{2}{n*t}} = \sqrt{\frac{2}{N}} .$$

It is apparent from the above formula, applying to small p, (≤ 0.01, i.e. ≤ 1 per cent) that $N^{-\frac{1}{2}}$ must be less than or equal to $p/3\sqrt{2}$ to allow the mean value of the measured polarization to exceed the mean error by a factor 3 (3 σ criterion, where σ is the standard error of the mean). For example, for p = 0.01, $N^{-\frac{1}{2}}$ must be approximately 0.0025, i.e. we require 0.25 per cent photometry.

The main drawback with this sequence of positions of the half-wave plate

is that the counts in the three channels bear little direct relation to the Stokes parameters, making casual inspection of the data awkward. Also, for a double-beam analyser, six separate counting channels are required and although this is still a simple and cheap proposition the next method to be described uses only four scalers and most important of all, is readily adapted to the measurement of circular polarization.

STOKES PARAMETER METHOD

Returning to equation (1), viz.,

$$N(\alpha) = \frac{1}{2} G (I \pm Q \cos 4\alpha \pm U \sin 4\alpha) \qquad \begin{array}{l} \text{Beam 1: } + \\ \text{Beam 2: } - \end{array}$$

and setting $\alpha = 0°$, $45°$ $(\pi/4)$, respectively gives

$$N(0) = \frac{1}{2} GI (1 \pm Q/I) : N(\pi/4) = \frac{1}{2} GI (1 \mp Q/I)$$

from which we get

$$\frac{Q}{I} = \frac{N(0) - N(\pi/4)}{N(0) + N(\pi/4)} \qquad \text{for Beam 1,}$$

$$\text{and} \quad \frac{Q}{I} = \frac{N(\pi/4) - N(0)}{N(0) + N(\pi/4)} \qquad \text{for Beam 2.}$$

Similarly, for $\alpha = \pi/8$, $3\pi/8$

$$\frac{U}{I} = \pm \frac{N(\pi/8) - N(3\pi/8)}{N(\pi/8) + N(3\pi/8)} \qquad \begin{array}{l} \text{Beam 1: } + \\ \text{Beam 2: } - \end{array}$$

Again, N can be understood as the number of counted photoelectrons. For small polarization $N(\alpha) \simeq \frac{1}{4} n*t$, where t is the total integration time. Assuming photon limited measurements describable by Poisson statistics, the mean error in each of the normalised Stokes parameters $p_x = Q/I$ and $p_y = U/I$ is easily derived to be

$$\Delta p_x = \sqrt{\frac{4\, N(0)\, N(\pi/4)}{(N(0) + N(\pi/4))^3}} \qquad \text{and} \qquad \Delta p_y = \sqrt{\frac{4N(\pi/8)\, N(3\pi/8)}{(N(\pi/8) + N(3\pi/8))^3}}$$

which, for small degrees of polarization, reduces to $\Delta p_x = \Delta p_y = (2/n*t)^{\frac{1}{2}}$, as expected.

Let $\varepsilon = (2/n*t)^{\frac{1}{2}}$.

The degree of polarization is $p = \left\{ p_x^2 + p_y^2 \right\}^{\frac{1}{2}}$ and the position angle is $\Theta = \frac{1}{2} \arctan (p_y/p_x)$, relative to the x-axis of the polarizer. The mean errors can be shown to be

$$\Delta p = \frac{1}{p} \left\{ p_x^2 \Delta p_x^2 + p_y^2 \Delta p_y^2 \right\}^{\frac{1}{2}} \simeq \varepsilon \quad \text{for } p \ll 1.00$$

and photon limited counts.

$$\Delta \Theta = \frac{p_x p_y}{2p^2} \left\{ \left(\frac{\Delta p_x}{p_x}\right)^2 + \left(\frac{\Delta p_y}{p_y}\right)^2 \right\}^{\frac{1}{2}} \simeq 28\overset{\circ}{.}65 \frac{\varepsilon}{p} , \quad \varepsilon \ll p .$$

Only two measurements are required to determine each Stokes parameter, and an obvious and simple way to utilise this technique is to employ the same pair of counting channels for each observation, i.e. record the Stokes parameters sequentially but within a very short time of each other. The electronic control system described in the next chapter is designed to enable intensity measurements to be taken at two click-stop positions of the half-wave plate, the counts being accumulated in two scalers, the values are printed out and the two new settings of the half-wave plate selected. The new counts are recorded in the same two scalers (which have been reset, of course) and finally printed out. It is not very difficult to make this entire sequence fully automatic.

Apart from the saving in equipment and the convenient display, the Stokes parameter method can be easily adapted to the measurement of the fourth parameter V/I which describes the circular polarization component of the light.

Consider the Mueller matrix of an ideal quarter-wave retarder oriented at $\pm 45^{\circ}$ with respect to the x-axis of the polarizer and placed in the

polarimeter prior to the half-wave plate; the Stokes Vector of the emergent beam is given by the product,

$$
\begin{bmatrix} 1 & 0 & 0 & 0 \\ 0 & 0 & 0 & \mp 1 \\ 0 & 0 & 1 & 0 \\ 0 & \pm 1 & 0 & 0 \end{bmatrix} \begin{bmatrix} I \\ Q \\ U \\ V \end{bmatrix} = \begin{bmatrix} I \\ \mp V \\ U \\ \pm Q \end{bmatrix}
$$

in words, the circular polarization component has been converted into a component of the linear polarization which can now be measured by setting the half-wave plate sequentially to 0° and 45°. The degree of circular polarization is simply given by

$$
q = \frac{V}{I} = \mp \frac{N'(0) - N'(\pi/4)}{N'(0) + N'(\pi/4)}
$$

where the $-$ sign applies to the case of the quarter-wave plate oriented at $+ 45^{\circ}$. Beam 2 of the polarimeter gives the negative of the value derived from Beam 1 if the counts (N') are subtracted in the same order as for Beam 1. Which orientation of the quarter-wave plate is involved can be determined empirically by measuring a laboratory lamp whose light has been circularly polarized with HNCP polaroid of known handedness. A more fundamental method will be described in Chapter 3.

Therefore, at least in principle, the Stokes Parameter method gives a very simple way of measuring all the Stokes parameters describing the polarization state of the incident light. Before going on to describe the instrumentation, some possible sources of systematic error in the polarimeter, arising from the non-ideal nature of some of the components, will be discussed.

2.6 Possible Sources of Systematic Error; Non-Ideal Polarimetric Elements

Firstly, consider again the ideal form of the intensity transmitted by a half-wave plate and double-beam analyser, viz.,

$$N(\alpha) = \frac{1}{2}G(I \pm Q \cos 4\alpha \pm U \sin 4\alpha)$$

If the initial angular setting of the half-wave plate is α_o instead of 0° and we define

$$(p_x)_a = \pm \frac{N(\alpha_o) - N(\alpha_o + \pi/4)}{N(\alpha_o) + N(\alpha_o + \pi/4)} \quad \text{etc.,}$$

then the normalised Stokes parameters referred to the frame of reference of the double-beam analyser are related to these apparent values (suffix a) by

$$\begin{bmatrix} (p_x)_a \\ (p_y)_a \end{bmatrix} = \begin{bmatrix} \pm \cos 4\alpha_o & \pm \sin 4\alpha_o \\ \mp \sin 4\alpha_o & \mp \cos 4\alpha_o \end{bmatrix} \begin{bmatrix} p_x \\ p_y \end{bmatrix}$$

Thus the degree of polarization $p = \left\{ p_x^2 + p_y^2 \right\}^{\frac{1}{2}} = \left\{ (p_x)_a^2 + (p_y)_a^2 \right\}^{\frac{1}{2}}$ is unaffected while the azimuth is rotated through $4\alpha_o$ from the analyser's frame of reference.

For the measurement of circular polarization the emergent intensity relation with the quarter-wave plate inserted at $+ 45^o$ was,

$$N'(\alpha) = \frac{1}{2}G(I \mp V \cos 4\alpha \pm U \sin 4\alpha)$$

and now, if the starting value of α is α_o (radians) we have,

$$q_a = \mp q \cos 4\alpha_o \pm p_y \sin 4\alpha_o \simeq \mp q \pm 4 p_y \alpha_o$$

for $\alpha_o \simeq 0$. In this case it is therefore important to ensure that α_o is very small, especially in the presence of a strong linear polarization component in the light. The effect described here is essentially linear-to-circular conversion (LCC). However, for small α_o this problem can be vir-

tually eliminated by one of two methods; (i) orientate the polarimeter such that the Stokes parameter $p_y = U/I$ is identically zero. Of course, this requires that the linear polarization component of the light be known or measured before the circular component. Case (ii), repeat the circular polarization measurement with the entire polarimeter rotated through $90°$ about the optical axis. By this procedure the sign of the linear Stokes parameter p_y is reversed while the true fractional circular polarization q is unaffected.

Linear-to-circular conversion can also arise if the quarter-wave plate is incorrectly set. Suppose that, relative to the ideal half-wave plate and double-beam analyser combination, the quarter-wave plate is oriented at an angle of $\pi/4 + \delta$, where δ is small. The intensity transmitted is approximately,

$$N(\alpha) = \tfrac{1}{2}G\left\{I \mp (V \pm 2U\delta)\cos 4\alpha \pm (U \mp 2Q\delta \mp 2V\delta)\sin 4\alpha\right\} .$$

The apparent fourth Stokes parameter derived from the counts in the usual way is

$$q_a = \mp \frac{N(0) - N(\pi/4)}{N(0) + N(\pi/4)}$$

and this is related to the real value of the fractional circular polarization, q, by

$$q_a = \mp q \mp 2p_y\delta .$$

It is not difficult to make $\delta \simeq 0.1°$ (~1/570 rads). However, the same measurement procedures as outlined above can be utilised to remove the LCC component.

Lastly, re-writing the expression for the intensity transmitted by a half-wave plate and double-beam analyser for the case when the analyser is

not ideal gives

$$N(\alpha) = \frac{1}{2}G(K_1 + K_2) \left\{ I \pm \left(\frac{1-\epsilon}{1+\epsilon}\right) \left(Q \cos 4\alpha + U \sin 4\alpha\right) \right\}$$

where $\epsilon = K_2/K_1$ and K_1 and K_2 are the intensity transmission coefficients for the analyser. For an ideal linear polarizer $K_2 = 0$, $K_1 = 1$. If the analyser is nearly perfect then $\epsilon \ll 1$, in which case

$$N(\alpha) \simeq \frac{1}{2}G(K_1 + K_2) \left\{ I \pm (1 - 2\epsilon) (Q \cos 4\alpha + U \sin 4\alpha) \right\}$$

Letting $(p_x)_a$ etc., stand for the apparent normalised Stokes parameters derived from the observed counts in the usual way then, $(p_x)_a = (1 - 2\epsilon) p_x$ and $(p_y)_a = (1 - 2\epsilon) p_y$ and, in fact, $p_a = p - 2\epsilon p$. The effect is simply to underestimate the degree of polarization without affecting the azimuth of vibration. Measurements with Polaroid pieces and on stars of known polarization indicate $\epsilon \lesssim 0.01$ for both beams. However, a less obvious consequence of an imperfect fixed analyser is that the radiation falling on the photocathode is now elliptically polarized and the azimuth of the ellipse oscillates slightly as a function of the half-wave plate orientation α. This may also introduce a small systematic error in the measured polarization. Some of these relations will be referred to again in subsequent chapters.

The remainder of the thesis is concerned with the description and application of a prototype, twin narrow band spectropolarimeter designed for exploratory work on polarization effects across the Hβ line profile. Specifically, in Chapter 3 an account of the several stages in the development of this instrument is given (more or less in chronological order to indicate how experience with the scanning system was acquired and new electronics developed). Sufficiently detailed coverage of the electronic control system is included and various calibrations and preliminary tests are also presented.

3. AN AUTOMATIC TWIN Hβ-SPECTROPOLARIMETER

3.1 Introduction

At the beginning of this study, in October 1971, a very basic photo-electric double-beam polarimeter incorporating a tilting interference filter, with a 2.5 Å passband and a normal incidence wavelength of 4872 Å, was already under construction at the Glasgow University Observatory. The only half-wave plate available for use with this instrument at that time was centred at λ = 5461 Å and was hand rotatable. After aligning the optics, some simple experiments using a D.C. amplifier and pen-recorder were carried out to determine if placing the filter prior to the half-wave plate introduced parasitic polarization. In this position, tilting the filter did seem to distort the instrumental polarization and so the filter was eventually placed behind the double-beam polarizer to yield two independent single-beam polarimeters as proposed in Chapter 2.

Before describing the development and layout of the polarimeter a discussion of the filter-tilting scanning monochromator is given.

3.2 The Hβ-Scanning Monochromator

A schematic layout of the polarimeter at this stage is shown in Fig. 3.1. When the half-wave plate is removed the instrument becomes a simple scanning monochromator, in this case, for the Hβ line profile. An eyepiece was occasionally used in Beam 2 for guiding purposes. The double-beam polarizer prism has already been described (see Fig. 2.3). It is a variant of the Foster (1938) design and although this type of prism is generally regarded as not being completely free from cross-talk between the beams it does allow a simpler and more compact optical design than a Wollaston prism and was already available at the Glasgow Observatory.
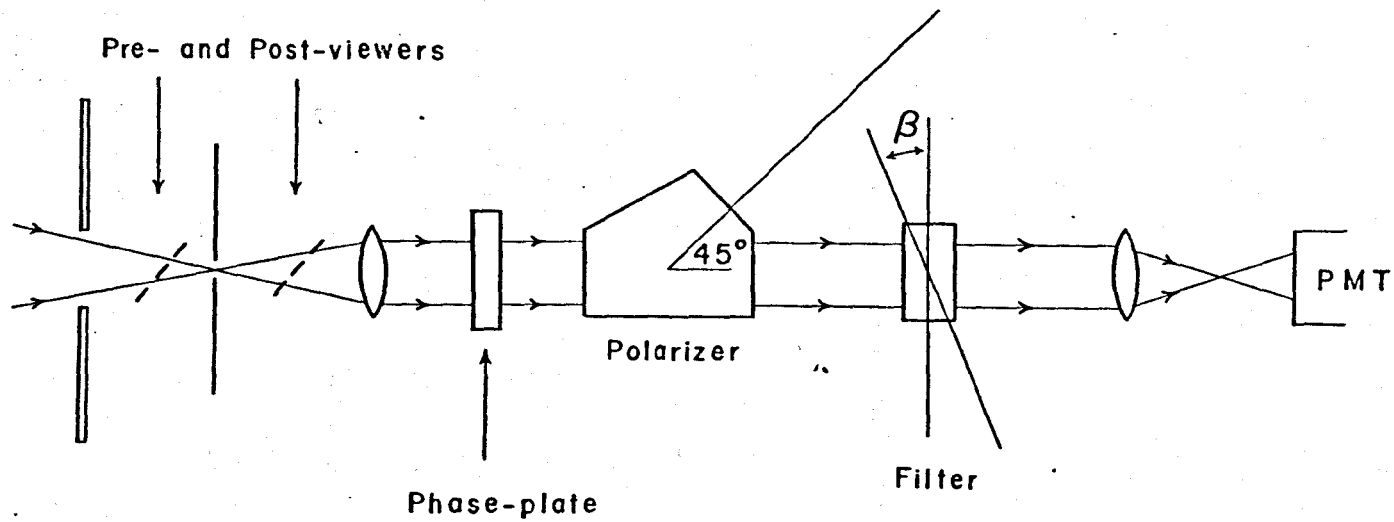
Fig. 3.1   Schematic layout of tilting-filter spectropolarimeter. An eyepiece or a second filter can be placed in the 45° beam. The angle of tilt (β) of the narrow band interference filter is shown, and the photomultiplier tube is indicated by PMT.

The filter itself is circular (25 mm diameter) and is mounted in a frame attached to a spindle set in a ball race. A lever arm is connected to this spindle, enabling the filter to be tilt-scanned by driving a micrometer against the arm. Return scans are achieved by tension in the coupling spring between the lever arm and the fixed micrometer mounting. By design, the angle of tilt (β) is related to the micrometer reading (x) by

$$\sin \beta = k(x - x_0) \qquad (1)$$

x_0 being the reading of the micrometer when the filter is at normal incidence and k is a factor related to the dimensions of the lever and micrometer scale.

Figure 3.2 shows the normalised signals as a function of micrometer setting for scans with the 2.5 Å filter of a hydrogen lamp (Hβ) and a zinc lamp (λ 4810.5 Å) taken in the laboratory, the peak for the latter line corresponding to a filter-tilt of about 12°. Since the wavelength passed at normal incidence is close to 4872 Å, a tilt from 0° to 12° corresponds to a scan of about 60 Å. It will be noted that at the wavelength of the zinc line, both the position of the filter passband and the halfwidth are just seen to be dependent on the direction of vibration of the polarized light.

Wavelength calibration can be applied by observing laboratory spectrum lamps. Combining equation (1) and the expression $\lambda = \lambda_0 \{1 - C\beta^2\}$ we have

$$\lambda = \lambda_0 \left\{ 1 - C \left[\sin^{-1} k(x - x_0) \right]^2 \right\} \qquad (2)$$

If k is assumed known from the design, equation (2) contains three unknowns: x_0, λ_0 and C. However, only two calibration spectral lines are required within the scanning range, as the position of normal incidence on the micrometer scale (x_0) is easily obtained by scanning one spectral line on both sides of normal incidence. The two remaining unknowns can be ob-
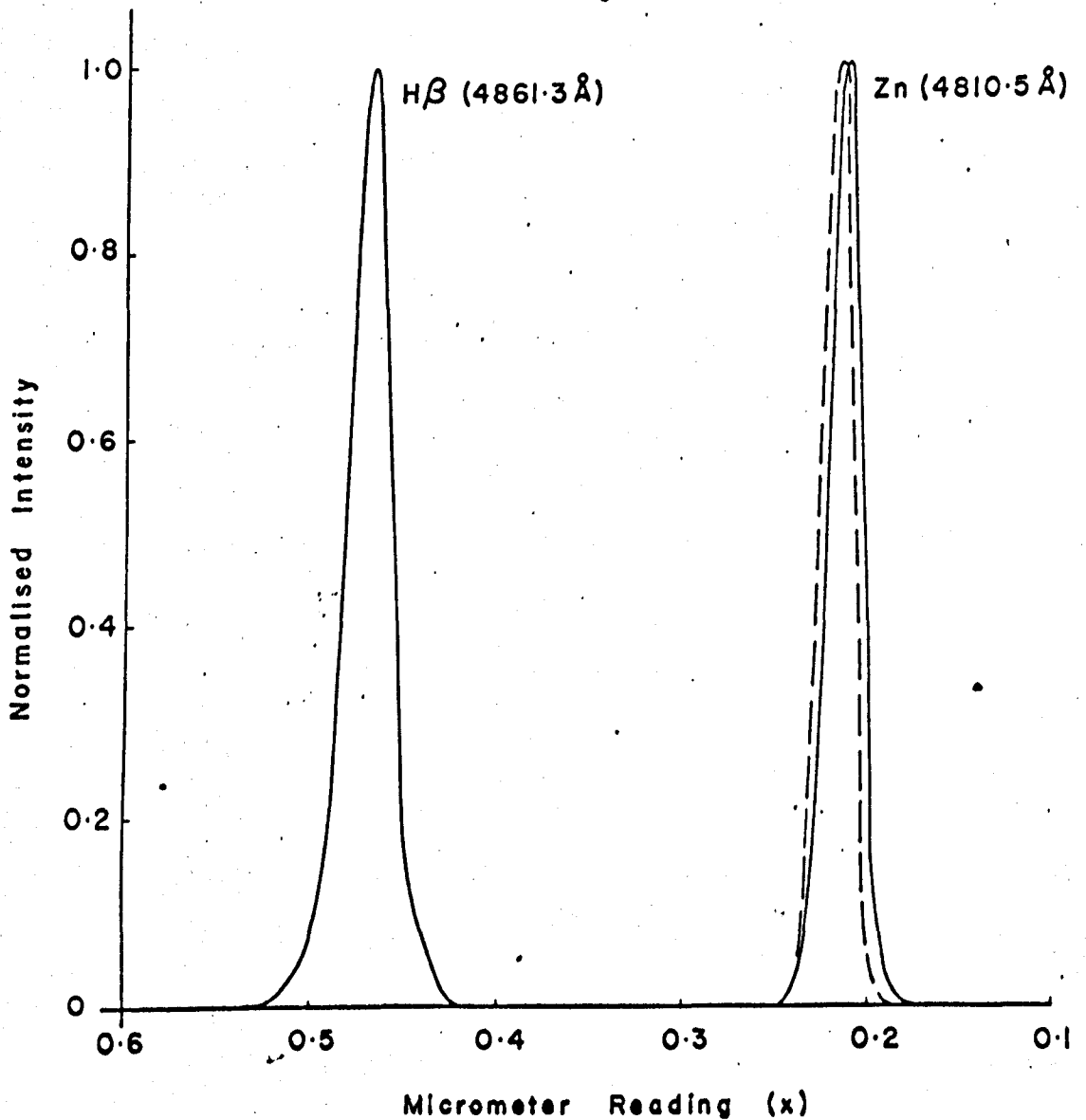
Fig. 3.2 Hβ tilt scans with a 2.5 Å filter of laboratory lamps (hydrogen and zinc), with normalised signal levels plotted against the micrometer reading. The separation of the passbands with direction of vibration of polarized light is just visible for the zinc line. The profile for the component polarized perpendicular to the plane of incidence is drawn dashed.

tained by recording the micrometer positions corresponding to the peak transmissions for the two spectral lines. Wavelength calibration curves for a particular temperature for the two directions of vibration of polarized light are displayed in Fig. 3.3. As anticipated, the calibration curve was found to be slightly dependent on temperature. In order to obtain reliable spectrophotometry, it may be necessary to provide a thermostated enclosure for the filter. However, since on-the-telescope calibration is easy in the final version of the polarimeter (Section 3.4) and the wavelength settings are always made empirically, by scanning the stellar Hβ line for example, temperature stabilization has not been included.

With the aid of the wavelength/tilt calibration curve it is possible to determine quantitatively first, the difference in the wavelength separation of the passbands according to the direction of vibration of polarized light and second, the broadening that the filter passband suffers with tilt.

At the extremity of our scanning range (the zinc line at λ 4810.5 $\overset{\circ}{A}$) the position of the passband shifts by less than 1 $\overset{\circ}{A}$ according to the direction of the vibration, the perpendicular component providing a passband at a longer wavelength. Over the small angles of tilt necessary to record the majority of stellar line profiles, this splitting effect might be neglected, i.e. for ordinary spectrophotometry the monochromator may be used without a polarizer.

In considering the scans of laboratory spectral lines, it is assumed that the lines have negligible width, so that the recorded outputs essentially display the profile of the filter at the wavelength of the line.

Assuming the calibration light to be accurately focussed onto a small diaphragm at the focus of the collimating lens then, after applying the wavelength/tilt calibration, the halfwidth of the filter profile, nominally
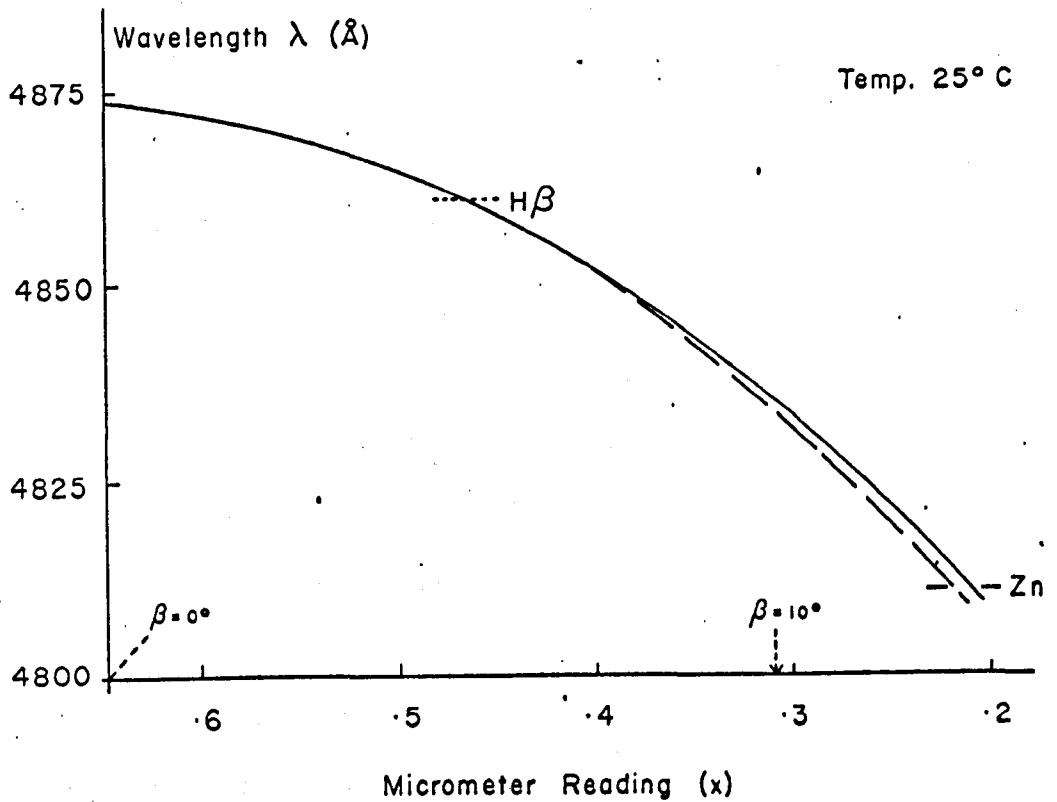
Fig. 3.3 Wavelength/tilt calibration curve, for a particular temperature, derived by application of equation (2). .Tilt is determined from micrometer displacements. The curve is illustrated for directions of vibration of polarized light parallel to and perpendicular to the plane of incidence. The latter component is indicated by the dashed curve.

2.2 Å at normal incidence (manufacturer's specification) increases to about 2.5 Å at 4861.3 (Hβ) and to about 3 Å at 4810.5 (Zn). If instead, divergent light is piped by fibre-optic tube to a diaphragm of larger aperture, a slightly greater rate of passband spread is noted but the relationship between λ and β is unaffected. At the extreme of the scan, the dependence on polarization of the passband halfwidth is just apparent, the difference being about 0.5 Å and the narrower profile corresponding to the component of polarization perpendicular to the plane of incidence.

Before any stellar observations are presented, a qualitative look is taken at the instrumental effects likely to distort the recorded profiles.

It is well known that the record from any scanning monochromator depends on the spectral feature being scanned and on the instrumental profile and halfwidth. In some studies the true spectral information is reclaimed when the instrumental properties are known.

With the tilting-filter instrument, the halfwidth is observed to increase by about 50 per cent over the complete scanning range. Over a typical broad absorption line the halfwidth changes from a value of 2 Å at one side of the line to 3 Å at the other. Now for such features, scans by instruments of 2 Å to 3 Å profile halfwidths would show little difference. Consequently, we would expect only slight distortions as a result of changes in halfwidth of this order during a scan.

In fact, experience has shown that useful scans of Hβ in early-type stars can also be achieved with filters of 10 Å halfwidth.

An increase in signal might be expected as the passband broadens. However, this effect is offset by the slightly more rapid decrease in the total transmittance of the filter with tilt. The systematic error intro-

duced into the photometry by the combined effect (approximately 5 per cent over a 35 Å scan) can be removed, if necessary, by using the monochromator to scan, for example, the continuous spectrum of a calibrated laboratory source.

From the above considerations and the results of the laboratory experiments it is concluded that it is possible to apply the tilting-filter technique to record broad stellar line profiles which, to a first approximation, would hardly be distorted. The results of preliminary observations are presented below.

Preliminary Line Profile Scans

Records of Hβ line profiles of different stars, taken by continuous scans with a D.C. amplifier and pen-recorder and with the instrument attached to the 50 cm telescope at Glasgow are reproduced in Figs. 3.4, 3.5 and 3.6. (Photocopies of the original tracings of these and other stars are contained in Appendix II). These curves are means, drawn by hand, through the noise on a single record. It will be remembered that these scans are not corrected for non-linearity in wavelength and that some distortion due to changes in instrumental halfwidth and changes in transmittance may be present. However, even at this stage there are apparent in the recorded profiles of stars, features which are dependent on spectral type and which clearly will not be removed by calibrations. For example, compare the scans of γ UMa (A0Vn), β Ori (B8Ia) and α Aur (G0III) (see Fig. 3.4).

In Fig. 3.5, scans of α Aur, of the blue sky and a rather simple simulated scan obtained by convoluting a region of the solar spectrum (Minnaert, 1940) around Hβ with a 2.5 Å wide rectangular instrumental function are compared. Although no spectrometer has such a rectangular profile, this very
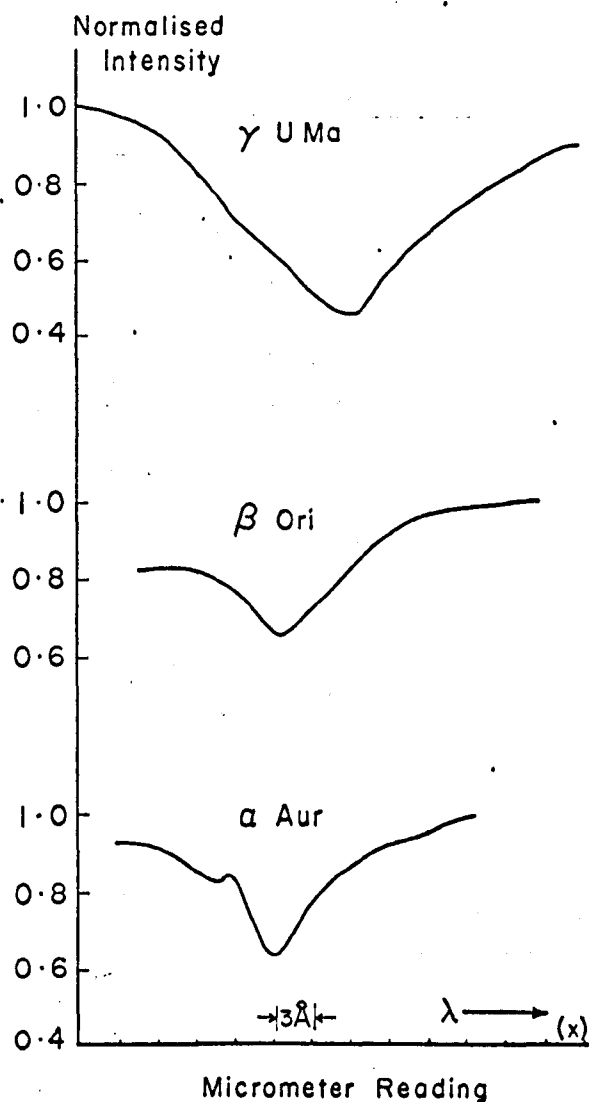
Fig. 3.4   Normalised records (2.5 Å resolution) of Hβ line profiles of
γ UMa (A0), β Ori (B8) and α Aur (G0) uncorrected for the non-
linearity of the wavelength scan.   The wavelength scale is in
arbitrary micrometer units.   Calibration marker pips are elec-
tronically imposed on the pen-recorder to facilitate subsequent
reduction.
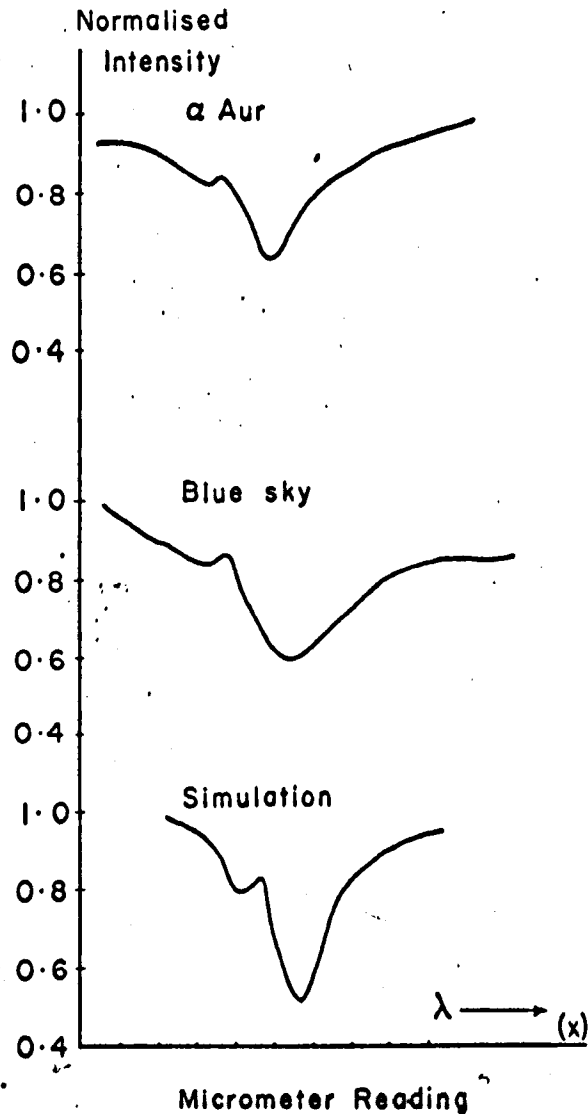
Fig. 3.5   Normalised records of Hβ line profiles of α Aur (G0) and the blue
           sky (Rayleigh scattered solar radiation (G2)). The bottom curve
           shows a simulated scan of the solar spectrum achieved by convolu-
           ting a high resolution spectrum (Minnaert atlas) with a 2.5 Å wide
           rectangular instrumental function. All spectra are displayed,
           with the non-linear wavelength scale of the instrument.

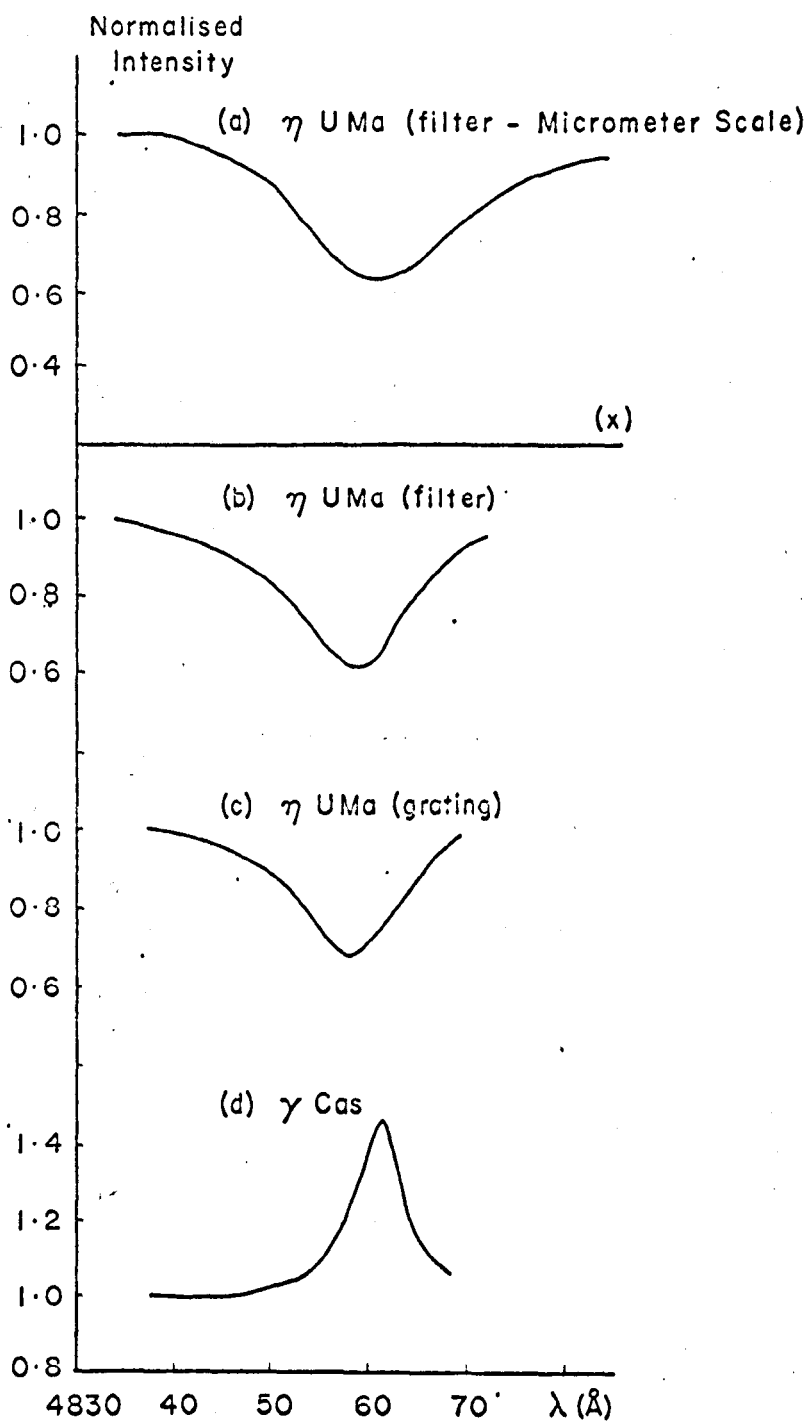Fig. 3.6   Figures 3.6(a) and 3.6(b) show the normalised records (2.5 Å
filter) of the Hβ line in η UMa (B3n) before and after calibra-
tion to a linear wavelength scale. A comparison record obtained
with a large photoelectric grating spectrometer and a larger
telescope aperture is reproduced in Fig. 3.6(c). For contrast,
the strong Hβ emission feature of γ Cas is also shown. The
wavelength scale commences at 4830 Å.

simplified instrumental function does successfully give a crude estimate of the profile obtained with a 2.5 Å filter. Except for the weak effect of Rayleigh scattering, scans of the blue sky (solar spectrum, G2) and of α Aur (GO III) are similar. Comparison with the derived convoluted scan shows that the scanning monochromator introduces remarkably little distortion to a recorded profile.

The effect of correcting the linear micrometer scale to a linear wavelength scale, by the wavelength/tilt calibration procedure described earlier, can be ascertained from Fig. 3.6 for the case of η UMa (B3n). Clearly, even before reduction to a linear wavelength scale, the recorded data gives a good indication of the shape of a line profile.

Without further reduction, the recorded Hβ profile of Fig. 3.6(b) compares extremely well with the profile of Fig. 3.6(c), recorded by a large photoelectric grating spectrometer attached to the 120 cm telescope at Asiago, Italy (~~Grainger and Ring, 1963~~ Clarke and Grainger, 1966). Because of the particularly poor seeing conditions prevailing on that occasion, the grating instrument was compelled to operate below its maximum resolution to enable the entire stellar seeing disc to be accepted. Sharply contrasting the wide, rotationally broadened profile of η UMa is the strong Hβ emission feature of the Be star γ Cas (Fig. 3.6(d)).

For the brighter stars the single channel line profile scans are not photon shot noise limited but rather are limited by scintillation noise and transparency changes occurring during the scans. The noise on the original records of the scans in Figs. 3.4, 3.5 and 3.6 is typically several per cent of the brightness level (see the next section and Appendix II). In the following section similar line profile scans are discussed with the instrument once again operating as a polarimeter.

3.3 Polarimetric Hβ Line Profile Scans

Polarimetry was initially performed by recording Hβ profiles by D.C. amplifier and pen-recorder at each of three positions of the half-wave plate separated by 120° (equivalent to 30° intervals). From the three intensities obtained at a given wavelength in the scan, the degree of polarization (p) and relative azimuth (θ) can be evaluated by Fessenkov's formula (see Section 2.5). However, although reasonable wavelength scans were obtained, transparency changes occurring during the time period ~~(~10 mins)~~ required (~10 mins) to record three line profile scans, limited the detectivity of polarization to about 2 - 3 per cent. Examples of actual pen-recorder tracings are shown in Figure 3.7. Therefore from the outset it was clear that, except under excellent transparency conditions, the polarimetry would have to be carried out quickly at each spectral point.

To achieve this the D.C. amplifier and pen-recorder were supplemented with a simple pulse counting system consisting of a commercial preamplifier, amplifier and discriminator followed by a six figure scaler/timer, of the writer's own design, employing cold-cathode neon tubes and TTL integrated circuit counters. A simple electronic gating system and timer allowed the signal to be counted for a preset time in the range 0 - 9 secs. The accumulated totals were then written down and the display cleared ready for re-starting. Meanwhile a companion observer rotated the half-wave plate through 120° to a new position and the count sequence was repeated. In this way the three intensities necessary for the Fessenkov method were obtained in about 15 - 30 secs at a discrete tilt/wavelength of the filter. The procedure was repeated many times at this wavelength to improve the mean value of p, before selecting another part of the line.

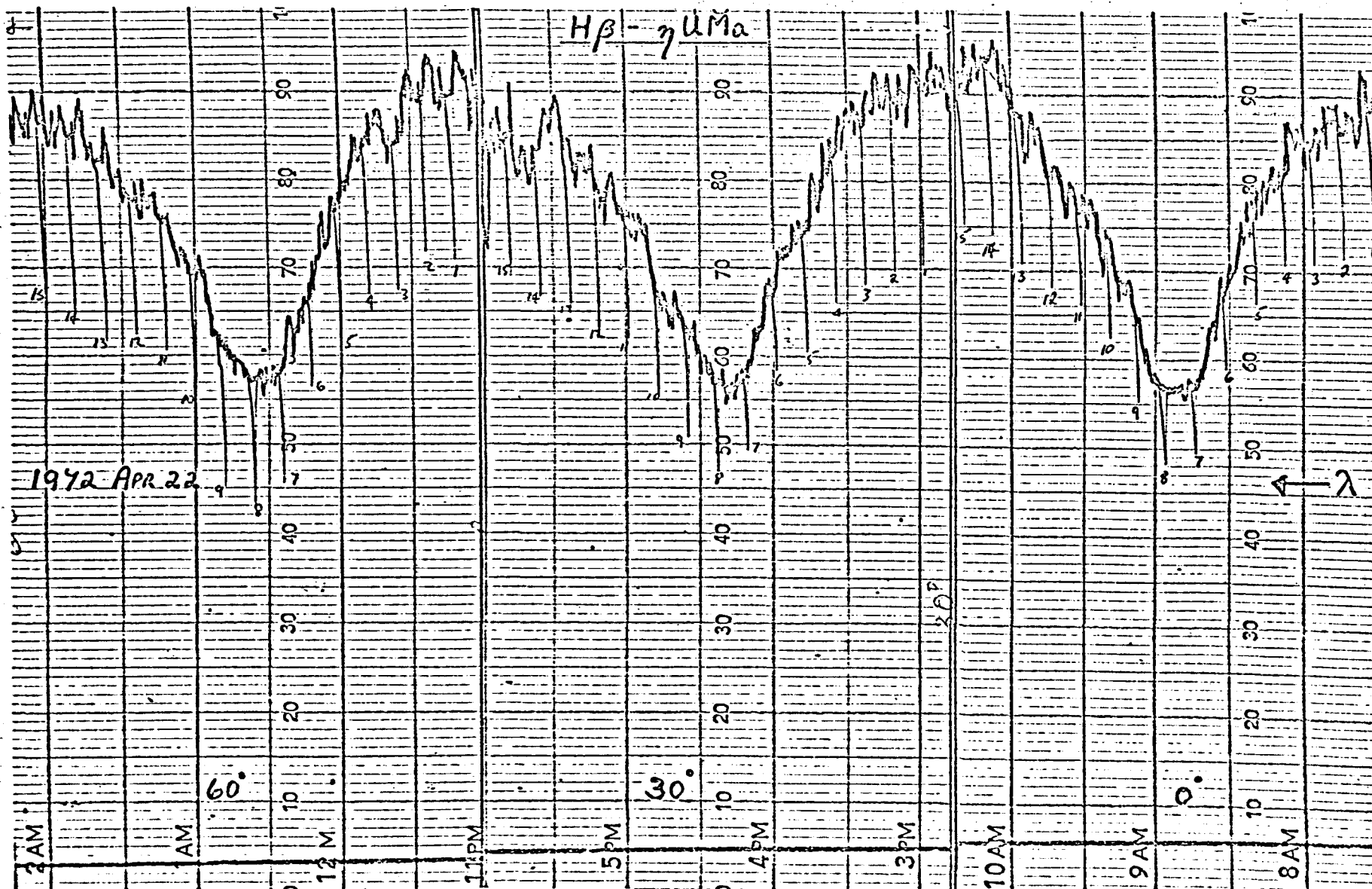To avoid the chore of recording the data by hand, and the associated

Fig. 3.7 Chart-recorder tracings (2.5 Å filter) of Hβ in η UMa, at three set positions (0°, 30° and 60°) of a half-wave plate relative to a fixed polarizer. Sharp vertical lines appearing in the profile are calibration marker pips electronically imposed each micrometer revolution.

time lag, an attempt was made to resurrect a 3-channel electronic system developed by Dr. Clarke some years previously and which employed a printer. Unfortunately this system, being out of regular use, was prone to mechanical failure of the printer. Nevertheless sufficient experience was gained with this system to establish that polarimetry by Clarke's slow chopping and integration method resulted in photon-limited polarimetry with a 2.5 Å passband filter and a 51 cm (20-inch) telescope.

To observe the effect of photon shot noise on the polarimetric data, it is convenient to evaluate the normalised Stokes parameters $p_x = Q/I$ and $p_y = U/I$ where,

$$p_x = p \cos 2\phi \quad \text{and} \quad p_y = p \sin 2\phi$$

where p is the degree of linear polarization and ϕ is the angle of the direction of vibration relative to the position of the first intensity measurement. When the light source is unpolarized and the instrumental polarization is zero, the average values for p_x and p_y over a very large number of measurements should then converge to zero. If the light source is unpolarized and p_x and p_y converge to constants, then these are the normalised Stokes parameters of the instrument (plus telescope) at the orientation and wavelength passband.

Pulse counting, single beam spectropolarimetric observations up to 1972 Oct 19 were made with relatively short integration times. Data taken at only two wavelength positions, corresponding to the centre of the line and a point in the continuum on the short wavelength (blue) side, were reported in a paper presented to IAU Colloquium No. 23 (1972), (Clarke and McLean, 1974a). These preliminary observations included the five stars listed in Table 3.1. Compared to results obtained later, the data shown in Table 3.1 is very poor and definitely indicates systematic instrumental polarization

Table 3.1   Preliminary observations of the normalised Stokes parameters p_x and p_y (in per cent) at the Hβ line and in the nearby continuum (1972 Oct 19)

Star	λ	p_x	p_y	Integ. Time (s)
α Lyr	Hβ	+ 0.41 ± 0.20	+ 0.82 ± 0.23	264
	cont.	− 0.05 ± 0.17	+ 0.44 ± 0.34	120
γ Cas [1]	Hβ	− 1.62 ± 0.37	+ 0.38 ± 0.44	216
	cont.	− 0.54 ± 0.46	+ 0.31 ± 0.57	120
ε Cas [2]	Hβ	− 0.77 ± 1.89	− 0.55 ± 0.73	144
	cont.	− 0.71 ± 0.89	+ 1.67 ± 0.72	120
γ UMa [3]	Hβ	− 0.49 ± 0.71	− 0.46 ± 1.06	240
	cont.	+ 0.12 ± 1.36	− 0.43 ± 0.44	96
ζ Ori	Hβ	− 0.77 ± 0.43	− 0.05 ± 0.56	288
	cont.	− 0.50 ± 0.27	+ 0.59 ± 0.38	288

NOTES: The errors have been obtained from repetitive measurements taken over 24 second periods and the total integration time and mean values of p_x, p_y built up from this series.

1   Well-known emission line variable star.

2   Listed by Tamburini and Thiessen (1961).

3   Listed by Clarke and Grainger (1966).

errors of about 1 per cent. However, the experience gained was sufficient to warrant the development of a new polarimetric system based on the same principles.

Beginning in the autumn of 1972, the design and construction of a new compact electronic control system for a twin narrow band polarimeter which would employ 4 set positions of a half-wave plate at angular intervals of $22\frac{1}{2}^{\circ}$ ($\pi/8$), was initiated; in practice, measurements are taken in pairs with angular separations of the half-wave plate equal to 45°, i.e. the Stokes Parameter Method (see Section 2.5). This system is simpler to construct electronically than a three-channel Fessenkov system and the pairs of intensities lead directly to the Stokes parameters. Several changes and additions were made to the original polarimeter described above, these and the final instrument are presented in the next section.

3.4 The Optical Arrangement of the Hβ-Spectropolarimeter

A cross-sectional view of the optical assembly of the final twin polarimeter is shown in Fig. 3.8. As before, the principal components are a collimating lens followed by a rotatable half-wave plate and a fixed double-beam polarizing prism giving a 45° separation of the outgoing beams. The instrument is shown attached to the Cassegrain focus of a telescope (usually the f/8, 51 cm Ritchey-Chrétien at Glasgow).

In the focal plane of the telescope is a two-position slide carrying a pair of different sized aperture stops. To enable the stellar image to be quickly centred in the aperture stop, two right angled prisms mounted in retractable tubes, with suitable eyepieces (e.g. Kellner x10), deflect the light beam by total internal reflection before and after the diaphragm holder. Variable illumination of the rear of the diaphragm (not shown in sketch) is provided by a miniature low voltage lamp.
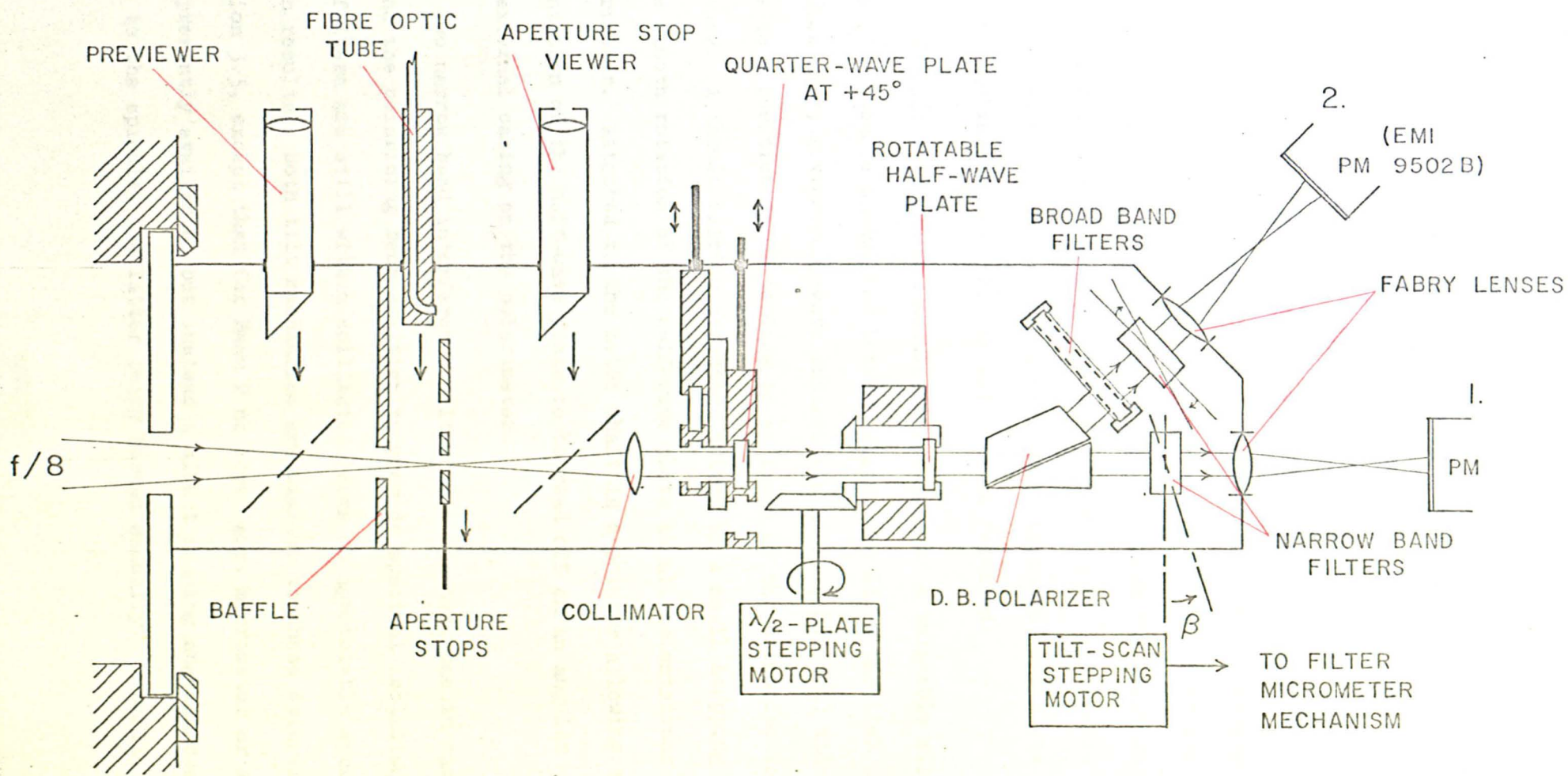
Fig. 3.8   Cross-sectional diagram of the final version of the twin Hβ-spectropolarimeter.   The photomultiplier tubes are indicated by PM.

Located very close to the diaphragm slide is a thin retractable pipe housing a fibre-optic tube the other end of which can be inserted into an aluminium box containing laboratory hydrogen and zinc lamps. The fibre-optic tubing is about 90 cm long and the unit containing the wavelength/tilt calibration lamps is easily made fast to the telescope near the polarimeter. This method for piping light to the polarimeter diaphragm does not simulate the telescope geometry and the beam incident on the interference filters is not well collimated. However, the technique allows the emission peaks of Hβ and the zinc line at λ 4810.5 $\overset{\circ}{A}$ (see Fig. 3.2) to be very easily and quickly correlated with the corresponding micrometer readings, while the polarimeter is on the telescope, and this is all that is required.

The basic polarization modulator consists of a rotatable mica phase plate (2 cm square sandwiched between glass, its edges parallel to the fast and slow axes) giving half-wave retardation at Hβ (4861.3 $\overset{\circ}{A}$) and mounted close to a position corresponding to an image of the telescope collecting aperture. A thrust bearing assembly, driven by a small stepping motor, ensures smooth rotation of the half-wave plate at all orientations of the polarimeter. Attached to the motor shaft is a pointer allowing the relative orientation of the half-wave plate to be read off on an angular scale on the external casing on the polarimeter.

Two narrow band interference filters are mounted, one in each beam, behind the polarizing beam splitter to provide spectral isolation. Since the filters are still within collimated beams no appreciable spread in bandwidth results. Both tilt mechanisms are similar to those described in Section 3.3, except that for Beam 2 no lever arm, micrometer or motor drive are presently available, but instead a direct reading angular scale is attached to the spindle, the latter being turned manually. A small, digitally

controlled stepping motor eventually replaced the synchronous motor drive system, originally used in conjunction with a pen-recorder, for line profile scanning. Two tilt mechanisms (lever arm type, direct tilt type) are available for each beam so that four filters can remain undisturbed in their mountings at any one time. Interchanging the pair of filters assigned to each beam is therefore a simple matter. Also available in one of the beams is a frame enabling 2" x 2" glass or gelatine filters to be inserted for broader passband measurements.

The last optical elements are two Fabry lenses. These lenses are fitted on the end faces of the instrument case and can be adjusted to transfer the image of the telescope collecting aperture onto the photocathodes of the photomultiplier tubes. For ease of transportation and interchanging of detectors, the photomultiplier housing, cooling jacket and preamplifier box were constructed as a single unit detachable from the end faces of the aluminium casing of the polarimeter.

It has already been shown in Section 2.5 that an ideal half-wave plate/ analyser combination does not modulate circularly polarized light, thus the instrument is essentially a linear polarimeter. To enable the measurement of the fourth Stokes parameter describing the circular polarization, a quarter-wave retarder for $H\beta$ with its reference axis at $+ 45°$ to the polarizing axis of Beam 1 (x-axis of system) must be inserted prior to the half-wave plate. To facilitate this, accurately machined two-position slides are located between the collimating lens and the half-wave plate. In one position, a quarter-wave plate can be set accurately parallel to the x-axis while in the second position it can be oriented at $+ 45°$. Usually, the second position is chosen $(+45°)$ and the other is left empty so that the instrument can be converted to a circular polarimeter by simply pushing in this slide to its

second position. Another identical slide, adjacent to the first, allows additional phase plates or calibration polarizers to be inserted easily.

The polarimeter casing itself is a jointed box machined from aluminium plate and therefore free from flexure; it is completely demountable. One face of the casing is detachable, giving access to the optical components for levelling and other adjustments. The overall length of the spectropolarimeter is 80 cm (31.5 ins) and it weighs approximately 18 kg (40 lbs).

3.5 Electronic Control System and Operational Modes

Having decided to concentrate the initial polarimetric investigations on the Hβ line, blue sensitive EMI 9502 B (S11 cathode) photomultiplier tubes were used. These are high gain devices with quantum efficiencies about 14 per cent near Hβ. Commercial preamplifiers were adapted for use with fast pulse counting by inserting a 680 Ω leakage resistor across the input to earth. With a 50 Ω coaxial line this arrangement gave negative pulses of ∼ 1.5 V peak. By suitably reverse terminating the line, a small linear integrated circuit (μA 710) wired as a pulse height discriminator also acted as line receiver. This device has a TTL* compatible output but the output pulse width is dependent on the time for which the input pulse exceeds the applied reference voltage. To standardise the pulse width the output from the μA 710 is fed directly to the Schmitt trigger input of a SN 74121 TTL monostable integrated circuit with a time constant of 100 ns. Both devices were mounted very close to the TTL counting circuitry. The bandwidth of the electronic system is about 1 - 10 MHz and is limited by the preamplifier, i.e. for average count rates $\gtrsim$ 1 MHz counting losses and non-linearity in gain are serious.

In practice, an average count rate of 5 x 10^5 counts per second was only rarely encountered (m_v = 0.0, Δλ = 10 Å, D = 91 cm) because of the

* TTL means Transistor Transistor Logic

narrow passbands involved. To enable the handling of higher count rates associated with use of the polarimeter on larger collectors, it will be necessary to employ a pulse counting system with a wider electronic bandwidth.

A block diagram of the entire polarimetric system is shown in Fig. 3.9. Note that each beam is provided with only two counting channels although four intensity measurements are required for a determination of the degree of linear polarization, p, and the azimuth, θ. The system is designed to measure the Stokes parameters one at a time. Each counting channel pre-scales by a factor 10 and has a five figure digital display employing cold cathode number tubes ("Nixies"). The counts from each channel (two per beam) are transferred in Binary Coded Decimal form to a 21 column, parallel input, digital printer. Electronically, Beam 2 is an exact replica of Beam 1.

Starting with the half-wave plate at some angular setting α, relative to the usual axes, the count sequence is initiated, enabling the standardised pulses originating from the two photomultipliers to enter independent count-ing channels for a preset time T. At the end of this time interval, the counters are inhibited and the stepping motor turns the half-wave plate through $45°$ ($7°5$ per step) to a new "click-stop" position ($\alpha + \pi/4$).

The step pulses are counted and the sixth pulse triggers a delayed auto-matic restart signal to the timer, but now the detector output pulses are fed into a second pair of independent counters. At the end of T seconds, the stepping motor returns the half-wave plate to orientation α and the cycle of discrete intensity measurements at these two orientations is repeated C times, the counts in each channel (two per beam) being accumulated. The number of cycles (C) can be preset in the range 0 – 9. When the last cycle is comple-ted the totals are automatically printed out by the digital printer and the
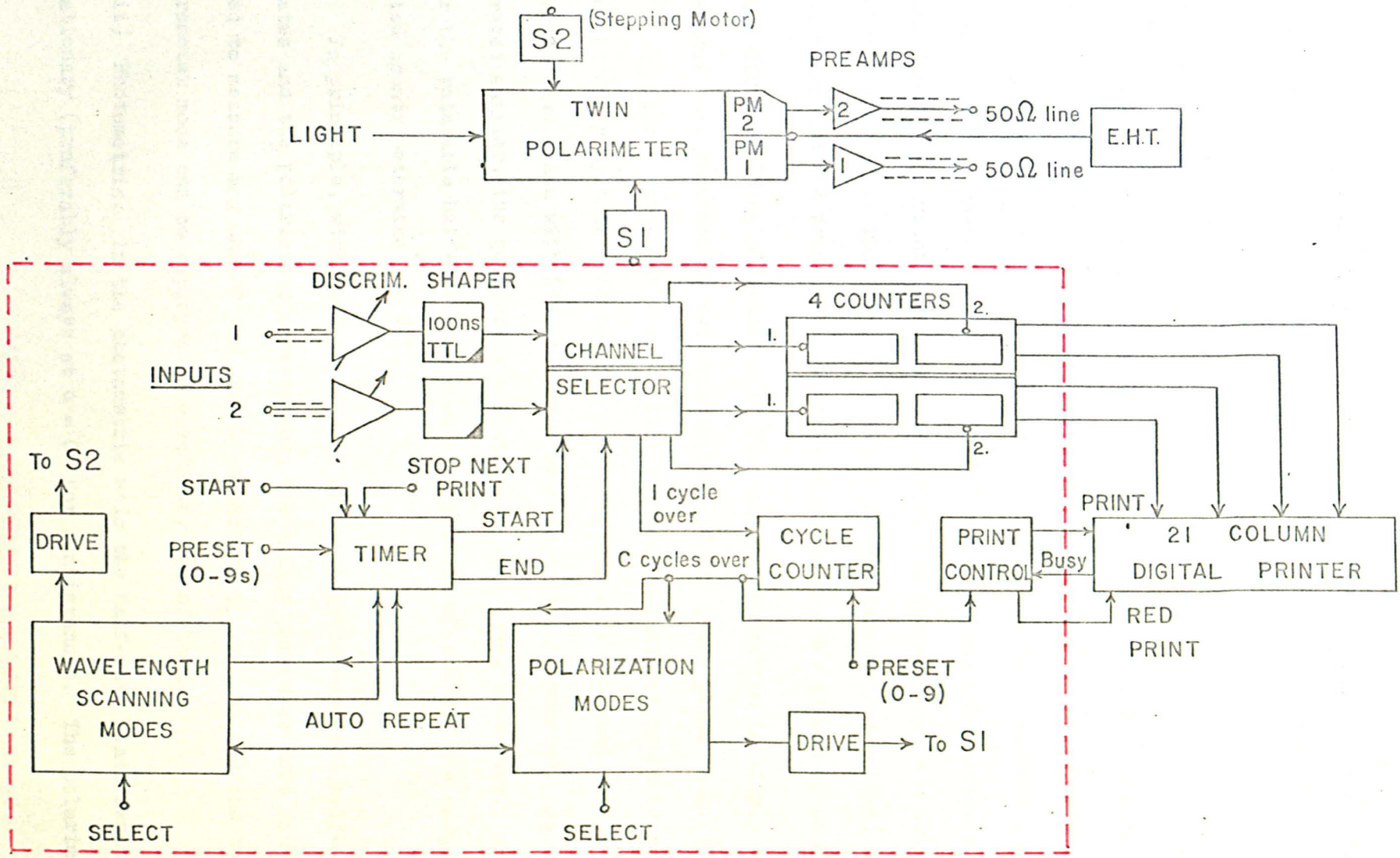
Fig. 3.9 Block diagram of polarimetric system. Enclosed area forms a single unit. The logic control circuitry employs 74 series TTL integrated circuits.

display cleared ready for restarting. Various optional modes of the polari-
meter are available according to the way in which the half-wave plate and
tilting-filter stepping motors are controlled from the front panel of the
display and control unit.

OPERATION MODES:

(i) Linear (or Two Parameter Mode): Intensity measurements are made at two
set positions of the half-wave plate, viz., $\alpha = 0^{\circ}$, 45°, corresponding to the
Stokes parameter $p_x = Q/I$. The signal is integrated for T seconds into each
channel, the two-channel cycle repeated C times and the accumulated counts
printed out. A similar sequence then occurs for the settings $\alpha = 22\frac{1}{2}^{\circ}$, $67\frac{1}{2}^{\circ}$,
yielding $p_y = U/I$. This entire procedure is automatically repeated, alter-
nate black and red print being used to identify the two groups of counts.

(ii) Circular (Single Parameter): This mode of operation is simply the
previous one, confined to two orientations of the phase plate, e.g. 0° and
45°. Obviously either of the two linear Stokes parameters could be studied
independently by this mode but its real usefulness is apparent when a
quarter-wave plate with its reference axis at $+ 45^{\circ}$ is inserted. As demon-
strated earlier, the quarter-wave plate acts as a $V \rightarrow Q$ converter. Hence,
for the rotatable half-wave plate working between 0° and 45° the accumu-
lated counts determine $q = V/I$.

In principle, with judicious usage of the quarter-wave and half-wave
plates and the polarimeter orientation, the single parameter mode can be
used to measure any one of the Stokes parameters p_x, p_y, q and the two
parameter mode can be employed to obtain any two of them.

(iii) Photometric: In the photometric mode the half-wave plate remains
stationary (preferably always at $\alpha = 0^{\circ}$ for consistency). The polarimeter

can therefore be used as a polarization sensitive double-beam photoelectric photometer. Only if the polarizing optics are removed does the instrument become a true photometer. As before, the signal is chopped for T seconds into each of the two channels and the cycle repeated C times. This electronic mode is best suited for recording the intensity of the sky background, dark counts from the photomultiplier tube or. the photometric signal when digitized line profile scans are being recorded by controlled tilting of the interference filters. If the filter in Beam 2 is at a fixed wavelength, and that in Beam 1 is used for tilt-scanning, the ratio of the signal outputs will compensate for scintillation and transparency changes during the line profile scan, when these are the dominant sources of noise. The instrument in this mode operates like a simple scanning monochromator.

(iv) Continuous Rotation: The stepping motor can also be made to step continuously (typically at ~ 20 Hz) independently of the pulse counting electronics.

(v) Four Quadrant Mode: This useful mode is identical to the single parameter mode inasmuch as it positions the half-wave plate at α or $\alpha + 45^{\circ}$ and channels the counts accordingly. However, after the printout occurs and the phase plate is returned to α, the display is automatically cleared, α is advanced (either direction is possible) by $22\frac{1}{2}^{\circ}$ and the sequence is restarted. Following each subsequent print, the half-wave plate will continue to advance by $22\frac{1}{2}^{\circ}$, eventually completing a rotation of 360°.

Wavelength Scanning:

Initially, line profile scans were made by D.C. amplifier, pen recorder and a synchronous motor drive as already described (Section 3.2). Later, some Hβ scans were taken by setting the micrometer which drives the tilt mechanism, by hand, to several discrete positions in turn and integrating

the signal counts for T = 3 seconds (1 cycle) at each spectral point. Fin-
ally, however, in early 1974, a small logic controlled stepping motor which
could turn the micrometer in integral revolutions was incorporated·in the
system. The motor was mounted on a slide to enable the gears to be easily
disengaged thereby allowing any starting micrometer reading to be set up.

Once a satisfactory number of polarimetric measurements have been com-
pleted at a given wavelength position, a control switch can be thrown which,
after the next print, will cause the wavelength scanning stepping motor to
drive the micrometer in the direction selected for the number of revolutions
selected (0 - 9). The oscillator controlling the pulsing of the stepping
motor is provided·with four speeds giving micrometer revolution rates of
0.1 rps, 0.3 rps, 1.0 rps and 2 rps. When the tilting motion is complete
the polarization measurement sequence is automatically restarted. At any
time during a polarimetric run at a particular wavelength, the observer can
alter the proposed direction of scan, number of micrometer revolutions (i.e.
wavelength interval) and, if necessary, the scanning speed in preparation
for the next wavelength change. For some applications it is convenient to
move on to a new wavelength after every printout and to reverse the scanning
sense after a certain number of spectral points have been studied. The
present system provides the following simple options, viz., 2, 3 or an inde-
terminate number of picture points in one scan direction before automatically
reversing direction. Examples of practical applications of these options are:
(i) alternate measurements on each wing of Hβ, or (ii) with the 3-point
mode, linear polarization across the line profile, i.e. continuum (red), line
centre, continuum (blue). In the "indeterminate" mode the scan will be in-
itiated following every print just as before, but no direction change will
occur. This mode enables an automated digitized spectral scan of the Hβ line
to be effected. Several profiles derived in this way will be shown later.
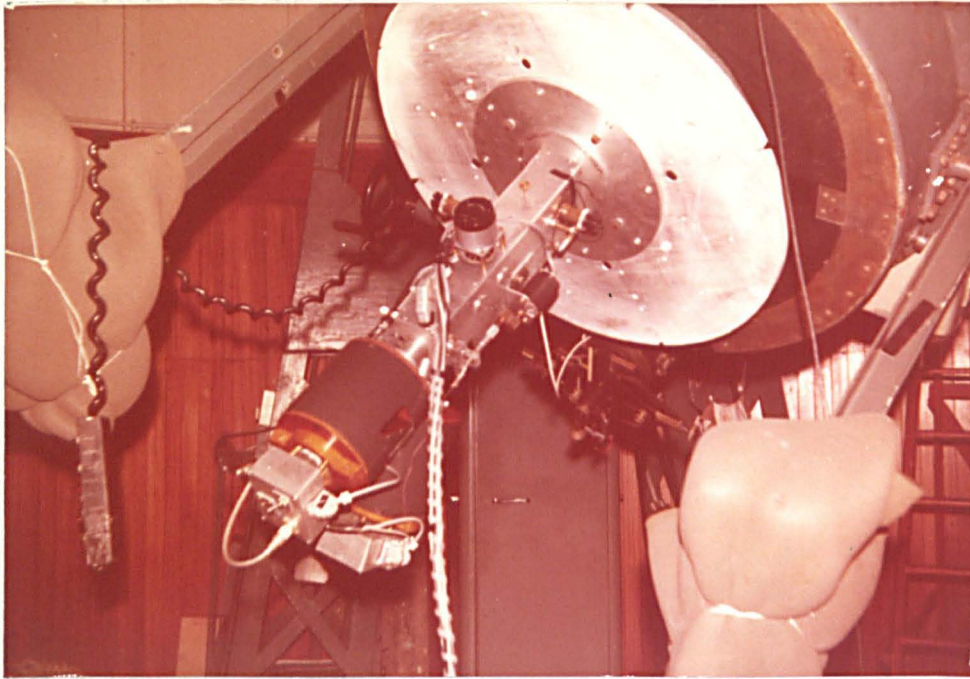
PLATE 1. The Hβ-spectropolarimeter attached to the 91 cm (36-inch) Yapp reflector at the Royal Greenwich Observatory, Herstmonceux. Both the half-wave plate stepping motor (upper face) and the micrometer (tilt) drive motor (side face) can be seen. Each photomultiplier casing is surrounded by a dry ice container.

PLATE 2. Electronic control system. From left-to-right are the pulse counting display and control cabinet, the digital printer and the Hewlett-Packard 9810 programmable calculator used in reducing the data. Power supplies for the preamplifiers and photomultiplier tubes are on the floor.

The electronic control system and pulse counting scalers form a single unit which, together with the digital printer, the EHT power supply for the photomultipliers and the spectropolarimeter itself, comprises a compact and complete system. Plates 1 and 2 show the spectropolarimeter attached to the 91 cm telescope at Herstmonceux, and the electronic control system, respectively. If regular wavelength calibration is required then the laboratory lamps and their power supplies are additional.

The entire system has twice been transported by car from Glasgow to Herstmonceux, Sussex, *and back* /and in each case the equipment was checked, reassembled and operational on the telescopes at either observatory in less than 3 hours.

In conclusion it may be remarked that a rough estimate of the overall cost of the polarimetric system just described including filters and machine-shop time is about £2500 - £3000. The comparatively low cost has been achieved because of the novel methods adopted, the use of some inexpensive optical and electronic components and because all of the special electronic control system was designed and constructed by the writer over a 6-month period.

3.6 Preliminary Tests and Astronomical Results

One of the first tests to be carried out on any new polarimeter is a check on its performance in analysing light which is completely (i.e. 100 per cent) polarized. The polarimeter was set up in the laboratory and light from a laboratory source, polarized by an HN22 Polaroid piece with its polarizing axis already marked by the manufacturer, was focussed onto the polarimeter diaphragm. The HN22 polarizer could be set to a variety of angles, relative to the x-axis, in $7^\circ.5$ steps. With the principal half-wave plate of the polarimeter removed, the HN22 polarizer was adjusted until it was accurately

crossed with Beam 1 of the double-beam polarizer. The half-wave plate was replaced and rotated until the minimum signal was again obtained, indicating that the retarder's axes were parallel to those of the polarizer. In this position the stepping motor shaft and the phase plate drive shaft were clamped together. With 25 Å interference filters set at tilts corresponding to Hβ in each beam of the instrument, light coming from a hydrogen lamp and polarized by HN22 Polaroid, was focussed onto the polarimeter diaphragm. The automatic system already described was then employed to measure the Stokes parameters for various known directions of vibration of the input light. In all cases, the measured degree of polarization, p, fell in the range 99 per cent to 100 per cent and the measured azimuth of vibration was within ± 0°.5 of the expected value. This method of aligning the half-wave plate along the x-axis of the double-beam polarizer is accurate to about ± 0°.25. However, when the orientation of the phase plate was checked by eye, it was found possible to utilise lines marked on the face of the plate-holder and parallel to the edges of the phase plate, as a means of establishing the required angular setting to within about ± 1°. Alignment of this accuracy is quite acceptable for linear polarization studies, especially for differential measurements.

To enable the optical tests to be completed the polarimeter was attached to the 51 cm (20-inch) telescope at Glasgow. With the photomultiplier tubes removed, but with 25 Å filters in the beams, sunlight (through a hazy sky) was focussed onto a small diaphragm. Using dummy photomultiplier housings, open at one end, the positions of the Fabry lenses were adjusted until a sharp image of the telescope collecting aperture was obtained on a thin paper screen at the position of the photocathode in each beam. Small adjustments to the optical alignment were carried out by observing back-reflections,

onto the diaphragm, from the various optical surfaces. Movement of the image of the telescope aperture on the photocathode was investigated by setting up a travelling microscope at the position corresponding to the detecting surface so as to view this image while rotating the half-wave plate. After very slight adjustment to the retarder's mounting, no movement of this image was observed to the limiting accuracy (about 20 μ) of the microscope.

To obtain polarization position angles in the equatorial co-ordinate system requires a knowledge of the orientation of the x-axis of the polarimeter in this reference frame. To determine this angle a line parallel to the polarizing axis of Beam 1 was transferred to the outside of the polarimeter casing and the telescope, with instrument attached, set in the meridian looking south. When the telescope is rotated about its declination axis until horizontal, the required angle is 90° plus the angle between the transferred line and the horizontal. This angle is easily read off using a protractor with a horizontal spirit-level. On the ~~only~~ two other telescopes with which the polarimeter has so far been used a slightly different technique was employed. In each case the telescopes were accurately pointed towards the zenith and the x-axis aligned directly in the equatorial system by turning the polarimeter about the optic axis using the telescope base rotator and corresponding angular scale.

Having obtained a satisfactory performance at 100 per cent polarization the polarimeter was then tested on a bright stellar source known to have low linear polarization, viz., α Lyr (AOV, $m_v = 0.03$). For this star, Behr (1959b) reports p = 0.025 per cent and Serkowski and Chojnacki (1969) give p = 0.024 per cent. The latter workers considered this value (with similar values for other stars) as typifying their instrumental polarization. With
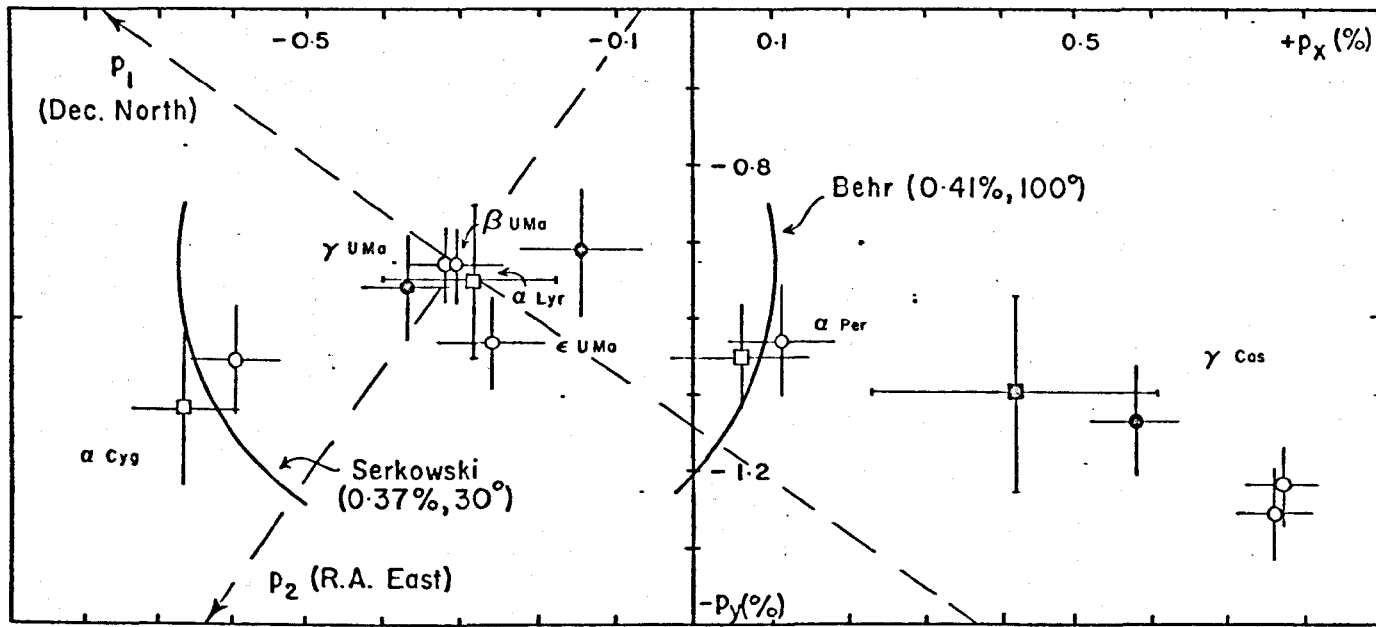
Fig. 3.10 Narrow band (Hβ) polarimetry of various stars plotted in the (p_x, p_y)-plane of the instrumental system. The equatorial reference frame is shown corrected for instrumental polarization by centering it on β UMa (p ≲ 0.005 per cent, Behr 1959b). All measurements were taken in 1973 September and October. Notice the strong indication of a reduced polarization at λ 4861 Å in γ Cas.

$\lambda/\Delta\lambda$

Key:
o   4835/25 (Beam 2)
□   4865/10 (Beam 1)
■   4861/3   "
●   4861/10   "

the polarimeter attached to the 51 cm telescope at the Glasgow University Observatory, linear polarization measurements were made on α Lyr using a 10 Å filter set at a wavelength of about 4865 Å in Beam 1 and a 25 Å filter set at 4835 Å in Beam 2. Referring the setting of the half-wave plate to the usual instrumental co-ordinate system, the observing sequence was as follows:

(i) Locate star, test photometric signal with half-wave plate at 0°.

(ii) Select the integration time per channel (T) and number of cycles (C).

(iii) Off-set the star and record sky background and dark background.

(iv) Re-centre star, select linear polarimetric mode.

When measurements taken with the half-wave plate rotated through 180° to a new but equivalent starting position were compared to those for $\alpha = 0^\circ$, the observed Stokes parameters were the same in each case, to within the accuracy of the polarimetry, typically ± 0.06 per cent.

A similar set of measurements was made for the star α Cyg (A2Ia, m_v = 1.26). Regarding the normalised Stokes parameters obtained from α Lyr as characterising the instrument's response to zero polarization, subtraction of these values from those measured for α Cyg therefore corrects, to good approximation, for instrumental polarization. The value of the instrumental polarization was $p \sim 1$ per cent and the derived degree of polarization and azimuth of vibration for α Cyg agreed well with the known values (see Fig. 3.10).

Several possible sources of the instrumental linear polarization are immediately apparent. For example, telescope optics (primary 51 cm mirror was due for re-aluminising), collimating lens (Fresnel reflection and re-fraction from the low f-ratio lens which may be slightly tilted), multiple reflections in the half-wave plate, or indeed, a combination of these. To

test for polarization introduced by the collimating lens and telescope optics another half-wave plate with its reference axes at 45° was inserted into the collimated beam. Ideally, the action of this component should yield U' = U, Q' = -Q, where primed quantities denote measurements with the additional half-wave plate in the beam. In fact, the U-parameter remained almost the same but the Q-parameter, although it changed sign as expected, was much larger numerically (more than doubled). There are at least two possible explanations for this result; either placement of the second phase plate at 45° in the optical beam has disturbed the instrument's response to zero polarization or, if this effect is negligible, then not all of the apparent polarization is caused by the fore-optics. Probably, the most likely source of the instrumental polarization is a combination of effects associated with the collimating lens and photocathode sensitivity. However, it was not considered worthwhile, at this stage, to pursue the matter further.

Choice of the best values for the channel integration time, T, and the number of two channel cycles, C, merits discussion. It is known that the power spectrum of scintillation contains frequencies from 1 Hz to 1 kHz but most of the power is in the frequency range 1 Hz to 20 Hz. For frequencies lower than 1 Hz (periods longer than 1 second) scintillation begins to mingle with transparency changes associated with mass motion of the air, i.e. with phenomena such as drifting cloud or approaching weather fronts. Since two intensity measurements at the same atmospheric transmission are required for each Stokes parameter, then values of T = 2, 3 or 4 seconds will give ample smoothing to all scintillation components down to 1 H_z. It is the components with periods comparable to T which introduce the most noise. Provided the fractional uncertainty in this noise is less than

photon noise then the atmospheric effects will be negligible. When photon noise is small, the chopping technique will smooth random variations in signal strength due to atmospheric effects, however, although repetitive measurements will improve the polarimetric precision by $1/\sqrt{n}$, n = number of observations, the precision may not improve by exactly $1/\sqrt{N}$, where N is the total photon count. The number of cycles C is chosen such that the accumulated counts in the two channels are high, say $\sim 10^5$, but the integration time per Stokes parameter measurement, 2CT, is short enough to permit both $p_x = Q/I$ and $p_y = U/I$ to be evaluated in less than 1 minute. Successive determinations can then be averaged and studied statistically. Although in the presence of cirrus cloud and haze, changes in atmospheric transparency will certainly occur during time intervals of 30 seconds or more, these effects are strongly smoothed out because a pair of corresponding intensities are accumulated every 6 seconds (if T = 3) and the sequence cycled 5 times. If P is the total number of pairs of printouts (each pair yields the parameters p_x and p_y and hence p and θ), then the total observation time is 4 PCT seconds. Since, for small p, the counts in each channel are $\simeq$ n*CT where n* is the average count rate, then the mean error in the average of P values of p_x, p_y or p, according to Poissonian statistics, is

$$\varepsilon = \left[\frac{1}{2CTP^2} \sum_{i=1}^{P}\left(1/n_i^*\right)\right]^{\frac{1}{2}} \simeq \left(\frac{1}{2n^*CTP}\right)^{\frac{1}{2}}$$

where the reduced form applies if n* is constant from print to print. In Fig. 3.11 the standard error of the mean, calculated from the data, together with ε (using the measured counts $N_{1_i} + N_{2_i} = 2n^*_i CT$) is plotted against P for the normalised Stokes parameter $p_x = Q/I$, measured for α Lyr. Other useful ways of displaying the polarimetric data statistically are also shown and discussed below.

α Lyr (11/9/73) $\lambda/\triangle\lambda = 4865/10$ (Å)

$p_1 = Q/I$
$p_2 = U/I$
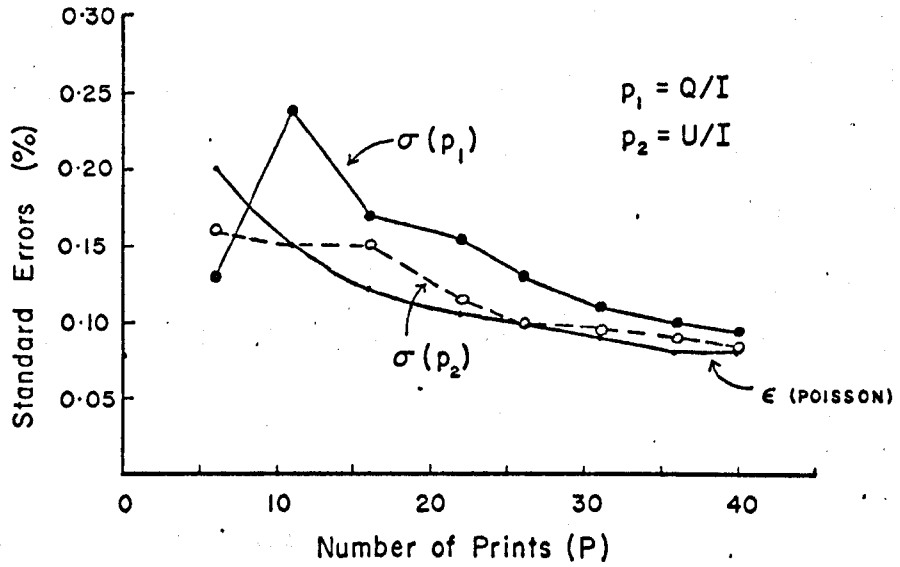
α Lyr: Photometric Data evaluated like Q/I

Number in Interval

C = 2
T = 2
P = 20
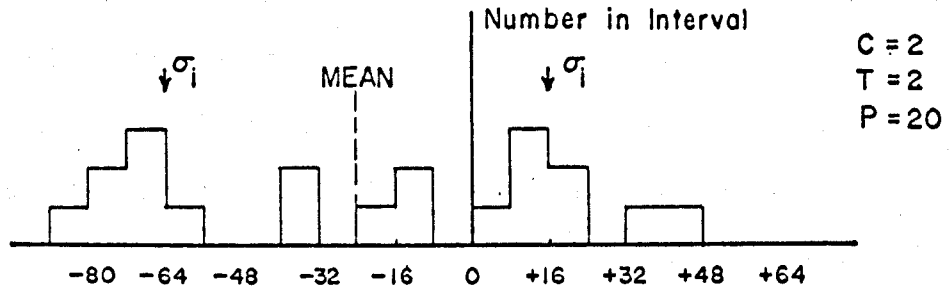
$10^4 p_1$

From the p_1's, σ_i (single observation) = 39×10^{-4}
From the counts, σ_i (Poisson) = 47×10^{-4}

Fig. 3.11   Methods of representing the statistics of the measured Stokes parameters.

Using the photometric mode and breaking up CT = 4s into (i) C = 1, T = 4s; (ii) C = 2, T = 2s; (iii) C = 4, T = 1s, about 20 prints in each mode were obtained for α Lyr. This data was reduced as if it represented a Stokes parameter. Such a test indicates the instrument's ability to s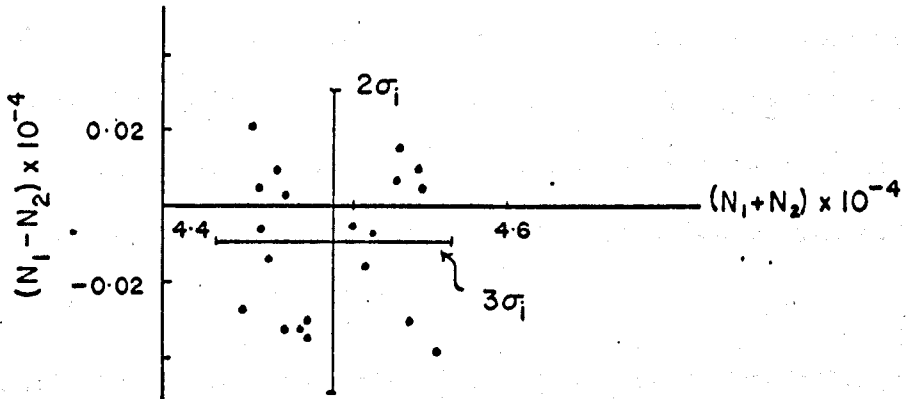mooth out random and systematic changes in signal level during the integrations. The samples illustrate that, under poor observing conditions (industrial haze, cirrus cloud) the apparent Stokes parameters are distributed about a mean value, which itself is reasonably close to zero when compared to the accuracy of a single observation assuming Poisson counting statistics. In practice, T = 2s or T = 3s are most used, however, a channel time of T = 5s, with C = 6, was successfully employed for the fainter (second magnitude) object, ε UMa, when observed through haze and thin cirrus.

Fig. 3.10 displays the normalised Stokes parameters (in per cent) in the instrumental reference frame and uncorrected for instrumental polarization, in a preliminary narrow band survey (2.5 Å, 10 Å, 25 Å passbands) of various bright stars. To obtain the point in the $p_x - p_y$ plane corresponding to unpolarized light the star β UMa was used as a standard. Arcs centred on this star and with radii equal to the degree of polarization, as obtained by other workers, are shown for α Cyg and α Per, and the equatorial position angles have also been inserted.

Listed in Table 3.2 is the apparent degree of circular polarization, q, uncorrected for instrumental effects, across Hβ in three peculiar, second magnitude stars. The polarimetric precision is typically ± 0.1 per cent (or ± 10 if q is expressed in units of 10^4). Positive (right-hand) circular polarization corresponds to a counter-clockwise rotation of the electric vector maximum with increasing time.

To investigate the instrument's response to circularly polarized light,

OBJECT	m_v (SP)	DATE	$\lambda/\Delta\lambda$ (Å)	INTEGRATION TIME (min)	$10^4 q$
α And	2·2 B9p	1973 Oct 11	4835/25	55	+ 52 ± 3
			4867/10	28	+ 50 ± 7
			4855/10	28	+ 44 ± 8
		1973 Oct 17	4835/25	38	+ 50 ± 4
			4866/3	19	+ 55 ± 14
			4856/3	19	+ 71 ± 13
ε U Ma	1·78 AOV pv	1973 Oct 17	4835/25	19	+ 59 ± 8
			4866/3	19	+ 31 ± 17
			4856/3	19	+ 44 ± 14
γ U Ma	2·54 AOV (n, v)	1973 Oct 10	4835/25	24	+ 48 ± 7
			4866/10	5	+ 70 ± 19
			4856/10	24	+ 29 ± 9

TABLE 3.2.   Apparent circular polarization (uncorrected for instrumental effects) on the wings of Hβ in 3 stars.   An observer of positive (right-handed) circular polarization sees a counterclockwise rotation of the electric vector (Gehrels (1974)).   According to the definition of Clarke and Grainger (1971) this polarization corresponds to a left-hand helix in space.

a pair of right-angled glass prisms were oriented to give two successive, co-planar, internal reflections of a collimated beam of light, completely linearly polarized at + 45° to the x-axis of the polarimeter. The plane of incidence and reflection was parallel to the y-axis. Resolving the incident beam into components polarized parallel and perpendicular to the plane of incidence, it can be shown that (see e.g., Clarke and Grainger, 1971), after two internal reflections, the perpendicular component suffers a retardation of nearly 270°. Thus, the emergent light is almost fully circularly polarized, with the electric vector maximum rotating clockwise with increasing time (left-handed circular polarization). In the "snapshot" picture of the wave components, this handedness corresponds to a right-handed helix in space. The instrumental circular polarization was about + 0.50 per cent.

A summary of the achievements of the study up until 1973 October is given below.

(a) A new filter-tilting Hβ scanning spectropolarimeter was designed, developed and tested in two stages:

  (i) Basic. Continuous Hβ tilt-scans (D.C. amplifier and chart-recorder) obtained at each of three fixed orientations of a half-wave plate (Fessenkov method). Later developed to a single channel pulse counting system. No automation.

  (ii) Twin. Fast polarimetry at fixed wavelengths (tilts) with a new pulse counting and almost completely automatic electronic control system.

  The Stokes parameter method is employed to obtain polarimetric data; only two counting channels per beam are required since the measurements related to Q and U are made sequentially and the counts printed out.

(b) Some simple laboratory tests on the polarimeter and scanning monochromator were carried out.

(c) Hβ polarimetry of various stars was obtained, though under relatively poor observing conditions, with passbands of 2.5 Å, 10 Å and 25 Å.

Advantages of the Method:

(a) The polarimeter is a twin device, i.e. two passbands are monitored independently.

(b) Clarke's method for averaging out scintillation and transparency can be successfully employed, enabling the data to be recorded with a precision essentially limited by photon shot noise. This enables a simple and compact pulse counting, data-logging system to be utilised.

(c) Scans of the Hβ line profile are obtained and calibration of the wavelength/micrometer scale, on the telescope, is easily achieved by piping H and Zn light to the polarimeter diaphragm by fibre-optic tube.

(d) Linear or circular polarization can be measured, i.e. each of the Stokes parameters p_x, p_y and q can be determined.

From 1973 November, the polarimeter was applied to astronomical observations on all possible occasions without further major interruptions for instrument development. The presentation of these various applications of the Hβ-spectropolarimeter and a discussion of the potential for future studies in astronomical narrow band polarimetry are the subject of Part II of this thesis.

PART II

(Applications)

4. ASTRONOMICAL APPLICATIONS

4.1 Some General Polarization Measurements

This section deals with those observations which were used to investigate the reliability of the polarimeter and to investigate the instrumental polarization. The polarimetric precision attainable under different observing conditions is also discussed.

In the six month period, 1973 Nov to 1974 April, the polarimeter was used with the following telescopes: 51 cm (Glasgow) regular use, 91 cm (Herstmonceux) two short runs, (1973 Nov 2 – Nov 15 and 1974 March 19 – 28) and the 250 cm Isaac Newton Telescope (Herstmonceux) from 1974 April 1 – 4. Only 18 "clear" nights were available during this period, the interval 1974 Jan/Feb being particularly barren of good weather. Less than 6 hours observation time was secured with moderate photometric skies, the bulk of the polarimetry being obtained under poor conditions, for example, low-lying haze and fog, thick cirrus and industrial smog!   Nevertheless, although the quantity of results is considerably less than desirable for a survey, the polarimetric precision typically achieved is about ± 0.02 per cent to ± 0.03 per cent and the indications are that, under any reasonable sky conditions, results are photon limited. Further, a precision of ± 0.01 per cent in any Stokes parameter is within the capabilities of this prototype instrument, given sufficient integration times. Since, in the applications of narrow band polarimetry discussed in this thesis, the emphasis is on <u>differential</u> linear or circular polarimetry across Hβ, a finite instrumental polarization appears as a constant offset or bias and is only a minor handicap.

Before describing particular applications, some general results are presented and discussed, particularly in the context of instrumental polarization.

As before, the basic observational procedure is:

(a) Locate star - test signal: Wavelength scan of Hβ (optional).

(b) Select the wavelength position, the channel integration time T and the number of cycles C, offset star and record "dark + sky background". (N.B. If the V/I parameter is required the background must be taken with the quarter-wave plate at 45° inserted).

(c) Re-centre star and commence polarimetry.

(d) Change to new wavelength and/or repeat "dark + sky background" as required.

For the observations recorded at Glasgow and for one run on the 91 cm telescope at Herstmonceux, Sussex, the counts accumulated and printed out were immediately transferred, at the telescope, to an electronic calculator. This machine was programmed to evaluate each individual Stokes parameter, in each beam, their running means and the running values of the standard error of the mean (σ) and other useful quantities, such as the approximate theoretical estimate of precision, ε. Usually, measurements were continued at a given wavelength until the value of σ was acceptable.

From 1973 Nov 1 until Dec 30 the second beam of the polarimeter contained an interference filter with a normal incidence wavelength of about 4860 Å and a passband of 25 Å. This filter was tilted to pass a wavelength of approximately 4835 ± 3 Å and remained fixed at that setting for all measurements taken over that two month period. The filters used in Beam 1 were either of the following: $\lambda/\Delta\lambda$ = 4872/2.5 Å or $\lambda/\Delta\lambda$ = 4869/10 Å. Later, another filter was obtained with $\lambda/\Delta\lambda$ = 4875/11 Å. Because of the micrometer and lever arm arrangement the filters used in Beam 1 could be reset very accurately to the same tilt (typically, to about ± 0.1 Å) thus ensuring identical image positions of the telescope collecting aperture on
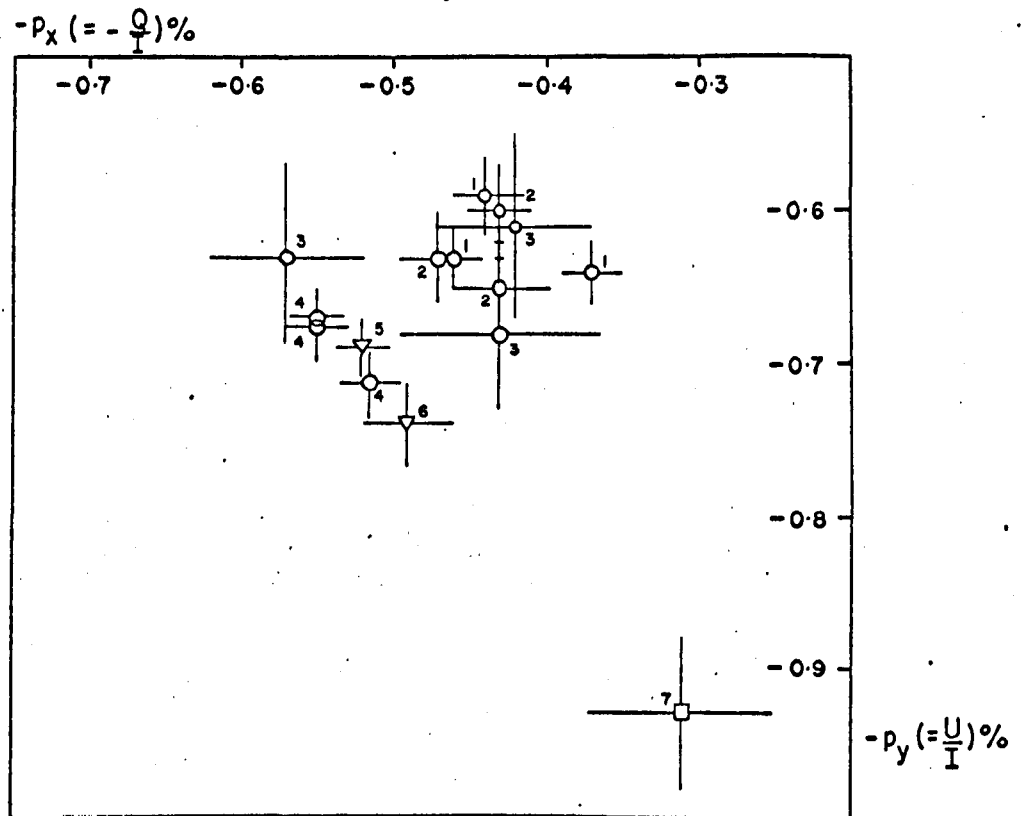
Fig. 4.1 Linear polarization measurements (Beam 2 only) of relatively unpolarized starlight on different dates and telescopes.

	STAR	DATE	TELESCOPE	PASSBAND
1	α Aur	1973 Nov 6	91 cm	4837/25 Å
2	β Cas	"	"	"
3	β Cas	1973 Nov 2	"	"
4	α Aur	1973 Nov 26	51 cm	"
5	α CMi	1974 Mar 20	91 cm	4861/10 Å
6	β UMa	1974 Mar 21	"	"
7	β UMa	1973 Oct 11	51 cm	4837/25 Å

the photocathode. Also, each orientation of the filter was considered as defining a separate instrumental polarization, to be calibrated against standard unpolarized stellar sources. For this purpose the following group of relatively bright stars proved useful:

Star	p (per cent)	
β Cas	.009 ± .009	Serkowski (1973)
α CMi	.005 ± .009	
α Aur	.028 ± .014	Serkowski and Chojnacki (1969)
α Lyr	.024 ± .014	
β UMa	.005 ± .020	Behr (1959b)

Of these stars, β Cas and α Aur were preferred because of their nearness to the stars which were selected for special study, for example, γ Cas.

A very brief measurement of the star ϕ Cas ($m_v = 5.0$), which has a large interstellar polarization, was performed as a check on the accuracy of the position angles in the equatorial co-ordinate frame. The average polarization derived by combining the results of both beams was $p = (3.9 \pm 0.4)$ per cent, $\Theta = 95° \pm 3°$. These values compare quite well with those of Serkowski (1973) viz., $p = 3.3$ per cent, $\Theta = 94°$, and those of Behr (1959b) viz., 3.5 per cent, $\Theta = 94°$. Therefore derived azimuths are certainly within $\pm 3°$ of the true azimuths in the equatorial system.

Slight differences in instrumental polarization were apparent between the 51 cm and 91 cm runs and for the same 91 cm telescope when used almost 6 months later, the condition of its primary mirror having deteriorated between the two observing sessions. However, these effects (see Fig. 4.1) are dominated by a telescope independent polarization intrinsic to the polarimeter with $p \simeq 0.8$ per cent and $q \simeq 0.5$ per cent. Figure 4.1 displays the
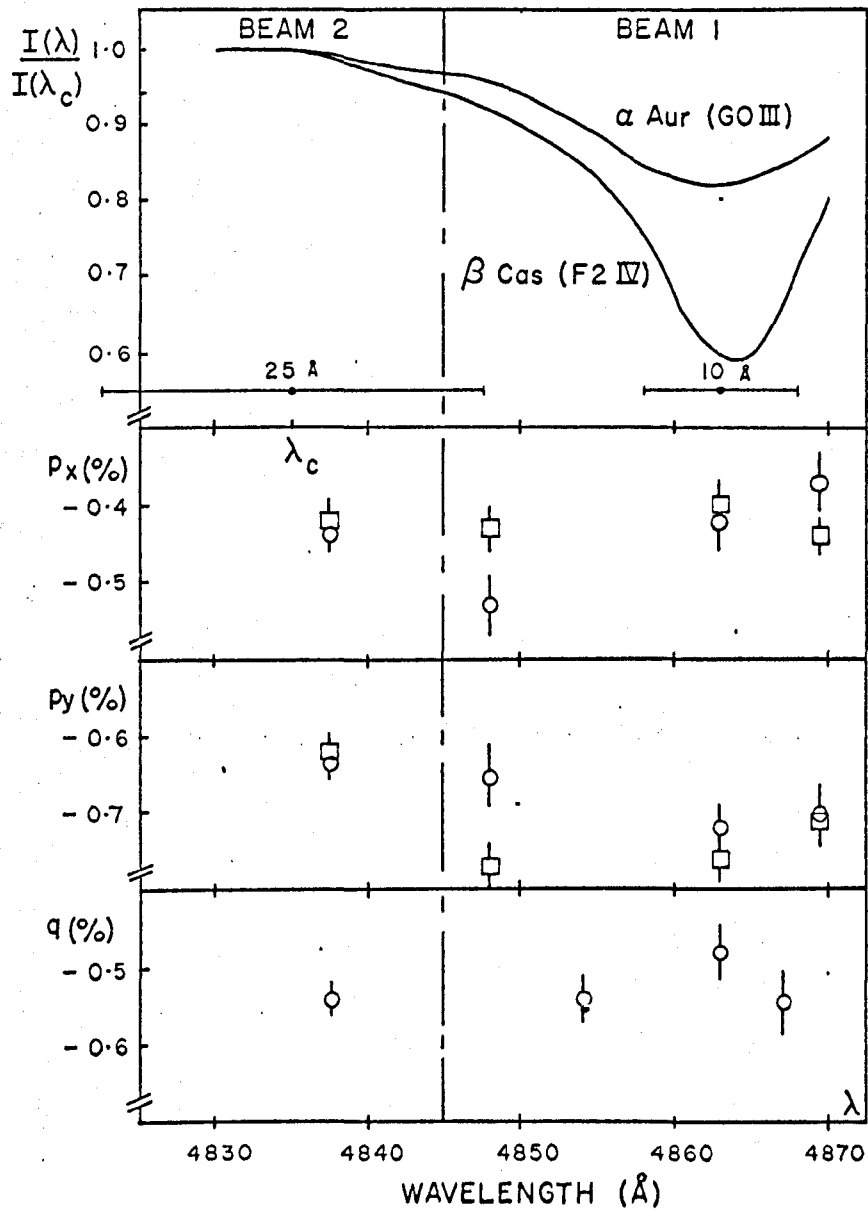
Fig. 4.2 Normalised Stokes parameters across Hβ in β Cas (o) and α Aur (□), demonstrating instrumental polarization and its dependence on the tilt-angle of the filter in Beam 1. The Hβ scans were obtained by tilt-scanning an interference filter of 10 Å passband and normal incidence wavelength of 4869 Å. Measurements with a 25 Å filter (Beam 2 only), just off the line, are also shown.

apparent polarization of β Cas, α Aur, α CMi and β UMa obtained with the 25 Å passband of Beam 2, while in Figure 4.2 a graphical illustration of the apparent Stokes Vector $\{I, Q, U, V\}$, in normalised form, is shown for β Cas and α Aur. The Hβ line profiles were obtained by tilt-scanning the 10 Å filter (λ_o = 4869 Å) and the normalised Stokes parameters were measured at discrete wavelengths. Clearly, only on the blue wing (largest tilts) is there any indication of a change in polarization with tilt and this effect is reduced by averaging the measurements for α Aur and β Cas.

In Figure 4.3 are reproduced, in a section of the $p_x - p_y$ plane, linear polarization measurements made across Hβ for several stars. The Stokes parameters are normalised and expressed as percentages. All measurements unless otherwise stated were obtained with the polarimeter attached to the 91 cm telescope at Herstmonceux. The polarimetric precision is typically ± 0.03 per cent and agreement, both in p and Θ, with the results of other workers is excellent. A discussion of the interesting reduction in polarization at the line centre of the Be-shell star γ Cas is given in Section 4.3. Notice that no such effect is evident for α Cyg and that the polarization differences across Hβ are much greater than those expected to arise by tilting the filter. In any case, the Stokes parameters obtained from β Cas and α Aur, at each tilt, serve to eliminate systematic errors due to this source.

Frequency distributions of the individual measured Stokes parameters are shown in Figure 4.4. The abscissa is the difference of any value from the mean (residual) and a convenient interval for this scale is 2σ, where σ is the standard error of the mean. The number of measurements falling within these intervals, expressed as a fraction of the total number, is plotted as ordinate. When the observed standard deviation of a single observation
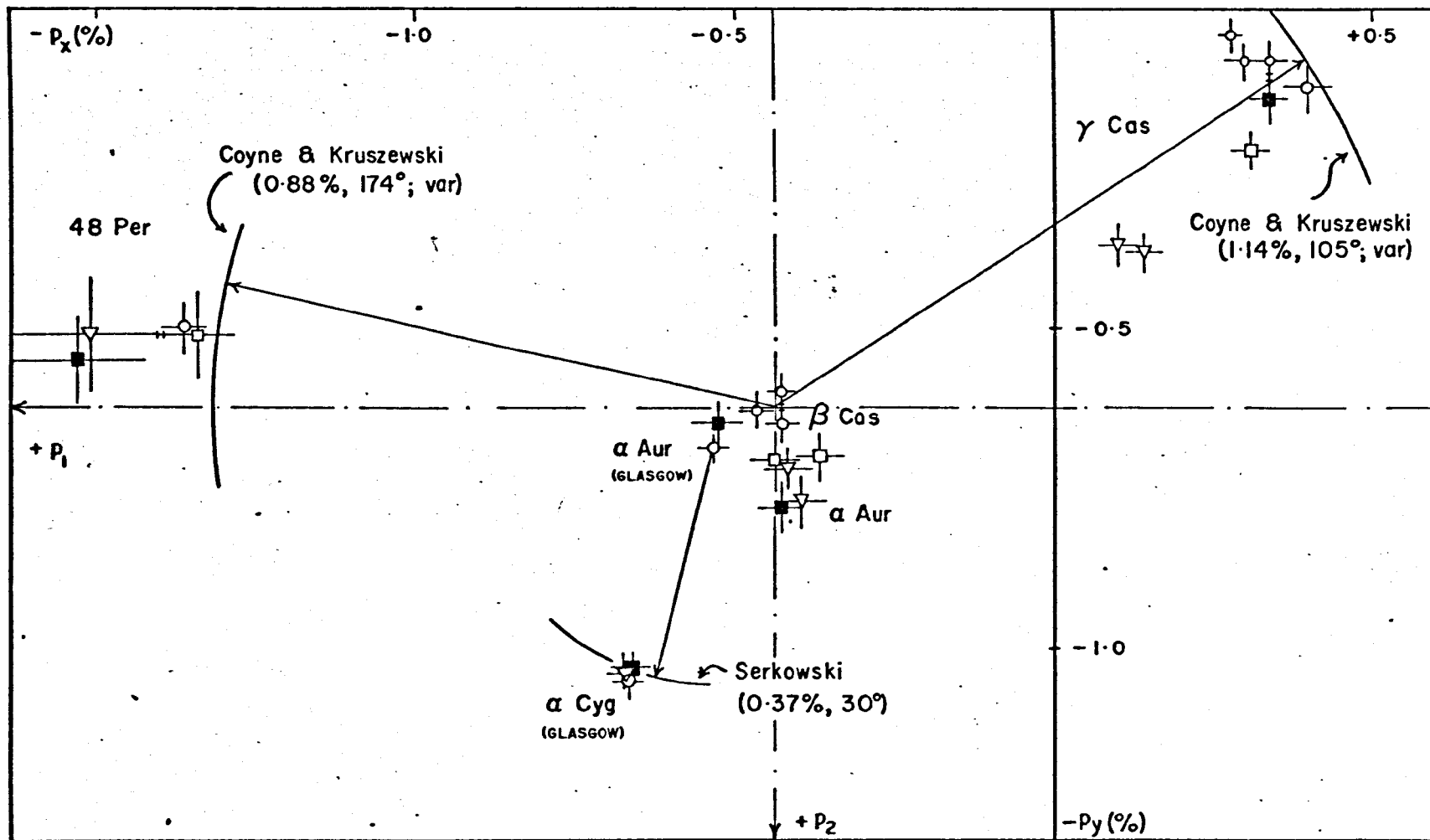
Fig. 4.3   Precision Hβ polarimetry of various stars with the following passbands: $\lambda/\Delta\lambda = 4835/25$ Å (o),
4869/10 Å (□), 4847/10 Å (■) and 4861/10 Å (▽).

($\sigma_i = \sigma \sqrt{n}$) is marked on the histogram, together with the equivalent Gaussian function, it is evident that the distributions follow the Normal Law of errors, despite the statistically small number of data points.

For γ Cas the histogram of p_x (= Q/I) seems to show structure, and although the likely cause of this is a lack of observations, it could also be the result of rapid and real time variations in the polarization of this star. Since a large number of observations are required to make frequency distributions statistically meaningful, time resolution of the polarimetry is degraded. However, the departure of the measured values from a good Gaussian fit may eventually prove to be a very useful method for detection of such variability. For example, if a more or less sudden change in the mean value of a Stokes parameter occurs during a long series of measurements, this would be likely to appear as a double-peaked distribution, whereas a slower variation would produce a broadened histogram. These ideas are applied again later in analysing the linear polarization of emission line stars.

Finally, it is encouraging to note that if σ_p is the expected error, based on Gaussian error combination of the idealised mean error, $\varepsilon = (2/n*t)^{\frac{1}{2}}$, for each individual measurement taken in time t, and which presumably describes photon limited polarimetry, then the ratio $r = \sigma/\sigma_p$ is nearly always less than 1.5 and typically less than 1.3, even for the brightest objects studied. For example, for α Aur ($m_v = 0.1$) $r = 1.29$ and it must be remembered that the observing conditions were non-photometric, hence a considerable contribution to the noise on the signal from α Aur is likely from scintillation and transparency effects. The largest value of r obtained was 2.0. and this was for a second magnitude star observed with the 2.5 m Isaac Newton Telescope. Therefore it appears that precisions of $\pm$ 0.02 per cent are ob-
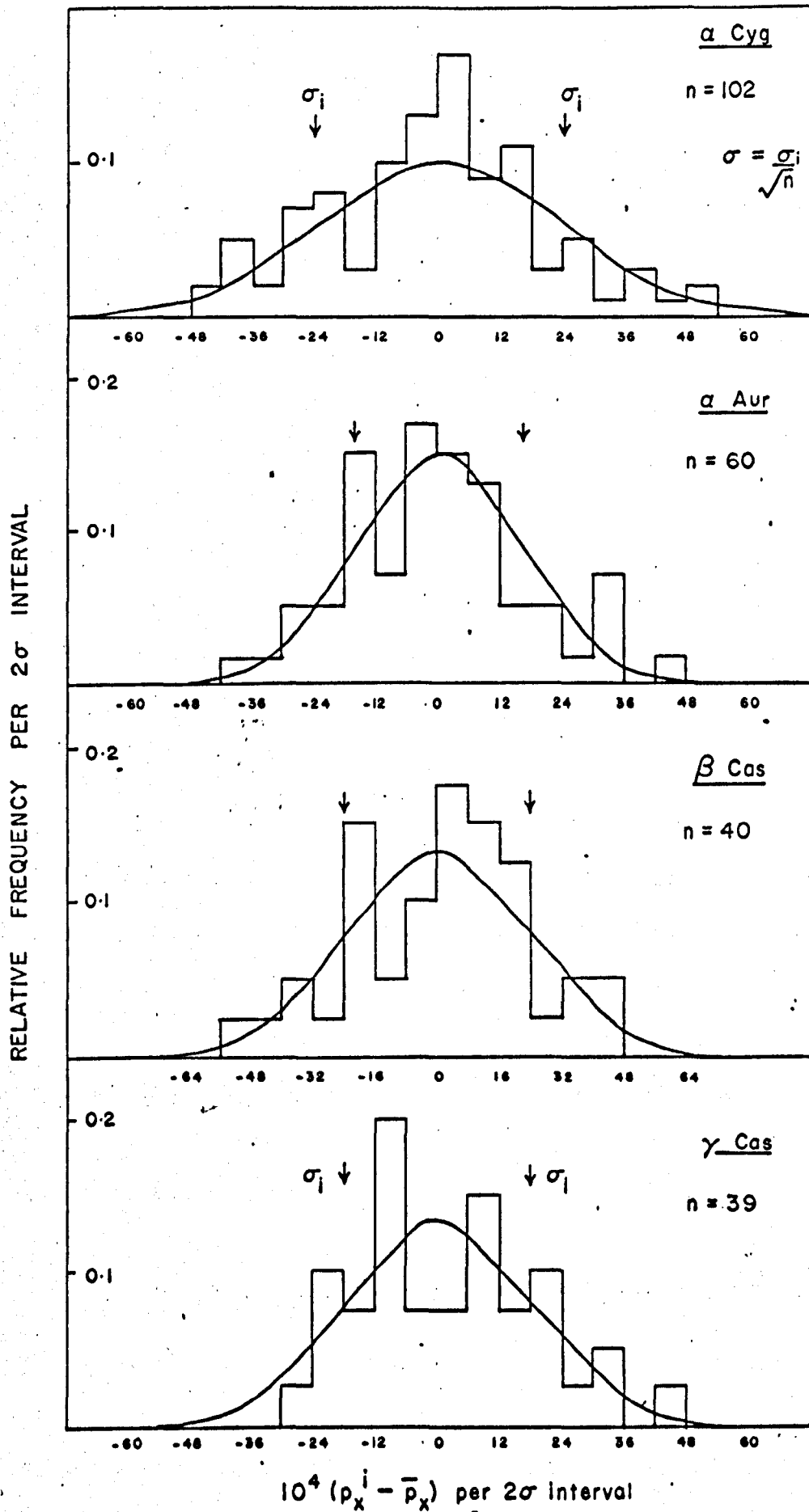
Fig. 4.4 Histograms illustrating the relative frequency of the individual parameter $p_x = Q/I$ for various stars. The binwidth is twice the standard error of the mean (σ) and the abscissa is the residual $(p_x^i - \overline{p}_x)$.

tainable in integration times which are always consistent with photon shot noise, to within a factor 2 at worst, even when photon noise is not the dominant source of error. Observations of the blue sky, emission line stars and magnetic stars are now reported.

4.2 Polarization Measurements across the Hβ Line in Blue Sky: The Grainger-Ring Effect.

Introduction

It has already been pointed out that the astronomical applications of narrow band spectropolarimetry are not confined to the measurement of effects connected with intrinsic stellar polarization. One such alternative study to which the Hβ-spectropolarimeter has been applied is the investigation of polarization effects within the Hβ line profile in the spectrum of the terrestrial blue sky light.

For a long time it seems to have been widely believed that the spectrum of the day sky is identical with that of the solar flux, apart from a few relatively faint dayglow emissions from the upper atmosphere. In fact, when the profiles of Fraunhofer lines in the spectrum of blue sky light are compared with line profiles from direct sunlight, the former are found to be less deep. This intensity "filling-in" effect was first reported by Grainger and Ring (1962a) who observed it in the H line of Ca(II) and later in Hβ and the sodium D lines (see Grainger 1962).

Noxon and Goody (1965) confirmed the existence of the filling-in effect in blue sky spectra and discovered that there are polarization changes across the line profiles. Their experimental method consisted of alternately viewing the sky through two optical channels, each containing suitably oriented polarizers, adjusted to equalise the output signals (Noxon 1968). Having obtained a balance at a certain fixed wavelength the spectrometer is allowed

to scan the line profile. Changes in the sky polarization with time and wavelength are negligible for short scans of limited range. Since the degree of polarization at a given wavelength in sky light is independent of the absolute incident intensity (according to single Rayleigh scattering $p = (1 - \cos^2\Theta)/(1 + \cos^2\Theta)$ where Θ = scattering angle), then the balance was not expected to be influenced by Fraunhofer lines. For the scanned lines, obvious departures of the polarization of the blue sky light were apparent across the profile, in the sense of reduced polarization. This they attributed to an unpolarized continuum component superimposed on the polarized scattered sunlight. Using the results of two scans carried out for mutually perpendicular orientations of the polarizer in one of the optical channels, Noxon and Goody state that it was proven that the "excess component must be polarized less than 2 per cent."

More recently, Pavlov, Teifel and Golovachev (1973) have reported photometric and polarimetric observations of the filling-in (Grainger-Ring) effect in the H, K, L and N Fraunhofer lines. They report that the "degree of polarization is always 2 - 6 per cent lower " at the line centre of the H and K lines than in the continuous spectrum while, for the L and N lines, the depolarization effect is considerably less and occasionally zero. The intensity filling-in is much stronger to shorter wavelengths.

Unfortunately the terminology employed in discussing the polarimetric measurements in the two cited works is a little confusing. It is difficult to reconcile the two statements in inverted commas, viz., the "excess component must be polarized less than 2 per cent" and the "degree of polarization is always 2 - 6 per cent lower" at the line centre. No mention is made of the direction of vibration or of the polarimetric precision.

Linear polarization measurements at discrete wavelength positions across
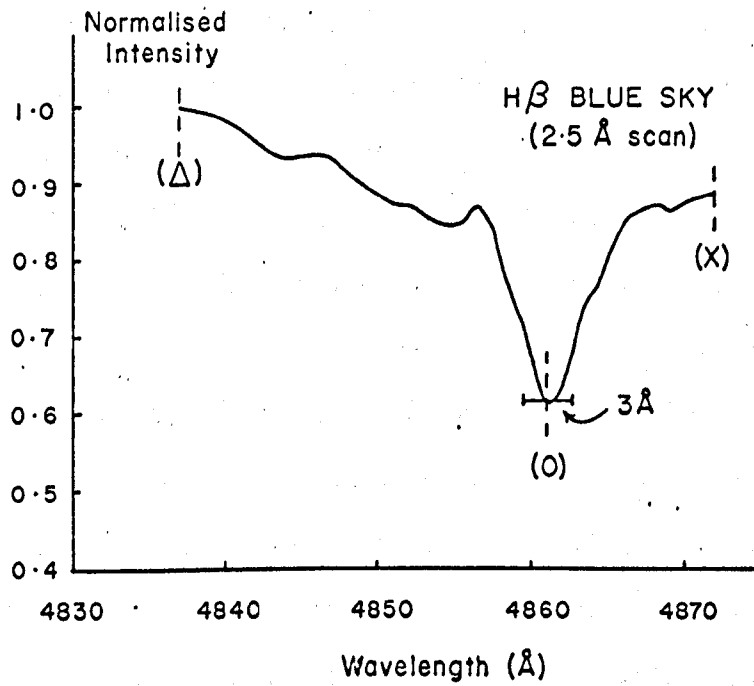
Fig. 4.5   An Hβ line profile in blue sky light obtained by tilt-scanning a
2.5 Å interference filter. Polarimetric measurements (see Figs.
4.6 and 4.7) were performed at three discrete wavelengths, viz.,
4872 Å (X), 4861 Å (O) and 4837 Å (Δ).

the Hβ line in blue sky obtained with the high throughput narrow band spectropolarimeter have already been presented in a preliminary note (Clarke and McLean 1974c) and are now described in more detail below.

OBSERVATIONS

For the blue sky observations the filter of 2.5 Å passband was used for tilt-scanning the Hβ line (4861 Å) in the usual way, and a broader filter (25 Å passband) was fixed in the other beam at about 4835 Å to act as a polarization monitor. Three spectral points (4872 Å, 4861 Å and 4837 Å) were chosen for measurement (see Fig. 4.5). An integration time of 6 seconds per channel (T = 3, C = 2) was selected thus enabling the two linear Stokes parameters (Q/I, U/I) to be measured in a total time of 24 seconds by the automatic polarimeter. Several determinations (usually five) were recorded at each of the three discrete wavelengths in turn and the sequence repeated many times. Each new wavelength setting was produced by rapidly turning the micrometer driving the tilt mechanism of the 2.5 Å filter by hand. The wavelength positions are therefore accurate to about $\pm$ 0.1 Å, neglecting the effects of temperature. From the results of the stellar observations described in the previous section, any differential change in the instrumental polarization caused by tilting the interference filter is $\Delta p \leqslant 0.05$ per cent. Although the blue sky is an extended source a small, circular, focal plane diaphragm subtending an angle of 10 arcsec was employed to minimise off-axis effects in the polarimetry, and this is not much larger than the diameter of a stellar seeing disc at Glasgow. In retrospect, it was probably possible to double this diameter, especially near twilight since, on the clearest day, the polarimetric observations appeared to be photon limited. However, count rates were quite high ($\sim 10^5 s^{-1}$) therefore the chosen diaphragm lessened any chance of counting losses.
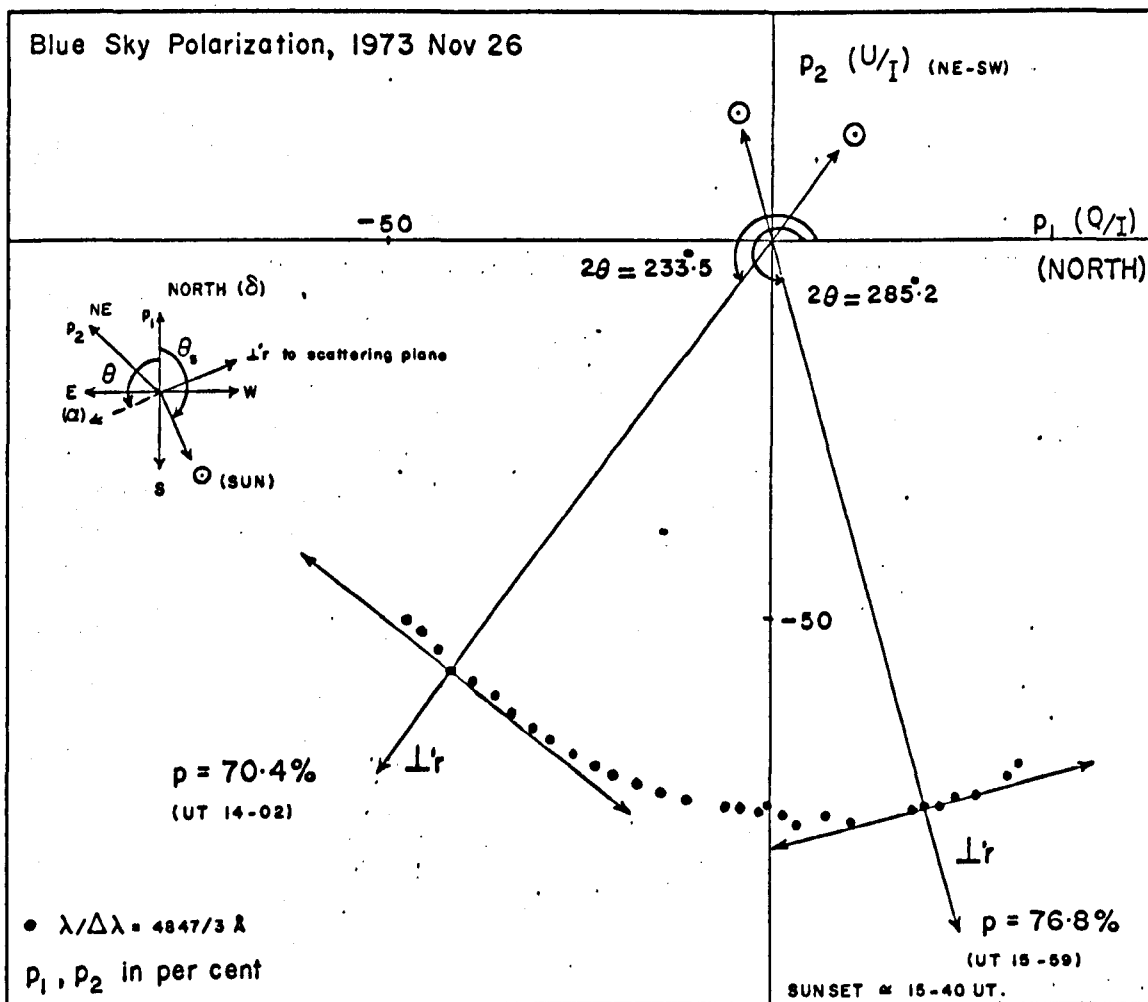
Fig. 4.6 Polarization of the zenith blue sky ($\lambda/\Delta\lambda$ = 4847/3 Å) on 1973 Nov. 26 plotted in the p_1 – p_2 plane of the equatorial co-ordinate system. The slow increase of p with time results from the change in scattering angle as the Sun moves across the sky. Assuming the vibrations are perpendicular to the scattering plane, the equatorial position angle, Θ, can be predicted if Θ_s is known. For the zenith,

$$\cos \Theta_s = \frac{\sin \delta_s - \sin \phi \cos Z_s}{\cos \phi \sin Z_s} \quad \text{and}$$

$$\cos Z_s = \sin \delta_s \sin \phi + \cos \delta_s \cos \phi \cos H_s \quad ,$$

where δ_s, Z_s and H_s are the declination, zenith distance and hour angle of the Sun respectively, and ϕ is the latitude. Then

$$\Theta = 270° - \Theta_s \quad .$$

Excellent agreement was obtained by taking the equatorial position angle of the x-axis of the polarimeter to be 91°, rather than the expected value, 90°.

Observations of the blue sky have been made with the polarimeter atta-
ched to both the 51 cm reflector at Glasgow and the 91 cm Yapp reflector at
the Royal Greenwich Observatory, Herstmonceux. The dimensions of the aper-
ture stops employed were chosen to give 10 arcsec angular resolution. Part
of an excellent run on the zenith blue sky at Glasgow, taken on 1973 Nov 26,
is displayed in Fig. 4.6 and Fig. 4.7; the observing conditions were near
perfect, with the sky clear and deep blue from mid-day well into twilight.
The run started at 13-15 UT and was terminated after sunset at 16-50 UT, by
which time the rate of decrease of the signal had become too rapid. During
the measurements, the degree of polarization of the zenith blue sky slowly
increased, because of the change in scattering angle between the zenith and
the Sun, reaching a maximum value of $p \simeq 0.76$ (i.e. 76 per cent) at sunset.

Figure 4.7 clearly shows that the degree of polarization is least for
the Hβ line centre. To evaluate the amount of depolarization and to inves-
tigate any time-dependence of the effect, the data was divided into blocks.
For each wavelength, a straight line was fitted by a least squares solution
to all the points within a block and the intercept and its standard error
calculated; formulae are given in, for example, Barford (1967).

When plotting p against time, allowance was made for the interval, as-
sumed constant, required to tilt the filter to a new wavelength setting.
This may lead to a small error in the time scale which, for this run, could
not be easily corrected. Such an error can be eliminated in future measure-
ments by use of the electronically-controlled wavelength scanning mode, added
in March 1974.

A similar fitting procedure was performed for the azimuth of vibration
(∅); the equatorial position angle is $\Theta = 90^{\circ} + \emptyset$. For example, for Block 1
(see Fig. 4.7), the intercept values of p and ∅ at λ 4837 Å and the line
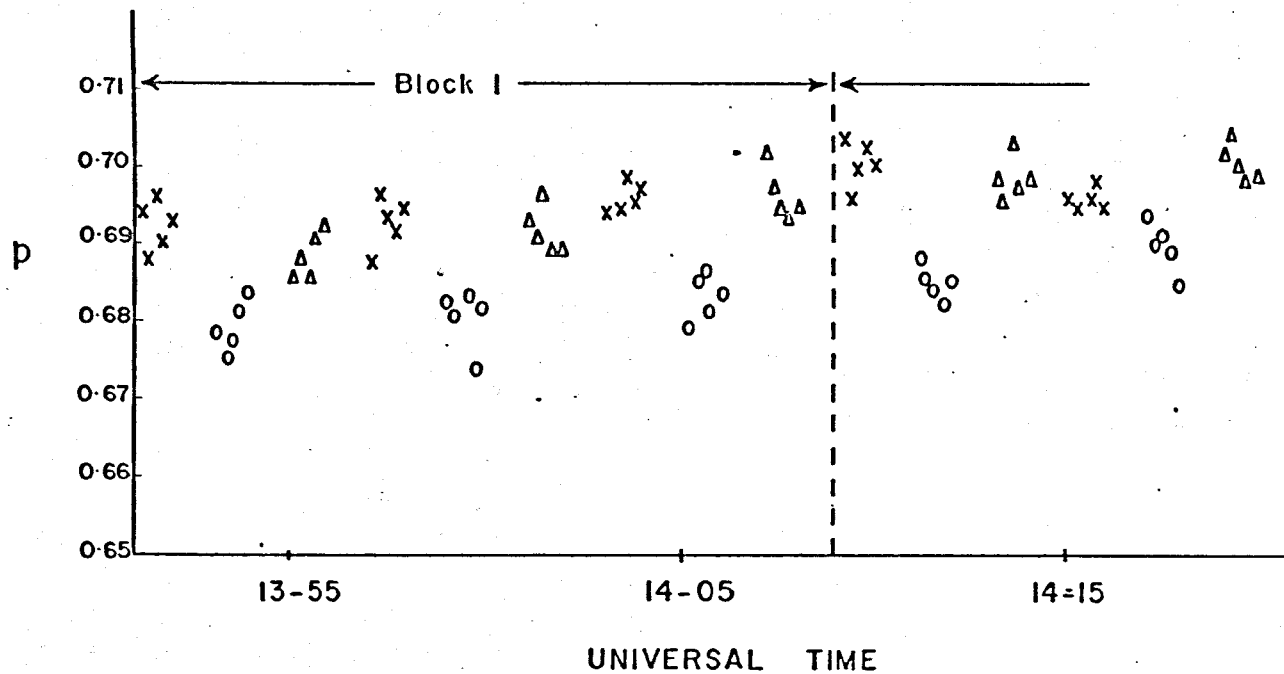
Fig. 4.7   The degree of linear polarization p at three wavelengths across the Hβ line in blue sky light plotted against universal time;   the designated block is part of a 3 hour observing·run on the zenith blue sky with an angular resolution of 10 arc sec at Glasgow on 1973 Nov 26.   An interval of 1 minute separates each change of wavelength setting, corresponding to the time required to move the micrometer driving the tilting filter.

centre, λ 4861 $\overset{o}{A}$, are respectively

$$p_o = 0.6915 \pm 0.0007 \quad , \qquad \emptyset_o = 21°9 \pm 0°5$$

$$p = 0.6782 \pm 0.0009 \quad , \qquad \emptyset = 22°0 \pm 0°6$$

i.e. $\quad p/p_o = 0.981 \pm 0.002 \quad$ and $\quad \emptyset - \emptyset_o = 0°1 \pm 0°8$

Examination of the ratio p/p_o and the difference in azimuths $\emptyset - \emptyset_o$ for each of the blocks $\left(\text{Figs. 4.8(a) and (b)}\right)$ revealed no systematic changes with time to within the uncertainties of the measurement. For the complete run, the average value of p/p_o was 0.984 ± 0.001 and the average value of $\emptyset - \emptyset_o$ was $0°1 \pm 0°2$.

If the added intensity component is unpolarized then, for points in the sky where the polarization is lower, the difference between p and p_o will also be lower. Hence, a depolarization ratio, p/p_o, is more meaningful than a polarization difference.

Using the Yapp telescope, observations on 1973 Nov 11 were made of both the zenith and the north celestial pole. The sky was not deep blue and the data (as evidenced by the monitor beam) showed small irregular variations in p, superimposed on the slower variation with scattering angle. For the same scattering angle the degree of polarization was lower than on 1973 Nov 26. These effects are probably indicative of a higher and more variable concentration of atmospheric aerosols.

As before, no change in the depolarization with time could be detected and no differences between the observed regions were revealed. However, there may be marginal evidence for a difference between the results of Nov 11 and Nov 26; the average values of p/p_o for the former being 0.988 ± 0.002 for the pole and 0.987 ± 0.002 for the zenith, while $\emptyset - \emptyset_o$ was $0°1 \pm 0°2$ for the two directions.
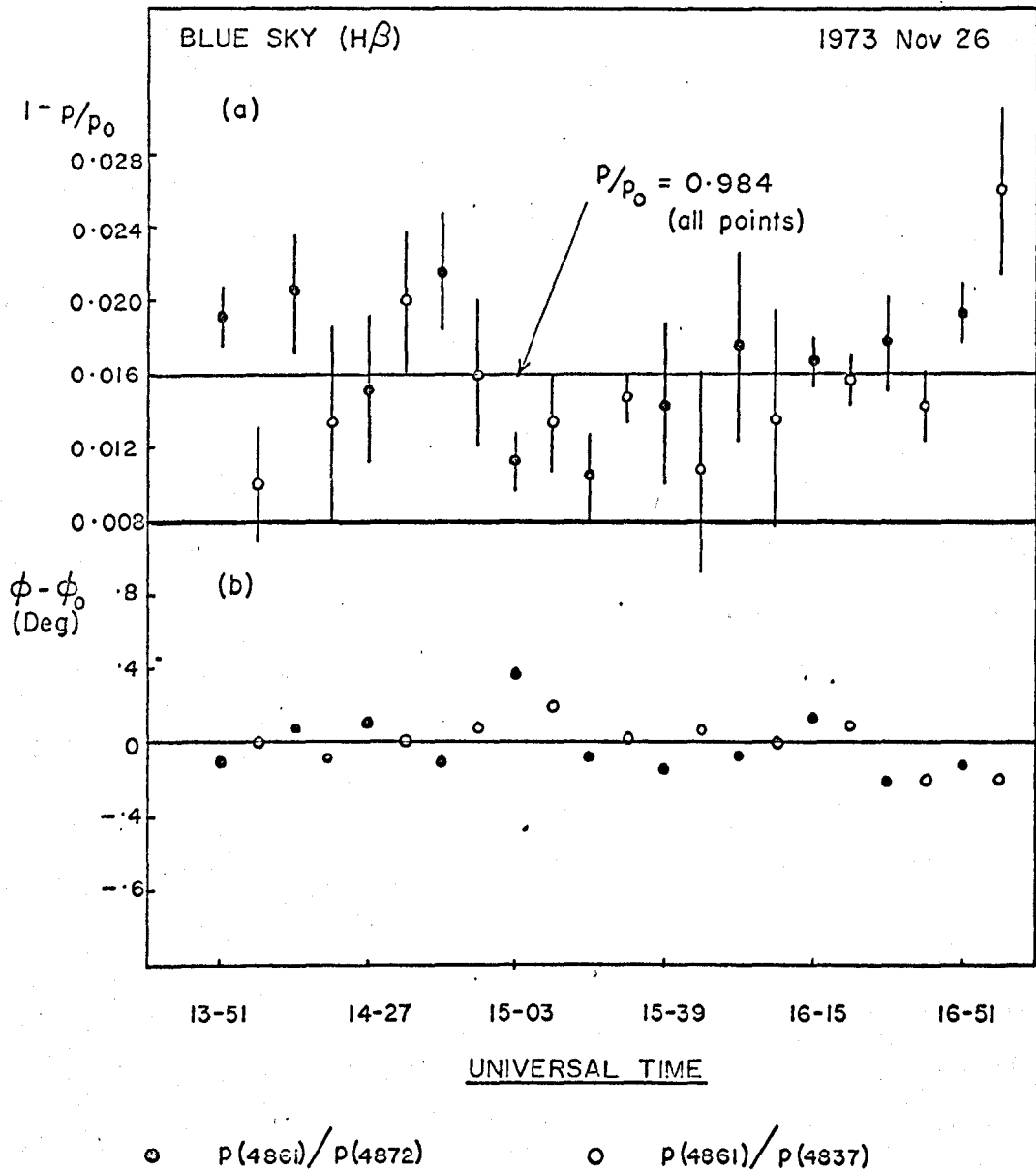
Fig. 4.8   (a) Plot of 1 - (p/p₀) against time, where p/p₀ is the mean de-
polarization ratio between the indicated wavelengths for each of
11 blocks of data (see Fig. 4.7).

(b) Corresponding variation in the azimuth difference $\phi - \phi_0$
with time. Error bars are not shown but those for Block 1 are
typical.

Discussion

The Stokes Vector observed at a point in the real terrestrial atmosphere can be written in the form,

$$W' = \left\{ I'(\lambda),\ p'(\Theta, \lambda)\ I'(\lambda),\ 0,\ q'(\Theta, \lambda)\ I'(\lambda) \right\}$$

where $|p'(\Theta, \lambda)|_{max} < 1$ and $p'(\Theta, \lambda)$ can be negative, (i.e. the vibrations are in the plane of scattering), and a small component of circular polarization is present. Neutral points occur above and below the Sun (Babinet and Brewster points) and above the antisolar direction (Arago point). Typically, a maximum of 75 per cent polarization is found at visible wavelengths on a clear sky approximately $90°$ away from the Sun. Comparison of the Rayleigh-Chandrasekhar theory (Chandrasekhar and Elbert 1951; see Coulson (1974) for review) with observations explains the departure from a maximum polarization of 100 per cent as follows. Multiple scattering dilutes 6 per cent, molecular anisotropy 6 per cent and reflection by the ground 5 per cent (this figure can only be a rough approximation) while a residual 8 per cent is presumed to be due to aerosols suspended in the atmosphere even when the sky is seen as hard blue.

A plausible explanation of the Grainger-Ring effect has been given by Brinkmann (1968). He has shown that, in air, part of the filling-in of the Fraunhofer lines in the blue sky can be accounted for by rotational Raman scattering in N_2 and O_2, (i.e. an inelastic scattering component). It is perhaps worthwhile to note that such a quasi-continuous component will also depolarize the continuum radiation. Seeking to explain the marked variability of the Grainger-Ring effect and the dependence on solar zenith angle recorded by Noxon and Goody, Hunten (1970) has demonstrated that analogous Raman effects in ground reflected radiation can be expected to produce such changes. It is well known that single Raman scattered light is partially linearly

polarized (7 per cent maximum) and, in fact, to accord with the upper limit of 2 per cent on the degree of polarization of the excess component reported by Noxon and Goody, Brinkmann proposed that multiple scattering and ground reflections would produce the necessary depolarization. Strictly speaking, any model of the atmosphere constructed to include the Grainger-Ring effect must incorporate Raman scattering in the transfer equation in the first instance. However, some physical insight into the usefulness (if any) of polarimetric observations across Fraunhofer lines may be gained by the following heuristic approach.

Suppose the final Stokes Vector of the blue sky radiation, at a given point, is regarded as being composed of a "normal" component $\{r(\lambda)I_0,$ $p'r(\lambda)I_0, 0, 0\}$ and an excess component $\{\rho I_0, \alpha\rho I_0, \beta\rho I_0, 0\}$. If I_{min} is the intensity of the blue sky at the Fraunhofer line centre before the excess component is added, then the ratio $R'_B = \dfrac{I_{min}}{I_0} \equiv R_\odot$, where $R_\odot$ is the ratio of the line centre to continuum intensity in direct sunlight. In the real blue sky,

$$R_B = \frac{I_{min} + \rho I_0}{I_0 + \rho I_0} \neq R_\odot ,$$

from which it can be shown that (Grainger and Ring 1962b),

$$\rho = \frac{R_B - R_\odot}{1 - R_B} .$$

For Hβ, Grainger (1962) gives the average value $\rho = 0.020 \pm 0.004$ at a site in the U.K. but also reports $\rho = 0.05$ for a high altitude location (Chacaltaya). Thus, the composite beam has Stokes Vector

$$W = \begin{bmatrix} (r(\lambda) + \rho)\, I_0 \\ (p'r(\lambda) + \alpha\rho)\, I_0 \\ \beta\rho I_0 \\ 0 \end{bmatrix} ,$$

and hence the degree of polarization p and azimuth of vibration $\emptyset$ (relative to the perpendicular to the scattering plane) are given by,

$$p^2 = \frac{\left(p'r(\lambda) + \alpha\rho\right)^2 + \beta^2\rho^2}{\left(r(\lambda) + \rho\right)^2} \quad ; \quad \tan 2\emptyset = \frac{\beta\rho}{\left(p'r(\lambda) + \alpha\rho\right)} .$$

At the Fraunhofer line centre, $r(\lambda) = R_\odot$ (corresponding to the values p, $\emptyset$ say) and in the blue sky continuum near the line, $r(\lambda) = 1$, corresponding to p_o, $\emptyset_o$). Confining attention to these two discrete wavelengths, and considering first all cases for which $\beta = 0$ then,

$$\emptyset - \emptyset_o = 0 \quad \text{and} \quad p = \frac{p_o(1 + \rho) + \alpha\rho(^1/R_\odot - 1)}{1 + \rho/R_\odot} .$$

Clearly, $\alpha = 0$ corresponds to an unpolarized excess component, $-1 \leq \alpha < 0$, to a component partially linearly polarized orthogonal to the normal Rayleigh component, and $0 < \alpha \leq +1$ to a partially linearly polarized component in the parallel direction.

As expected, $\alpha \leq 0$, leads to a reduction in the degree of polarization at the line centre (i.e. $p < p_o$); however, even if α is positive a depolarization can still result. In fact, ignoring trivial solutions, the condition $p = p_o$ occurs for $\alpha = p_o$, independent of ρ. In other words, an excess component linearly polarized (with degree of polarization less than p_o) <u>parallel</u> to the Rayleigh component still produces a depolarization at the centre of the Fraunhofer line. This result is a consequence of the relative strengths of the polarized and unpolarized intensity components comprising the composite beam. Further, the observed depolarization, p/p_o, can be produced, with <u>no</u> rotation of the azimuth of vibration, by an infinite number of combinations of ρ and α, e.g. with $R_\odot = 0.6$, $p_o = 0.60$ and $p = 0.59$, then suitable pairs are (0.028, +0.05), (0.025, 0.00) and (0.023, -0.05). To disentangle the polarization properties of

the excess component therefore requires very accurate polarimetry and a knowledge of ρ.

When $\beta \neq 0$, that is, the polarization of the excess component is neither parallel nor orthogonal to the scattering plane, then $\phi - \phi_0 \neq 0$. However, since $\beta\rho$ and $\alpha\rho$ are small quantities ($\sim 5 \times 10^{-4}$) then,

$$\phi - \phi_0 \simeq \frac{(1 - R_\odot)}{2 R_\odot} \cdot \frac{\rho}{p'} \cdot \beta .$$

$$= \frac{(1 - R_\odot)}{2 R_\odot} \cdot \frac{\rho}{p'} \cdot p_e \sin 2\phi_e$$

where p_e and ϕ_e are the degree of polarization and azimuth of vibration of the excess component. Inserting typical values, e.g. $R_\odot = 0.60$, $p' = 0.60$, $\rho = 0.02$, $p_e = 0.05$ (5 per cent) and $\phi_e = 45^\circ$, gives

$$\left| \phi - \phi_0 \right|_{max} \simeq 2' \quad (\text{i.e. } 0^\circ.03)$$

Assuming an unpolarized added component ($\alpha = \beta = 0$) and using the observed value of p/p_0 for 1973 Nov 26 with $R_\odot = 0.6$ gives $\rho = 0.025 \pm 0.002$. However, relating the above discussion to the blue sky observations indicates that the polarimetric precision, about ± 0.1 per cent, achieved over short runs such as Block 1, is insufficient to discriminate between an unpolarized excess component and one which is weakly partially linearly polarized in an arbitrary direction. Further, without a knowledge of ρ it is impossible to decide on the nature of the polarization, even when it is definitely known that there is no rotation of the azimuth of vibration across the Fraunhofer line.

Although these findings are perhaps disappointing when such reasonable accuracy has been obtained, it must be remembered that much higher polarimetric precisions are possible given sufficient integration time, compare

$\sigma \sim \pm$ 0.01 per cent for stellar work. Increasing the angular extent of the patch of blue sky observed, making measurements on the north celestial pole rather than the zenith or, better, tracking a point on the Sun's declination arc at the solar rate should help in improving the polarimetry. Further, measurements of Fraunhofer lines such as the H line of Ca II may be more profitable since the filling-in is greater towards the violet. Measurements from a high altitude location would also be worthwhile.

Since the Raman-scattering explanation of the Grainger-Ring effect is open to very few observational tests, it would probably be worthwhile to push this method to the limits of detectability in order to distinguish polarimetrically between Raman effects and, for example, unpolarized aerosol fluorescence.

4.3 Intrinsic Polarization of Be Stars: Discovery of a Reduced Polarization at the Hβ Line Centre in γ Cas

Introduction

Historically, O and B stars have been of interest in polarimetry because they are inherently bright enough for their light to probe the interstellar medium to great distances, and are therefore useful in the study of interstellar polarization. That certain of these stars may exhibit intrinsic polarization was first revealed after Behr (1959b) reported the variability in white light of the linear polarization of γ Cas. This result, and similar reports of variability in X Oph (Shakhovskoj 1962) and X^2 Ori (Vitriczenko and Efimov 1965) however, met with comparatively little interest. In a survey of the wavelength dependence of polarization, Coyne and Gehrels (1967) found several new early-type objects with variable polarization, while a new tool in identifying early-type stars with intrinsic polarization was introduced by Serkowski (1968). He found that emission-line stars exhibit a

peculiar wavelength dependence of polarization becoming abnormally low in the ultraviolet. More recently, Coyne and Kruszewski (1969) and Coyne (1971) using a series of broad band filters have observed the polarization-wavelength curve in the region 3000 Å to 1 μm in a large number of Be stars. Dips in the polarization at the wavelengths of the Balmer and Paschen limits of hydrogen are attributed to electron-scattering in an asymmetric circum-stellar cloud modified by unpolarized radiation from hydrogen recombination and by hydrogen bound-free opacity within the cloud. A model of the Be star ζ Tau incorporating these features, together with a free-free emission com-ponent required to explain the decrease in p in the infrared (out to 2.2 μm), has been published by Capps, Coyne and Dyck (1973). Serkowski (1971) poin-ted out that the only rapidly rotating early-type stars that show measurable intrinsic polarization in broad wavelength bands are those that have extended atmospheres or envelopes, as evidenced by the presence of emission lines.

The available broad band measurements smooth out the variation of pola-rization with wavelength and some of the passbands include emission lines, such as the Balmer lines, known to be variable from spectroscopic evidence. Therefore, it seemed reasonable to expect that moderate and high-resolution spectropolarimetric observations of Be stars and similar objects (fast rota-tors, eclipsing binaries and late-type supergiant stars) would reveal pola-rization effects within their line profiles (Clarke and McLean 1974a, pro-posal made to IAU Colloquium No. 23 (1972)).

In the next section, observations made with the twin Hβ-spectropolari-meter of three Be-shell stars, viz., γ Cas, ζ Tau and 48 Per, and of the blue supergiant α Cyg, are reported. A reduced polarization has been discovered at the centre of the Hβ emission feature in γ Cas (Clarke and McLean 1974b) and a similar effect found in ζ Tau. This latter result confirms unpublished

measurements of lower spectral resolution made by Zellner and Serkowski (1972), and is consistent with recent observations of a depolarization effect at Hα in this star (Coyne 1974, personal communication).

Observations

Although several preliminary observations of γ Cas (m_v = 2.8 v, BOpe) prior to 1973 Nov indicated that there was a fall in the degree of polarization at the Hβ line, the polarimetric precision was insufficient to establish the fact unequivocally. To investigate the suggested effect more thoroughly, further observations were made, with longer integration times, on the emission feature and on each wing. A filter of 10 Å passband (λ_o = 4869 Å) was used for scanning the Hβ line and a broader filter (25 Å) was tilted to pass a wavelength of about 4835 Å and remained fixed in Beam 2 to act as a monitor (as described in Section 4.1). The 10 Å filter was selected for this investigation to maximise the amount of light collected. It is clear from Fig. 4.9(a) that continuous tilting of the 10 Å filter provides a useful record of the stellar line profile. Wavelength-tilt calibration was achieved in the usual way by piping light from laboratory lamps to the polarimeter diaphragm by fibre-optic tube. After examination of the line profile, the discrete wavelengths of 4847, 4863 and 4869 Å were chosen for the polarimetric observations; the longest wavelength corresponds to the filter being at normal incidence in the collimated beam.

Observations of the linear polarization at these wavelengths were taken over integration times typically of 30 minutes. The Stokes parameters were determined about 40 times during this interval and mean values obtained with their standard errors. Comparison measurements made at precisely the same wavelengths (i.e. tilts) on β Cas and α Aur enabled the instrumental polarization to be subtracted out. A mean error of σ = ± 0.0003 (i.e. 0.03 per cent)
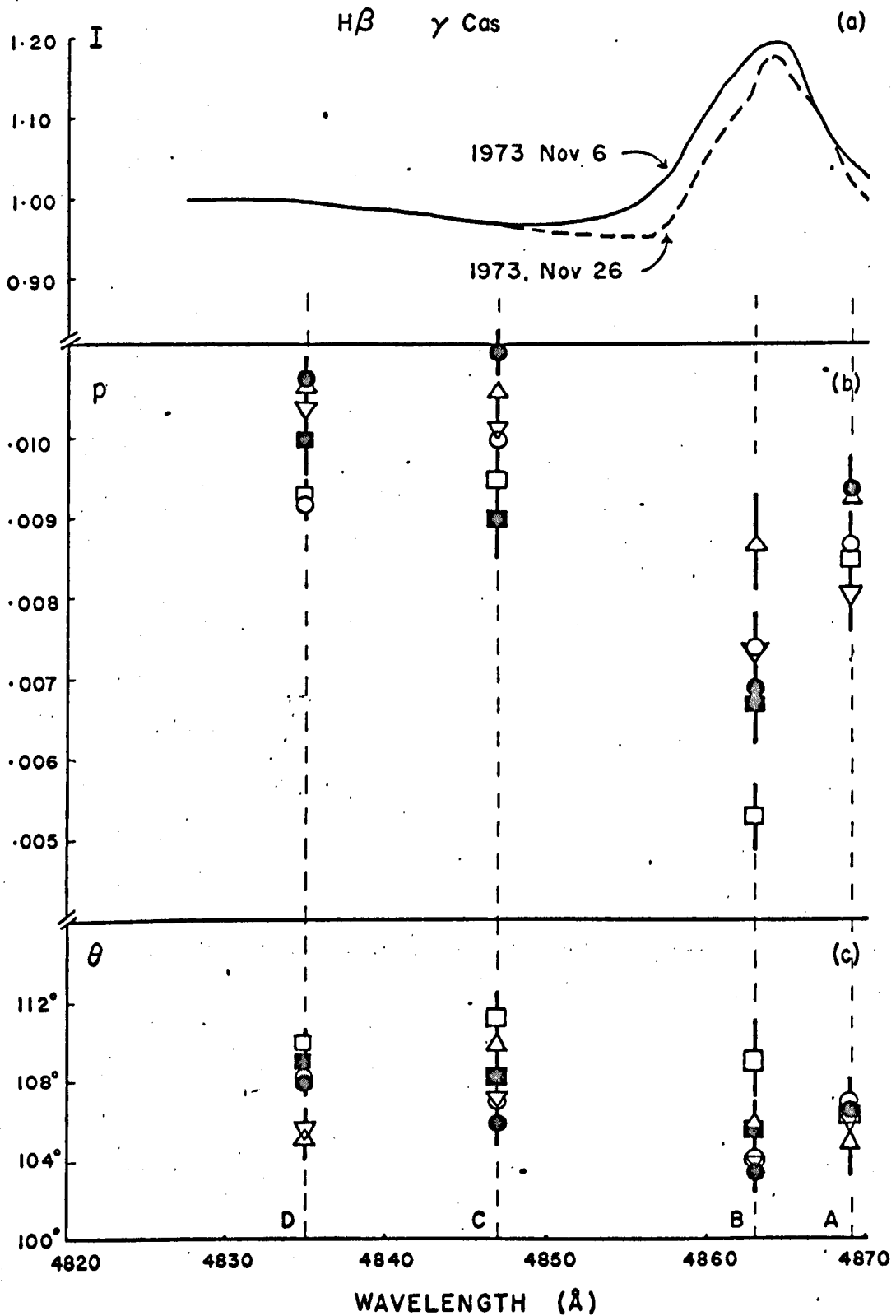
Fig. 4.9 (a) Normalised wavelength scan of the Hβ emission feature in γ Cas obtained by tilting a 10 Å interference filter. Labels A, B and C indicate the discrete wavelengths isolated for polarimetry by the 10 Å filter while the monitor 25 Å filter (Beam 2) is labelled D. Values of p, in decimal fractions, are displayed in (b) and the azimuth of the direction of vibration, θ, (equatorial co-ordinates) in (c) for six nights, 1973 November 3 (△), November 5 (▽), November 6 (○), and November 26 (□), December 14 (●), December 30 (■).

in each Stokes parameter was typical for γ Cas and $\pm$ 0.02 per cent typical for β Cas and α Aur but, of course, the integration times for α Aur were shorter (about 15 minutes).

Measurements

Fig. 4.9(b) and (c) illustrates measurements taken with the polarimeter attached to either the 91 cm telescope at Herstmonceux or the 51 cm telescope at Glasgow. Clearly, there is a marked dip in the degree of polarization, p, across the emission feature. For example, comparing values of p at $\lambda\lambda$ 4847 $\overset{o}{A}$ and 4863 $\overset{o}{A}$ for 1973 Nov 6, the difference was about 0.0026 (0.26 per cent) while on 1973 Nov 26, it was much larger, 0.0042 (0.42 per cent). On other occasions the degree of polarization at λ 4847 $\overset{o}{A}$ is not the same as on the two dates mentioned. The individual values of p on Nov 6 and Nov 26 were obtained (after correction for instrumental polarization) to a precision of $\sigma = \pm$ 0.0004 (i.e. $\pm$ 0.04 per cent) for the line values and to $\sigma = \pm$ 0.0002 for the values at λ 4835 $\overset{o}{A}$. Not only is the depolarization effect strongly evident, it is clearly variable.

Since each sequential measurement within the line is accompanied by a simultaneous measurement in the monitor beam, these latter values can therefore reveal any time dependent broad band polarization changes which might otherwise render interpretation of the Hβ line observations difficult. In fact, on all six nights, the difference between any two of the three mean values of p, Θ obtained at $\lambda/\Delta\lambda$ = 4835/25 was less than the sum of the derived standard errors of those means. This useful test is both stringent and quickly applied. Hence, these values have been combined to obtain nightly mean values which have been plotted in Fig. 4.9(b) and (c), (Label D). Light from the line centre being passed by the wings of the 25 $\overset{o}{A}$ filter profile would result in a reduction of the degree of polarization at λ 4835 $\overset{o}{A}$. If

Table 4.1   Hβ Polarimetry of 48 Per and ζ Tau

Star	Date (1973)	λ/Δλ Å	p (%)	Θ (degrees)
48 Per (m$_v$ = 4.03, B3Vpe)	Nov 4	4869/10	0.98 ± 0.11	171 ± 4
	"	4861/10	1.02 ± 0.13	175 ± 4
	"	4854/10	1.09 ± 0.13	175 ± 4
	"	4837/25	0.89 ± 0.05	174 ± 2
ζ Tau (m$_v$ = 3.0, B2 IV pe)	Nov 6	4869/10	1.34 ± 0.07	31.4 ± 1.5
		4837/25	1.56 ± 0.07	34.1 ± 1.2
	"	4861/10	1.07 ± 0.05	32.9 ± 1.5
		4837/25	1.49 ± 0.035	34.3 ± 0.8
	"	4853/10	1.31 ± 0.05	33.2 ± 1.1
		4837/25	1.68 ± 0.044	33.9 ± 0.7
	Mean	4837/25	1.57 ± 0.06	34.1 ± 0.5
	Nov 26	4869/10	1.20 ± 0.06	32.4 ± 1.4
		4837/25	1.43 ± 0.05	33.4 ± 0.9
	"	4861/10	0.91 ± 0.06	32.7 ± 1.9
		4837/25	1.48 ± 0.04	34.2 ± 0.7
	"	4848/10	1.54 ± 0.05	32.5 ± 0.9
		4837/25	1.48 ± 0.04	34.6 ± 0.7
	Mean	4837/25	1.46 ± 0.02	34.1 ± 0.5

this was the case, then the observed night to night variations at that wavelength should be closely correlated with those at λ 4861 Å. However, inspection of, for example, the data for Nov 6 and Nov 26 shows that the polarization at the line centre is markedly different while no corresponding differences occur at the other wavelengths. For a Gaussian filter profile centred on λ 4835 Å, the transmission factor is only 5 per cent at λ 4861.Å; this factor is more than doubled for an Airy function. Therefore, variability on the line wings, rather than at the line centre, should most affect the monitor beam measurements. From the diagram it can be seen that the degree of polarization at the line centre was almost the same on the dates Dec 14, Dec 30 and only slightly different at λ 4835 Å. In contrast to these values, the degree of polarization at λ 4847 Å is quite different for the two nights by an amount greater than three times the standard error in the mean separation. Further, the overall impression gained from the diagram of Fig. 4.9 is that there is a shift in the absolute value of the degree of polarization measured on different nights while the general shape of the depolarization effect remains unchanged. These arguments lead to the important conclusion that more than one effect may be responsible for the observed polarization structure and variability across Hβ in γ Cas.

A similar series of measurements was performed on two other well known emission-line shell stars, viz., ζ Tau (m_V = 3.0, B2 IV pe) and 48 Per (m_V = 4.03, B3 V pe). The results are displayed in Table 4.1. Reproduced in Fig. 4.10(a) is a 10 Å tilt-scan of the shallow Hβ line profile of ζ Tau. Some evidence is apparent at this resolution for the complex emission and shell-absorption structure well known to be present at Hβ in this star.

For 48 Per, no effect was apparent to within the precision of the measurements obtained which are poorer than for γ Cas because the star is fainter.
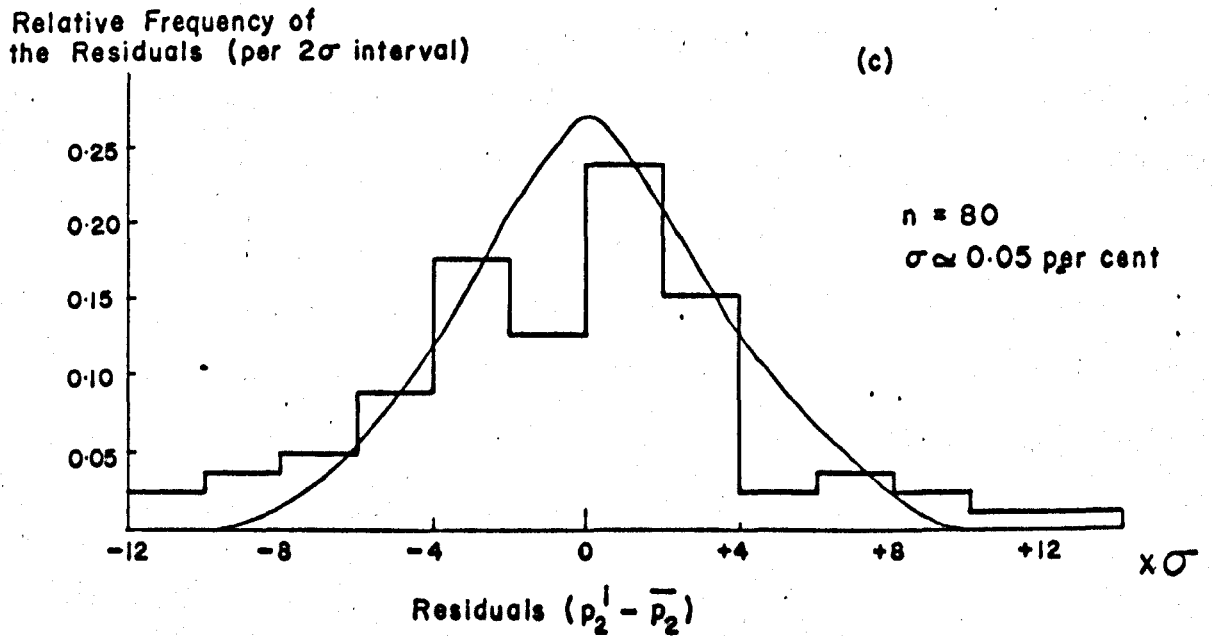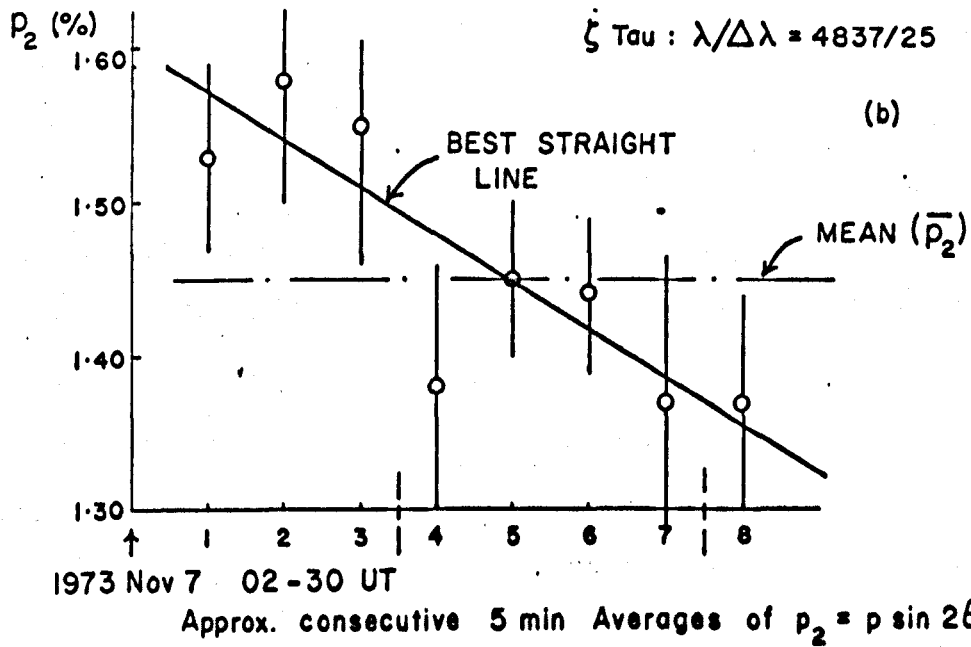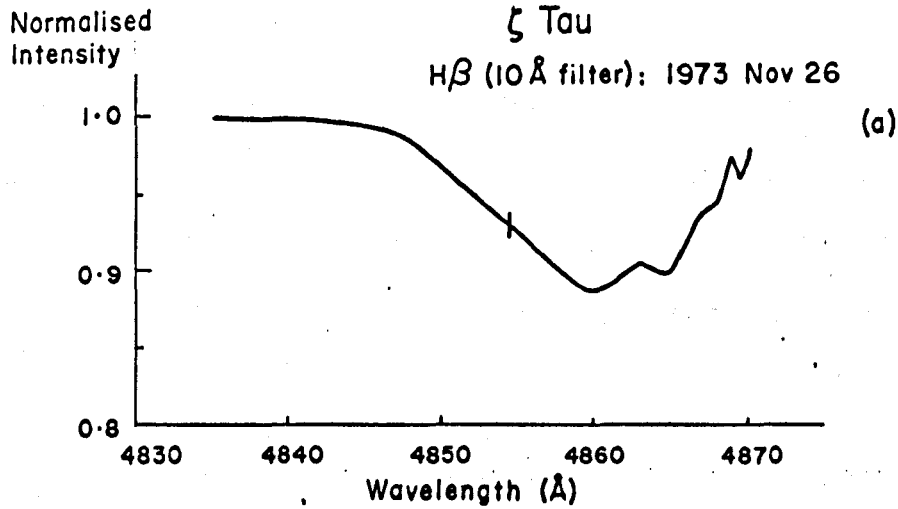
Fig. 3.10 (a) 10 Å tilt-scan of Hβ in ζ Tau. (b) Variation of p₂ with time at λ/Δλ = 4837/25 Å on 1973 Nov 6. (c) Histogram showing the relative frequency of the residuals for all the data of (b).

Much longer integration times or use of a larger collector will be required to further investigate this star. However, the reduced polarization at Hβ is clearly evident in ζ Tau on 1973 Nov 6 and again on Nov 26 although on the earlier date, the monitor beam gives diverse results for three sequential runs. Detection of such time variability during line profile measurements is precisely why the monitor beam is used. However, before any conclusions can be drawn regarding the intrinsic nature of the effect, possible instrumental sources must be considered.

It has already been shown in Section 4.1 that altering the tilt of the interference filter used for scanning the line profile results in a small change in the instrumental polarization which only becomes important at large angles of tilt. For that reason measurements are made on comparison stars at each tilt to ensure complete elimination of any systematic error from this source. The filter in the monitor beam remains at a fixed tilt and therefore does not suffer from this effect. Further, care is taken to tilt both filters in such a direction that reflected light from one beam cannot pass directly into the other beam. Light reflected back into the polarizing prism from either filter should not be capable of entering the other beam, at least to a first approximation, since the two components are orthogonally polarized. Finally, a similar discrepancy between consecutive measurements at $\lambda/\Delta\lambda = 4835/25$ Å was not observed for any of the stars α Aur, β Cas, γ Cas and 48 Per observed on the same night and for the same star, ζ Tau, on a different night.

A histogram of all the values of the larger of the two linear Stokes parameters, $p_2 = U/I = p \sin 2\theta$, obtained at $\lambda/\Delta\lambda = 4835/25$ Å on Nov 6 is reproduced in Fig. 4.10(c) while a plot of almost consecutive 5-minute averages of p_2 is given in Fig. 4.10(b). Although the precision is reduced by averaging over such short time intervals, the change is still apparent and it

is clear that it occurred most strongly near the time when the 10 Å filter was tilted, yet there is no evidence to support an association of the two. In the histogram, the decrease in p_1 appears as a skew distribution with a preponderance of negative residuals.

These measurements amply demonstrate the importance and the advantages of a monitor beam and a line profile scanning device in the polarimetric study of variable stars.

Discussion

Since the emission at Hβ is localised to the stellar neighbourhood, then the observation of a reduction in polarization indicates directly that a substantial part of the polarization is intrinsic to the star. The strongest polarization variability is associated with the emission feature which is itself variable.

As far as can be seen from the reported observations, there is no evidence for any rotation of the azimuth of vibration across the Hβ feature of either γ Cas or ζ Tau (see Fig. 4.9(c); Table 4.1). If this is in fact the case, then the depolarization effect can only be produced by the superposition of an orthogonally polarized component, or by the superposition of an unpolarized component, or by a combination of both. The simplest mechanism to consider is the addition of an unpolarized emission component of intensity xI where I is the original total intensity at the centre of the underlying absorption line. If p_0 refers to the degree of polarization in the nearby continuum and p_1 to that at the wavelength of the line, then $p_1/p_0 = 1/(1+x)$. Depolarization ratios for the γ Cas measurements of Fig. 4.9 are displayed in Table 4.2.

In order to produce an effective depolarization ratio of 0.80 (for

Table 4.2   Polarization Ratios across Hβ in γ Cas

JULIAN DATE (244,0000 +)	p (%) (λ4835)	$\dfrac{p(\lambda 4847)}{p(\lambda 4835)}$	$\dfrac{p(\lambda 4861)}{p(\lambda 4835)}$	$\dfrac{p(\lambda 4861)}{p(\lambda 4847)}$
1990.40	1.07 ± 0.04	0.99 ± 0.05	0.81 ± 0.04	0.82 ± 0.06
1992.50	1.04 ± 0.03	0.97 ± 0.05	0.71 "	0.73 "
1993.38	0.92 ± 0.02	1.09 ± 0.03	0.80 "	0.74 ± 0.05
2013.26	0.93 ± 0.02	1.02 ± 0.03	0.57 "	0.56 "
2030.50	1.07 ± 0.02	1.04 ± 0.03	0.74 "	0.71 ± 0.06
2047.50	1.01 ± 0.05	0.89 ± 0.05	0.66 "	0.74 ± 0.06

Table 4.3   Linear Polarization Measurements across Hβ in α Cyg (A2Ia)

JULIAN DATE (244,0000 +)	λ/Δλ (Å)	p per cent	θ (deg)	Integ. Time (Min)
2030.25	4861/10	0.377 ± 0.025	35 ± 2	30
	4847/10	0.367 ± 0.025	35 ± 2	30
	4835/25	0.400 ± 0.019	38 ± 1.5	60

example, p(4861)/p(4835) in γ Cas on Nov 6) then an added unpolarized flux equal to 25 per cent of the original flux is required, while to obtain p(4861)/p(4835) equal to 0.50 requires x = 100 per cent, which is still just consistent with the strength of Hβ emission and underlying absorption in γ Cas. Only one digitized scan of the Hβ line in γ Cas was taken on each occasion and that on 1973 Nov 26 contained two spectral points fewer than the scan taken on Nov 6, hence, the normalised profiles shown in Fig. 4.9(a) are not directly comparable. The apparent constancy of the values of p on the wings and nearby continuum of Hβ on the two nights mentioned above contrasts with the large changes occurring at the line centre. Clearly, future studies must include frequent, calibrated scans of the line profile, in order to test the hypothesis that the polarization variations are related to the emission strength.

From spectroscopic evidence (Underhill, 1960) it is estimated that the radius of the region producing hydrogen emission is about 10 stellar radii, while the main body of gas lies at 2 or 3 stellar radii from the star, thus lending support to the idea that the hydrogen emission does not suffer scattering in the circumstellar cloud and is therefore likely to be unpolarized.

The model for the continuum polarization of the Be-shell star, ζ Tau, given by Capps, Coyne and Dyck (1973), involving electron-scattering, modified by hydrogen absorption, in an optically thin, ionized equatorial disc, is, apart from the simplified geometry, likely to be complicated by intrinsic polarization produced by the rapidly rotating underlying star. Hutchings (1970) has calculated absorption- and emission-line profiles for a rotating, geometrically distorted star. He found that the observed profiles in the spectrum of γ Cas were fitted best by those computed for an O8 star, rotating at break-up velocity, with a rotationally ejected outer envelope. The

envelope is almost disc-like at the contact point with the stellar equator but very extensive perpendicular to this plane at several stellar radii. Although such a computational method may not produce a unique model, the "doughnut-shaped" shell together with a rapidly rotating O8 star might also explain the observed variations in the continuum polarization and the line profile polarization of γ Cas reported here.

Polarization to be expected from rotationally distorted early-type stars has already been discussed in Section 1.2; the points of concern here are:

1. Whichever mechanism is involved in producing the polarization properties of the light from Be-shell stars, (e.g. scattering in an optically thin disc of ionized hydrogen or radiative transfer in rotationally distorted extended atmospheres), hydrogen emission occurs in optically thin regions on the fringes of the stellar "atmosphere." Hence, the depolarization effect across Hβ establishes the presence of intrinsic polarization.

2. High resolution/high precision polarimetry on emission line wings, together with wavelength scans of the profile, may reveal further polarization structure associated with rotation effects. Correlations between polarization and spectral variations may also be revealed. For example, if the circumstellar shells are produced by mass loss, it is possible that a time lag may occur between changes in emission strength and continuum polarization. Marginal evidence for small additional polarization effects in the wings of Hβ is suggested by the measurements reported here. Further observations, perhaps with the 2.5 Å filter, are certainly needed.

For comparison with the Be-shell stars, observations were made on another star, with an extended atmosphere, known to show broad band polarization, namely, α Cyg (A2 I a). This star is a highly luminous supergiant,

which shows Hα emission and variability in other Balmer lines. It shows no evidence of a shell spectrum but line profile changes indicate possible radial movements of its atmosphere (Underhill, 1966). Polarization measurements at three wavelengths across the Hβ line are given in Table 4.3. To the precision of these observations ($\sigma \simeq \pm 0.02$ per cent), no polarizational effects are apparent and the measurements agree very well with the broad band values given by Serkowski and Chojnacki (1969), i.e. $p = 0.37 \pm 0.018$, $\theta = 30°$. However, since α Cyg is not a rapidly rotating star, intrinsic polarization arising in the extended atmosphere is probably unlikely to result in any net effect, in either the continuum or the line. Measurements across the Hα emission feature would settle the nature of the polarization of this star.

Polarimetry with high spectral resolution of objects in the categories discussed or referred to in this section has only just begun and widespread discoveries can be expected in the future.

4.4 Magnetic Stars – Intrinsic Linear and Circular Polarization Associated with the Zeeman Effect in Hβ.

Introduction

A powerful, and perhaps the most topical, application of narrow band spectropolarimetry concerns the detection of magnetic phenomena by measurement of the intrinsic polarization of spectral lines. Reported in this section are linear and circular polarization measurements made on the Hβ line of a small selection of magnetic and suspected magnetic stars.

The first stellar magnetic field detected was in the peculiar A-type (Ap) star 78 Virginis (Babcock 1947). Measurement of the field strength was achieved by recording, side by side, high dispersion spectra in left- and right-circularly polarized light and then using the systematic displacement

between the absorption lines in the two spectra. This displacement is produced by the longitudinal Zeeman effect in absorption. Briefly, in the normal Zeeman effect, a single spectral line appears split into three independent, polarized components – the Zeeman triplet – when the atomic transition occurs in an external magnetic field. When the resulting spectrum is viewed in a direction at right angles to the applied field (transverse Zeeman effect), a central component (π), linearly polarized parallel to the field, is seen, together with two displaced components (σ) polarized perpendicular to the field and of half the intensity of the π component. For a field directed toward the observer (longitudinal Zeeman effect), only two circularly polarized, displaced components (σ) of equal intensity and opposite handedness appear. If the Zeeman triplet is viewed in an arbitrary direction, the σ components are elliptically polarized and the relative intensity of the π, σ components altered. The wavelength separation of the σ components from the undisplaced central component is proportional to the strength of the applied field.

Stellar magnetic fields have been detected by photographic methods (Babcock 1962) in about 100 stars, mostly of early spectral type, and a catalogue has been compiled by Babcock (1958). Also contained in that catalogue is a list of stars in which magnetic fields are probable but not firmly established, and others in which the spectral lines are too broad to permit any measurements of Zeeman splitting. According to Preston (1969), the precision attainable is about 150 to 200 gauss standard error in suitable sharp-lined stars. For stars in which the narrow metallic lines are broadened by stellar rotation and those in which the magnetic field is very weak, detection from the absorption line profiles alone is rendered impossible by the very small separation of the σ components compared to the line width. How-

ever, in all cases, residual circular polarization in the wings of the un-
resolved profile can be used to yield the value of the effective longitudinal
component of the magnetic field. Photoelectric polarimeters are superior to
photographic instruments in this regard and have been regularly employed in
very high precision observations of the Sun. Recently, several workers
have adapted the same technique for application to stellar measurements.

Intrinsic linear polarization in magnetic Ap stars has been a controver-
sial topic for many years. Thiessen (1961) reported variable linear polariza-
tion for HD71866 and suggested that it was not of interstellar origin, but
associated with the magnetic properties of this star. He also reported large
linear polarization effects related to the measurement of equivalent widths
of the spectral lines of certain stars (Tamburini and Thiessen 1961). These
results were repudiated by other people on the basis of overanalysis or mis-
interpretation. Isolated evidence, such as the report by Clarke and Grainger
(1966) of a polarization effect across Hβ in γ UMa, appears to have gone almost
unnoticed. Survey measurements in broad or unfiltered passbands by Hiltner
and Mook (1967), and Serkowski and Chojnacki (1969) produced negative results.
Since a Zeeman triplet observed without spectral resolution is unpolarized,
it is apparent that the higher throughput of broad band polarimetry is off-
set by the smallness of any residual intrinsic polarization arising from, for
example, line blanketing or the slope of the spectral energy curve. The
method adopted in this work relies on the rapid wavelength variation of pola-
rization expected across a spectral line affected by a magnetic field, in
comparison to the slowly changing wavelength dependence of the interstellar
component.

It has been encouraging and stimulating to note that a considerable
interest has developed over the past four or five years in photoelectric

polarimetry of magnetic or suspected magnetic stars. Recent advances have
already been summarised in Section 1.3. Some of the stars observed during
the course of this work were also observed independently by other researchers
using different techniques. For example, Borra and Landstreet (1973) have
employed a coudé photoelectric Pockels cell polarimeter to survey 23 bright
stars for circular polarization in the wings of metallic lines, while Kemp
and Wolstencroft (1973c, 1974) have used discrete narrow band interference
filters for Hβ polarimetry with a single beam polarimeter employing a photo-
elastic modulator.

The fractional circular polarization on the wings of a Balmer line,
such as Hβ, is typically 50 to 100 times smaller than for sharper metallic
lines, such as those of CrI. A passband of about 10 Å will cover most of
one wing of Hβ while a passband of about 0.2 Å is required for sharp lines.
Consequently, assuming the same optical transmittance, about 50 times more
signal is obtained with the Balmer line. In practice, a larger increase in
signal is probably attainable because methods involving a high-resolution
line profile scanner often require a coudé telescope system with the added
drawback of time-dependent instrumental polarization produced by the oblique
reflections in the mirror train. Off-setting these disadvantages somewhat,
is the useful feature of the coudé system in permitting a choice to be made
of several spectral lines with high Landé g-factors. A very high resolution
method is superior provided a large enough collector is available and there
are obvious advantages if a multi-channel instrument can be employed. How-
ever, taking account of the complexity involved and the need for a large
collector, and remembering the importance of hydrogen emission in Be stars,
discrete narrow band interference filters for Hβ were selected for the work
on magnetic stars reported here. The additional feature of the Hβ-spectro-

polarimeter, already described, to obtain a record of the line profile by tilt-scanning and the two-beam facility for simultaneous measurement on, for example, each wing of the line, are important advantages of this method.

OBSERVATIONS

So far, the sample of stars studied for linear and circular polarization effects across Hβ is small and restricted to Ap stars. This is partly a consequence of observing conditions but also because many of the most interesting magnetic and suspected magnetic stars are fainter than m_v = 4.0, thus a large collector is essential.

The strength of polarization in a line profile, $I(\lambda)$, is determined by the effective magnetic field H_e, in the region of line formation, that is the mean component along the line of sight $(H_e = H \cos \gamma)$, and by the spectral slope, $dI/d\lambda$. Let $r(\lambda)$ represent the intensity profile of one of the σ components, in a Zeeman triplet, convoluted with the instrumental profile of the scanning monochromator. Representing the Zeeman splitting by $\Delta\lambda$, where

$$\Delta\lambda = \frac{e}{4\pi mc^2} g \lambda_o^2 (H \cos \gamma) \quad ,$$

then for the case in which the Zeeman splitting is negligible compared to the line width, the resultant intensity profile and the fourth Stokes parameter (V) are given by,

$$I(\lambda) = r(\lambda + \Delta\lambda) + r(\lambda - \Delta\lambda)$$
$$V(\lambda) = r(\lambda + \Delta\lambda) - r(\lambda - \Delta\lambda)$$

since $\Delta\lambda \ll \lambda$ these expressions can be rewritten as,

$$I(\lambda) \simeq 2r(\lambda)$$
$$V(\lambda) \simeq 2\Delta\lambda \cdot \frac{dr(\lambda)}{d\lambda}$$
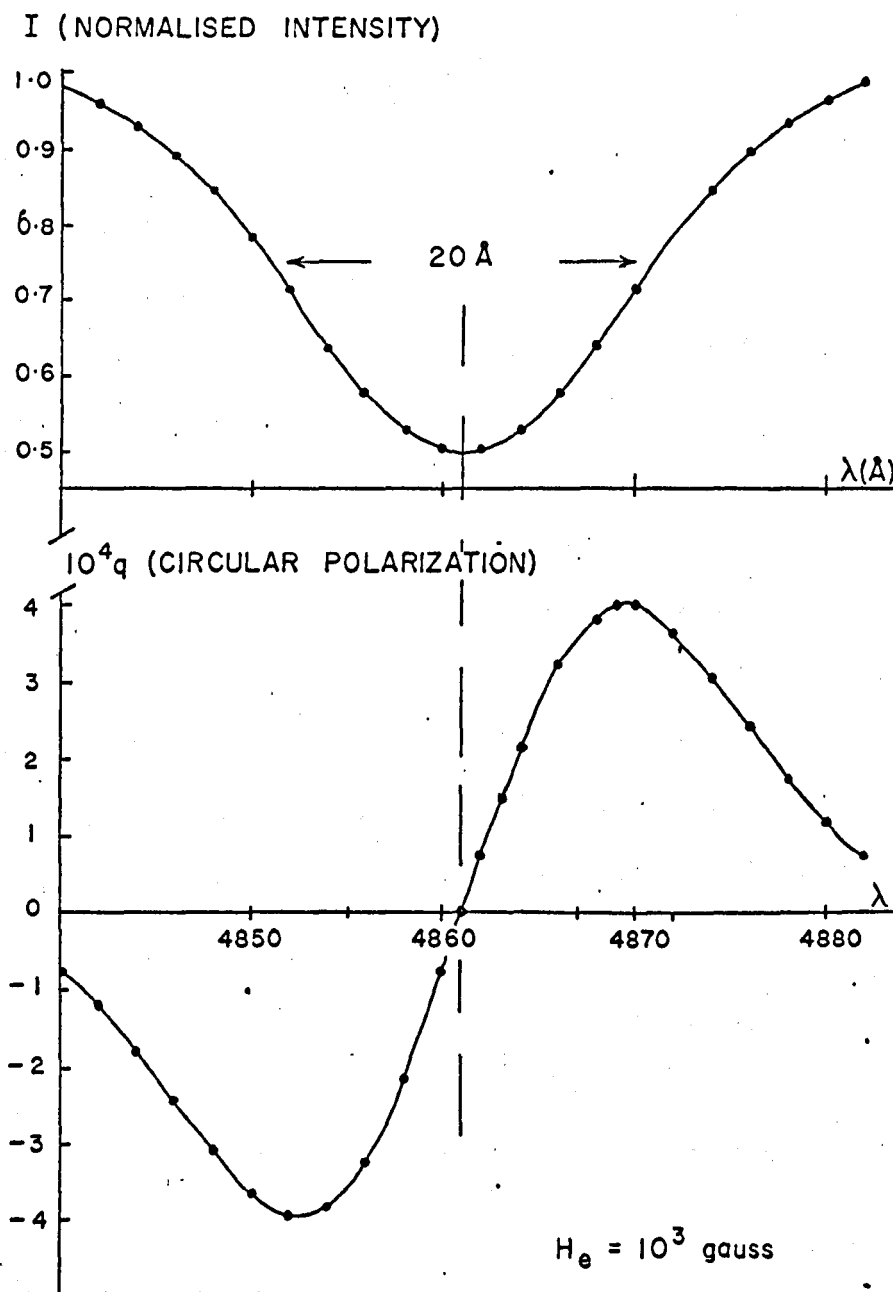
Fig. 4.11   Fractional circular polarization q (in units of 10^4), across a broad, idealised (Gaussian) Hβ line profile in which the Zeeman splitting due to a magnetic field of 1 kilogauss is completely unresolved.

giving for the fractional circular polarization, $q(\lambda) = V/I$, at wavelength λ near the Balmer line Hβ (λ_o = 4861.3 $\overset{o}{A}$),.

$$q(\lambda) \simeq 1.104 \times 10^{-5} \, H_e \, \frac{dI(\lambda)/d\lambda}{I(\lambda)} \qquad (1)$$

where H_e is in gauss.

The important point is that the measured line profile $I(\lambda)$ and fractional circular polarization $q(\lambda)$, at wavelength setting λ, together give all the information required to derive H_e. It is not necessary to know the instrument or stellar line profile separately.

Figure 4.11 shows the antisymmetric variation of $q(\lambda)$ across a normalised Gaussian line with a full width at half maximum transmittance (FWHM) of 20 $\overset{o}{A}$ and residual intensity 0.5 at the line centre, for a magnetic field of 1 kilogauss. Profiles of approximately this width and depth are obtained by tilt-scanning the Hβ line, in early-type stars, with an interference filter of 10 $\overset{o}{A}$ passband. Notice that for this magnitude of field the separation of the σ components ($2\Delta\lambda$) is only 0.022 $\overset{o}{A}$.

Since the resolution used for all the observations reported here (10 $\overset{o}{A}$) is comparable to the width of one line wing, the fitting procedure amounts to evaluating the mean circular polarization and mean normalised gradients of the two line wings, that is,

$$q^* = \frac{1}{2}\left[q_{RED} - q_{BLUE}\right] \quad \text{and} \quad g = \frac{1}{2}\left[\left(\frac{dI}{d\lambda}/I\right)_{RED} - \left(\frac{dI}{d\lambda}/I\right)_{BLUE}\right] \quad ,$$

and inserting these in equation (1).

Measurements were made by first tilt-scanning a 40 - 50 $\overset{o}{A}$ band across Hβ with a 10 $\overset{o}{A}$ filter to obtain the line profile. The scans are not centred on Hβ because of the normal incidence wavelength cut-off of the available

Table 4.4   Circular Polarization at Hβ in eight Ap Stars

	(1)		(2)	(3)	(4)	(5)	(6)	(7)
STAR	m_v	Sp	JULIAN DATE (244,0000+)	$10^4 q*$	MEAN GRAD. $g(Å^{-1})$	H_e (gauss)	TOTAL INTEG. TIME (min)	NOTES (incl. telescope)
α And	2.2	B9p	1992.375	+ 0.7 ± 1.8	0.040	+ 159 ± 409	69.5	(a), 1, 91 cm
			1998.3	− 2.7 ± 1.6	"	− 615 ± 364	87.6	(b), 1, "
β Aur	2.1	A0p	1992.625	+ 0.2 ± 2.7	0.056	+ 32 ± 440	26.0	(a), 1, "
α² CVn	2.9	A0p	1999.71	− 4.9 ± 4.0	0.035	−1270 ± 1040	17.6	(b), 1, "
			2142.48	− 3.9 ± 2.3	0.034	−1039 ± 613	13.5	(b), 2, 250 cm
β CrB	3.7	F0p	2142.58	− 1.7 ± 1.8	0.034	− 455 ± 482	32.0	(b), 2, "
γ Cyg	2.2	F8Ib	2047.50	− 4.2 ± 10.5	0.030	−1280 ± 3200	20.0	(a), 1, 51 cm
α Dra	3.6	A0p	2142.54	− 1.7 ± 1.7	0.024	− 645 ± 645	24.0	(a), 2, 250 cm
52 Her	4.8	A3p	2142.66	+ 1.4 ± 2.2	0.030	+ 425 ± 664	30.0	(b), 2, "
15 UMa	4.5	A2-F4m	2142.50	− 2.4 ± 2.2	0.032	− 679 ± 764	22.0	(b), 2, "

NOTES:

(a) Sign of q   same for both wings.

(b) Sign of q   changes from one wing to the other.

1. Sequential measurements of q with one beam.

2. Simultaneous   "   " " using both beams.

filters. Positions about $\pm$ 6 Å either side of the line centre, corresponding as closely as possible to the points of steepest gradient, were selected and the circular polarization measured at these wavelengths. Several determinations of q are obtained from which a mean value and its standard error can be derived. Instrumental circular polarization at each of the wavelength settings used was assumed to be given by the results for β Cas and α Aur, and was subtracted out. No attempt was made to remove LCC effects by repeating the measurements with the polarimeter rotated through 90°. This is justified for the present observations because all of the stars selected have a weak component of interstellar linear polarization. Intrinsic linear polarization of Hβ, if any exists in these stars, should be approximately symmetric across the line, hence any contribution to q from this source will be minimised by taking the antisymmetric mean, q*.

The accumulated data is summarised in Table 4.4. Sequential measurements across the line, using a single 10 Å filter, were made when the polarimeter was attached to the two smaller collectors, while for the run on the 2.5 m Isaac Newton Telescope, two 10 Å filters were employed to obtain simultaneous observations of each wing. Column (2) of Table 4.4 gives the Julian date at the beginning of each run and column (3) the antisymmetric mean circular polarization, q*, in terms of the convenient unit 10^4; (10^4q* = 1 is equivalent to q* = 0.01 per cent). A real effect appears as a circular polarization which reverses sign from one wing to the other, but, because of rotational effects and non-uniformity of the magnetic field over the projected stellar disc, the magnitudes of q may be different for each wing. In column (4) is given the mean value of the normalised line profile gradient, g, and in column (5) is the effective magnetic field H_e and its standard error, derived from equation (1). Positive q*/g implies a field
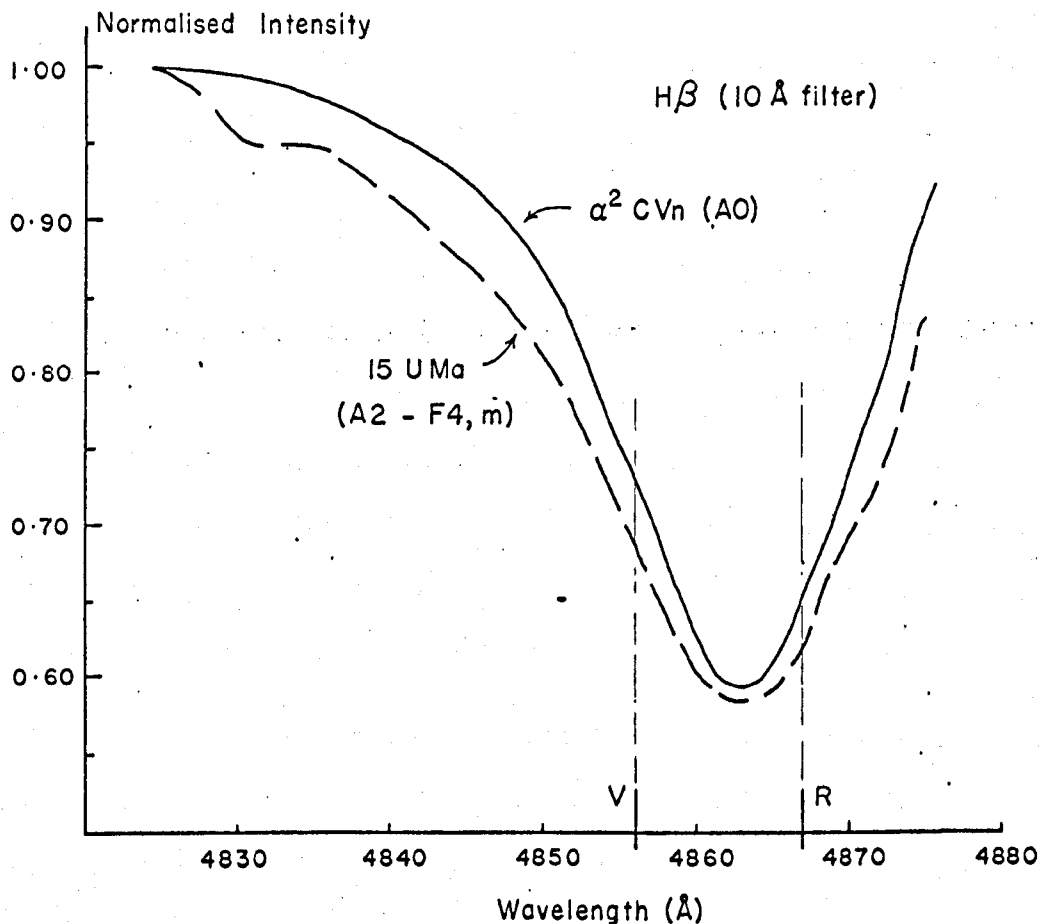
Fig. 4.12 (a) Hβ line profiles of two Ap stars obtained by tilt-scanning of
a 10 Å interference filter (λ_0 4875 Å). Fixed positions used for
circular polarimetry are indicated by V and R.
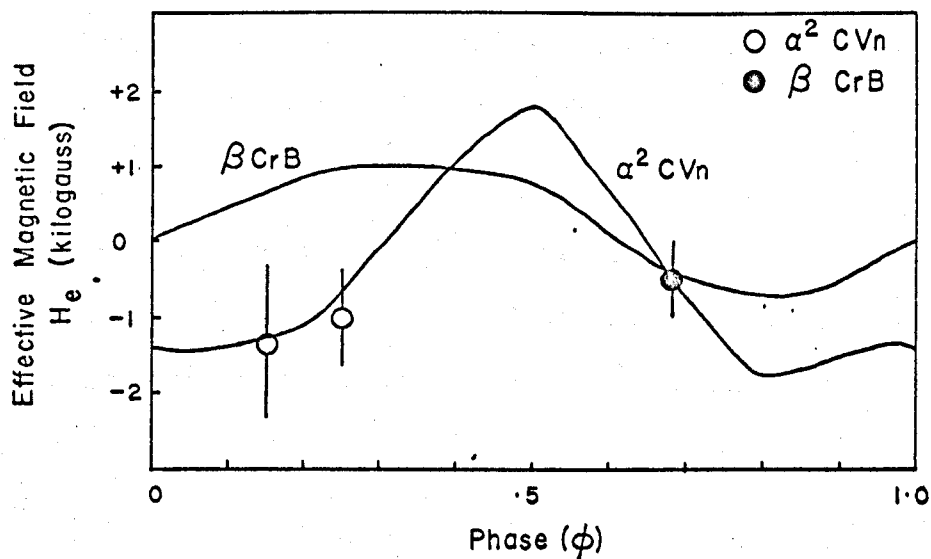

Fig. 4.12 (b) Idealised phase curves for α^2 CVn and β CrB reproduced from
Kemp and Wolstencroft (1974), Pyper (1969), Jarzebowski (1965) and
Preston and Sturch (1967) respectively.

directed toward the observer and positive (right-hand) circular polarization corresponds, as usual, to a counterclockwise rotation of the electric vector with increasing time.

Typical Hβ scans of two Ap stars are reproduced in Fig. 4.12(a). The fractional error at any point in each profile is less than 0.01 (i.e. 1 per cent). Consequently, the shape of Hβ in the metal rich star, 15 UMa, is real and, in fact, a similar but less pronounced kink in the blue wing is also apparent for β CrB. This star has spectral type F0, intermediate between the peculiar classification A2-F4 of 15 UMa and the structure in the spectrum in each case is probably due to lines of ionised iron.

Idealised phase curves for the periodic magnetic variables α^2CVn and β CrB are shown in Fig. 4.12(b). That for α^2CVn is a reproduction of one given by Kemp and Wolstencroft (1974), who derived it from the work of Pyper (1969), modified by the writer to agree with the shape reported by Jarzebowski (1965). The phase curve of β CrB is taken from Preston and Sturch (1967). Of course, these curves are derived from metallic lines rather than the Balmer lines. To obtain the phase, $\emptyset$, at the epoch of observation the following ephemerides, given by the above authors, were used: JD 2439012.61 + 5.46939E for α^2CVn and JD 2434217.5 + 18.487E for β CrB.

In addition to the circular polarization observations linear polarization measurements across Hβ for four early-type peculiar stars were also obtained and these are displayed in Table 4.5. All the observations shown in Table 4.5 were obtained with the polarimeter attached to either the 51 cm or the 91 cm telescope.

Discussion

As is evident from column (5) of Table 4.4, none of the measurements of H_e are statistically significant, that is in no case did the mean value of

the magnetic field exceed $3\sigma_H$, where σ_H equals the standard error of the mean. The average value of σ_H, about 500 gauss, is excellent for the range of stars investigated and for the integration times involved. Hence, although only upper limits on the effective longitudinal magnetic fields of the eight stars listed can be given, certain encouraging trends can be demonstrated without criticism of overanalysis. Of the eight stars observed, three are known magnetic stars and the others categorised as having intermittent fields, very weak fields or broadened spectral lines.

Referring to Fig. 4.11(b), it is apparent that the two results for α^2CVn and the single value for β CrB are in good agreement with the expected field strengths at the phases of observation. In addition, the positive magnetic field derived for 52 Her is consistent with Babcock's finding that this irregular variable always has a field of positive polarity. Although a positive field was present on each occasion that Babcock observed this star, many of the spectrograms listed in his catalogue did not yield, for one reason or another, statistically meaningful quantitative values for H_e. The minimum well defined value was + 840 gauss, hence the result reported here, + 425 $\pm$ 664 gauss is quite feasible.

Since 52 Her was the faintest star observed in the entire programme and it was studied with the largest collector (2.5 m INT), it is worthwhile to consider the integration times involved. To yield a convincing demonstration of the presence of a field of about + 425 gauss would require an improvement in the precision of $q*$ by a factor 5, that is an integration time of 12.5 hours would be needed! The error in $q*$ includes correction for instrumental polarization. In mitigation it must be pointed out that the observations of 52 Her were carried out under very poor photometric conditions, namely, a thick layer of cirrus cloud illuminated by the full Moon, leading to a count

rate reduced by about one stellar magnitude (i.e. a factor 2.5). Therefore, under good atmospheric transparency conditions; an integration time of 5 hours should enable a precision of $\pm$ 0.004 per cent ($\pm$ 0.4 x 10^{-4}) to be attained and hence $\sigma_H \simeq$ 120 gauss. With the same collector, and allowing for the same transparency loss factor, this precision should be possible in about 20 min on a second magnitude star (count rate $\sim$ 5 x $10^5 s^{-1}$). Comparing the standard error for α^2 CVn with the photon counts reveals that the integration time is too long by a factor of two, indicating that under the hazy conditions encountered the data was not strictly photon limited.

Circular polarization measurements were also made at $\lambda/\Delta\lambda$ = 4835/25 $\overset{o}{A}$ for α Aur, β Cas, α And and β Aur. In each case the standard error of the mean derived from the data was $\sigma \sim \pm$ 0.01 per cent. Since the divergence of the four mean values of q was $\sim \pm \sigma$, these values were combined to form an average instrumental polarization to a precision of $\sim \pm$ 0.005 per cent.

Of the other stars listed in Table 4.4, viz., α And, β Aur, γ Cyg, α Dra and 15 UMa, the latter, 15 UMa probably warrants further investigation since it shows a sign reversal of q from one wing to the other. It is tabulated, together with α Dra, in Babcock's catalogue under the heading "magnetic field probable but not firmly established."

Borra and Landstreet (1973) have reported the appearance of a variable reversing field exceeding 10^3 gauss for a short time in γ Cyg, but the brief observation given here is not good enough to check this.

β Aur is a bright A0 star for which no field is known. The results given here are consistent with this to a precision $\sigma_H = \pm$ 440 gauss.

Several measurements of the well known manganese star α And were made prior to those tabulated, but the best results were achieved during the 91 cm run in 1973 Nov. This star, the second brightest (after ε UMa) of the Ap

stars with rotationally broadened lines, gives no indication of a magnetic field at the level σ_H = 364 gauss, which is an important result. Recently, a few isolated measurements made independently by other workers have been published, for example, Borra and Landstreet (1973) give σ_H = 440 gauss (one observation of λ 4254.4 Å) while Kemp and Wolstencroft (1974) reported two results with values of σ_H of 30 gauss and 50 gauss respectively, using 15 Å filters on Hβ.

The precision quoted by the latter workers may be an overestimate by a factor of 2 or 3, because of the application of an approximate formula involving the equivalent width of the spectral line (W) and the FWHM of the filter (F). Assuming that (i) the Zeeman splitting is completely unresolved; (ii) the filter function is Gaussian; (iii) the filter is substantially wider than the spectral line; and (iv) the line is centred at a half-transmission point of the filter, this leads to H_e (gauss) $\simeq 6.6(F^2/W) 10^4 q*$, where F, W are in angstroms (Kemp and Wolstencroft 1973a). In Ap stars, condition (iii) is no longer satisfied for $F \simeq 15$ Å or less. Using the given expression with $F = 10$ Å for α^2 CVn resulted in a value of H_e smaller by a factor 3 than that derived by the line profile method and, of course, the apparent precision was overvalued by the same amount. For $F \simeq 15$ Å the discrepancy may be less serious. Dr. Kemp agrees (personal communication) that this rule-of-thumb is only strictly valid for the case for which it was derived, viz., OB X-ray binaries in which the equivalent width of Hβ is ~ 2 Å or less.

It can be concluded from these preliminary observations that magnetic fields of ~ 500 gauss or more can be detected with 10 Å resolution in a wide range of A-type stars, in integration times of a few hours with a suitably large collector. For stars of later spectral type, in which Hβ is weaker and narrower, use of the 2.5 Å filter would be profitable. However, the technique

Table 4.5   Linear Polarization at Hβ in four Ap stars.

STAR	m_v	Sp	JULIAN DATE (244,0000 +)	$\lambda/\Delta\lambda$ (Å)	p (per cent)	θ (deg)	INTEG. TIME (min)
α And	2.2	B9p	*	4863/10	0.37 ± 0.14	134 ± 11	28
				4835/25	0.13 ± 0.08	29 ± 18	"
ε Cas	3.4	B3III	1990.5	4861/10	0.31 ± 0.17	110 ± 15	18
				4835/25	0.45 ± 0.09	130 ± 6	34
γ UMa	2.5	A0nv	2132.5	4861/10	0.16 ± 0.04	26 ± 8	240
				4875/11	0.14 ± 0.05	41 ± 11	115
				4800/200	0.05 ± 0.04	169 ± 30	32
ε UMa	1.8	A0pv	1967.4	4861/10	0.40 ± 0.14	20 ± 10	42
				4835/25	0.11 ± 0.08	58 ± 20	"

* Mean of two observations: JD 244,1966.5 and JD 244,1967.5

becomes most powerful when combined with linear polarimetry at Hβ, hence enabling, for example, magnetic and electron-scattering phenomena to be distinguished.

Of the four stars measured for linear polarization effects across Hβ (see Table 4.5), both α And and ε UMa show no differences to within the precision obtained, viz., ± 0.14 per cent. Both of these stars exhibit rotational broadening of their spectra. A few measurements of higher precision made recently by Kemp and Wolstencroft (1974) indicated an intrinsic linear polarization, probably variable, of $p \simeq 0.03$ per cent in α And. For ε UMa the position regarding either intrinsic linear polarization or a magnetic field is still unresolved. The only published narrow band polarization measurements of this star are those of Borra and Landstreet (1973), who find no evidence of a magnetic field at the level of $\sigma_H = 130$ gauss (circular polarimetry; one observation).

A "five per cent" polarization effect in the equivalent width of Hβ in ε Cas has been claimed by Tamburini and Thiessen (1961). However, with 10 Å resolution and a precision of ± 0.17 per cent there is no evidence of any differential polarization across the line. In fact, the results shown in Table 4.5 agree quite well with those of Behr (1959b), viz., $p = 0.35$ per cent, $\theta = 120°$.

Unfortunately, the only prolonged observations of γ UMa (AOnv) were made under severe, low-transparency conditions due to fog. Hence, the integration times given in Table 4.5 are very long but are consistent with the count rate which was observed on that occasion. Statistically significant results are just obtained at wavelengths λλ 4861 Å and 4875 Å, while the value of p for the broad blue filter (Δλ ~ 200 Å) is smaller and compares well with the broad band polarization given by Behr (1959b), viz., $p \simeq 0.04$ per

cent. Since the azimuth for the measurement at $\lambda/\Delta\lambda = 4800/200$ Å is poorly defined, it is difficult to ascertain whether or not a real rotation of the position angle has occurred. These results require to be substantiated under better observing conditions and time variability should be searched for.

If the line polarization reported here is real, then it is about 25 times smaller than that reported by Clarke and Grainger (1966). Although Dervis (1970) also claimed to have established the presence of a strong Balmer line polarization effect in this star, his result is stated as "p = 11 ± 5 per cent", which is really meaningless.

The measurements by Clarke and Grainger were obtained by recording the Hβ line profile, with a photoelectric grating monochromator, for two orthogonal orientations of a polarizer placed <u>after</u> the exit aperture. Thus only one component of the linear polarization was determined. Reduction of the two scans was achieved by first matching the centroids of the line profiles and then forming ratios at several discrete points across the line. A differential polarization amounting to 5 per cent was found at the Hβ line centre; the polarimetric precision was ± 0.5 per cent to ± 1.0 per cent. This method of deriving the polarimetric quantity is potentially troublesome, since any mismatching of the wavelength points to be ratioed will produce an apparent differential polarization following the shape of the spectral line.

Further investigation of γ UMa is definitely warranted, with special emphasis on very accurate circular polarimetry on the wings of Hβ, to establish the longitudinal component of any magnetic field present. If this field is very small ($q^* \lesssim 0.01$ per cent), while the linear polarization is large ($p \simeq 0.10$ per cent) and shows a rotation of θ across the line, then a magnetic origin may be difficult to support. Since γ UMa is a rapid rotator a plausible explanation may be the mechanism predicted by Öhman.

5. CONCLUSIONS

5.1 Summary

In the previous chapters the design, development and application of a photoelectric Hβ-spectropolarimeter has been presented and discussed. Not only has it been established that this instrument performs satisfactorily as a narrow band linear or circular polarimeter, but an original contribution to the study of Be- and Ap-stars has been achieved by the observational work.

By tilt-scanning narrow band interference filters of either 2.5 Å or 10 Å passband, digitized line profiles of the Hβ line (λ 4861.3 Å) are obtained. Polarimetry can then be performed at discrete points across the spectral feature with a resolution of approximately 3 Å or 10 Å. On-the-telescope calibration of the wavelength/angle of tilt relationship is accomplished by piping light from laboratory sources to the polarimeter diaphragm by fibre-optic tube.

A fixed double-beam polarizing prism, preceded by a rotatable mica half-wave plate, enables measurements to be performed simultaneously, by single beam polarimetry, at two independent wavelengths and passbands. Four click-stop settings of the half-wave plate, relative to one of the polarizing axes of the double-beam analyser, are used, in pairs, to obtain the two linear Stokes parameters p_x = Q/I and p_y = U/I. To record the degree of circular polarization, q = V/I, a quarter-wave plate, with its reference axis at $+45^o$ to one axis of the double-beam polarizer, is inserted to act as a V→Q converter; q is yielded by intensity measurements at the same two orientations of the half-wave plate used to determine p_x.

Wavelength scanning and the polarimetric measurement sequence are fully automated, with pulse counting electronics being employed to display and record the signals. Short integrations (~3s) are used at each half-wave

plate setting and every pair of measurements, corresponding to p_x, p_y or q, is cycled several times before the accumulated counts are printed out. This method is quite effective in smoothing out both random and systematic errors arising from atmospheric effects such as scintillation, transparency drifts and extinction.

Many of the stellar measurements were obtained under relatively poor observing conditions. Nevertheless, it has been shown that, on most occasions, mean values of any of the normalised Stokes parameters p_x, p_y, q can be obtained to an accuracy essentially controlled by the fundamental limit of the photoelectron production rate, i.e. by photon (or quantum) noise. In all cases in which intrinsic time variability of the source was not suspected, the polarimetric precision was within a factor 2, at worst, of the idealised theoretical error derived from Poisson counting statistics. Several consistent measurements, on various stars, with a 25 Å passband yielded a standard error in the mean value of the Stokes parameter of $\sigma = \pm 0.01$ per cent of total intensity. Precisions of ± 0.02 per cent to ± 0.03 per cent were typical for studies involving the 10 Å filters.

Observationally, the achievements of the study have been as follows:

(a) Application of the polarimeter to the study of the "filling-in" (Grainger-Ring) effect in the Hβ line of blue sky light revealed the expected decrease in polarization across the line. These measurements, made with 2.5 Å resolution, are believed to be the first of this kind for Hβ and the polarimetric precision ($\sigma \sim \pm 0.1$ per cent) is probably better than that obtained by previous workers studying other Fraunhofer lines. It is demonstrated that even when the intensity filling-in factor, ρ, is known, the nature of the polarization of the excess radiation component can only be deduced if very high precision pola-

rimetry of the line profile is obtained (say, $\sigma \pm 0.01$ per cent).

(b)   Observations of Be-shell stars, with 10 Å resolution, led to the disco-
very of a reduced polarization at the line centre of the Hβ emission
feature in γ Cas.   A similar result was obtained for ζ Tau.   These
measurements give direct proof that much of the observed polarization
of the light from these stars is intrinsic, i.e. the polarization occurs
close to or within the star, rather than in the interstellar medium.
Definite time variability and intriguing evidence for further polariza-
tion structure on the line wings was observed for each star.   A similar
result for Hα in ζ Tau has been reported by Coyne (personal communica-
tion).

(c)   Measurements across the Hβ line profile of the blue supergiant star α
Cyg, which has a very extended atmosphere and shows Hα emission, gave
no evidence of any differential polarization effect to within a precision
of ± 0.02 per cent of total intensity.

(d)   Upper limits to the longitudinal magnetic fields of several stars were
obtained by circular polarimetry of the Zeeman effect on the line wings
of Hβ, with 10 Å resolution.   Good qualitative agreement was found for
three stars of known field strength (α^2 CVn, β CrB, 52 Her), although
the integration times were too short to permit 3σ values to be obtained.
Results given for the broad-lined Am star, α And, are discussed and com-
pared to recent measurements made independently by other workers.   As
far as is known, the upper limits for the stars 15 UMa, α Dra and β Aur
are original.

(e)   Four peculiar A-type stars, about which little is known regarding the
presence of a magnetic field, were investigated for intrinsic linear
polarization of Hβ.   Upper limits on any differential effect were ob-
tained for three of these stars, viz., α And, ε UMa and ε Cas.   The

result for α And has now been superseded by observations, with higher precision, by Kemp and Wolstencroft (1974). For the fourth object, γ UMa, a rapidly rotating star, there is just a hint of the presence of intrinsic polarization amounting to p = 0.15 per cent in the Hβ line compared to p = 0.04 per cent in a 200 Å band centred near the line. Further measurements involving linear and circular polarimetry of Hβ and a wider passband should be carried out for all of these stars, especially γ UMa.

(f)   From the various Hβ line profiles shown it is apparent that tilt-scanning of narrow band interference filters is a very useful and simple method of recording stellar (and other) line profiles.

The principal advantages of the polarimetric system are:

(i)   Simplicity of design (both optically and electronically).

(ii)   Compactness; easily operated at a Cassegrain focus.

(iii)   High throughput at high resolution is obtained, and all of the stellar seeing disc is accepted, by using narrow band interference filters.

(iv)   The basic linear polarimeter is easily converted to measure circular polarization.

(v)   A permanent record of the stellar line profile is easily obtained by tilt-scanning of the narrow band interference filters.

(vi)   By using a double-beam polarizing prism and each beam as a single channel polarimeter, two independent wavelengths and passbands can be studied simultaneously.

(vii)   Chopping back and forth between two click-stop orientations of a rotatable half-wave plate for short pulse counting integrations of about 3 s (Clarke's method), provides a simple and reasonably

efficient means of smoothing out signal noise of atmospheric origin. (viii) The system is easily transportable ·and relatively inexpensive.

5.2 Areas for Improvement

Three areas- in which the polarimetric system could be improved are immediately apparent, viz., instrumental polarization, achromatic polarimetric ·elements, higher speed pulse counting.

The question of instrumental polarization is quite important when small variations in polarization with time or wavelength are being sought. In the Hβ-spectropolarimeter, instrumental polarization is not small but it can, apparently, be fairly well characterised by measurements of so-called unpolarized standard stars (see, ·e.g. Serkowski 1974). Such corrections, when applied to observations of stars of known polarization, lead to results which compare very well, at the ± 0.02 per cent level, with those of Behr (1959b), Serkowski and Chojnacki (1969) and Coyne and Kruszewski (1969).

Corrections to a precision higher than ± 0.01 per cent are often unnecessary for many differential polarization measurements but, in any case, very few standard stars are characterised to a precision of say ± 0.005 per cent, at present. Of more importance are those instrumental instabilities which could result in a change in instrumental polarization during a particular, probably long, observing run. No such effects have so far been encountered at the 0.01 per cent level.

There seems little doubt that part of the instrumental polarization is due to the collimating lens. The presence of this lens is essential to maintain the resolving power of the interference filters, however a lens of higher optical quality or higher f/ratio may be helpful.

Extending the wavelength range over which the polarimeter can operate,

by incorporating achromatic phase plates, would be most useful. This would enable, for example, simultaneous high resolution measurements to be made at Hα and Hβ and also allow various broad band observations to be made in support of the line measurements.

Fast-response amplifiers and high speed scalers with electronic bandwidths of ∼100 MHz would be extremely advantageous for blue sky and bright star work especially when atmospheric conditions were good.

Other features which might be added are, (i) a paper tape punch, to run in parallel with the digital printer, giving a computer-readable output; and (ii) automation of the tilt-scanning mechanism in Beam 2 of the polarimeter. The latter would be essential for simultaneous work at Hβ and Hα.

5.3 Future Studies

Polarization measurements of certain spectral features with high resolution are of considerable importance to astrophysics. This is especially true when exceedingly high precisions of about ± 0.001 per cent can be obtained or when the narrow band polarization observations are supplemented with broad band polarimetry and spectrophotometric measurements. Some topics awaiting full development are outlined below.

Blue sky; Moon; Planets:

Establishing the polarization state of the excess radiation component, causing the filling-in (Grainger-Ring) effect in the Fraunhofer lines in blue sky, is a challenging study which has obvious possibilities for extension to the study of planetary atmospheres. Detection of luminescence, which could also result in a filling-in of certain spectral lines, might be possible polarimetrically in the light from the Moon, and other planetary objects without atmospheres.

Ae, Be stars:

Not all Ae and Be stars exhibit polarization in broad bands and some emission line stars which do show polarization, but not shell spectra, give little broad band evidence that the polarization is intrinsic. Line profile polarimetry, especially of emission features, is a new and important tool in the study of these stars and should enable more realistic and detailed models to be constructed.

Correlation of the polarization of the Balmer lines with the strength and structure of the emission line profile, continuum polarization and light variations, and rotational velocity should be searched for. Such information will improve our understanding of the scattering geometry and the effects of mass loss, radiative transfer and rotational distortion on the star and its envelope. If the presence of a circumstellar shell is related to the evolutionary stage of the star then an interesting correlation may be found between age and intrinsic polarization. Simultaneous measurements at Hα and Hβ could be very useful because the scattering/*-absorption* optical depths are quite different.

Other Emission Line Stars:

Every star showing hydrogen emission, regardless of spectral type, should be investigated for intrinsic polarization effects by observations of its line profiles. Slowly rotating stars are not precluded since line polarization could be produced by some other means, for example, asymmetric scattering from hot spots or resonance scattering.

Rapidly Rotating Stars:

These stars are obvious candidates for study. Polarization of the continuum flux of rotationally distorted early-type stars and the possibility of line profile effects has already been discussed in this thesis. If the star

is rotating near break-up velocity and occasionally ejects material, many of the features of emission line shell stars may be apparent.

Binary Systems:

Binary star systems may exhibit many of the properties of emission line shell stars and rapid rotators. Tidal distortion or perhaps asymmetric illumination, both of which may be functions of orbital phase, may be manifest in differences in polarization between spectral lines and very broad bands. Complex effects might occur if one, or both, of the stars have strong magnetic fields.

Magnetic and Suspected Magnetic Stars:

Insight into the magnetic field geometry and direct evidence of the stellar rotation can be gained through observations of the intrinsic linear polarization of periodic magnetic variables. Evidence for a transverse component of the magnetic field should be sought in all known magnetic stars despite the restrictions on the magnitude of p imposed by LTE. By photoelectric circular polarization measurements on line wings, the longitudinal component of the stellar magnetic field can be deduced. This technique can be applied to so-called "irregular variables" to search for periodicities, to stars of all spectral classes not so far investigated for magnetic fields, to magnetic white dwarfs and to studies of the optical counterparts of X-ray sources and possible neutron star and black-hole candidates. Simultaneous measurements at, say, $H\beta$ and $H\alpha$, would be most useful in all cases since this would provide information on the distribution of the magnetic field with height above the photosphere.

Interstellar Material:

Narrow band polarimetry of interstellar absorption features such as the λ 4430 Å line can reveal the presence of impurity atoms in the interstellar grains.

Nebulae:

Hydrogen emission polarized by scattering in a dense localised dust cloud may show structure and spatial variations or time variability related to the dynamical structure of the cloud.

From the above list, which is not claimed to be exhaustive, it should be quite apparent that a fascinating and, as yet, virtually untapped wealth of medium-to-high resolution polarization phenomena await observation and interpretation.

GLOSSARY OF SYMBOLS

α arbitrary orientation of the rotating half-wave plate of the pola-
rimeter with respect to the Cartesian axes of the fixed polarizer;
angular diameter of stellar seeing disc.

α_o residual orientation error when the half-wave plate is assumed to
be aligned with the axes of the polarizer.

β external angle of tilt for the interference filters; $\beta = 0$ corres-
ponds to the filters positioned at normal incidence in the colli-
mated beams.

C   number of repetitions (cycles) of the two channel integrations,
each of time T. Time for C cycles is 2CT seconds.

ε mean error in the degree of polarization and each of the normalised
Stokes parameters. For small polarization and Poisson counting
statistics, $\varepsilon = (2/n*t)^{\frac{1}{2}}$, where n* is the measured count rate inte-
grated for t/4 seconds at each of four position angles of the half-
wave plate.

FWHM   full width at half maximum transmittance of a filter or spectral pro-
file - the passband (also $\Delta\lambda$, F); measured in angstroms ($\mathring{A}$).

g   mean normalised gradient of the red and blue wings of a spectral
line profile.

H_e effective longitudinal magnetic field ($H_e = H \cos \gamma$).

I   intensity, the first Stokes parameter.

IAU   International Astronomical Union.

L   luminosité, throughput.

LCC   linear to circular conversion of polarized light.

λ wavelength of light.

m_v stellar magnitude (visual).

N   number of counted photoelectrons.

p   degree of linear polarization, $p = (Q^2 + U^2)^{\frac{1}{2}}/I$

p_x, p_y normalised linear Stokes parameters, $p_x = Q/I$, $p_y = U/I$ or

$p_x = p \cos 2\phi$ and $p_y = p \sin 2\phi$.

p_1, p_2 normalised linear Stokes parameters referred to equatorial co-ordinate system.

q   degree of circular polarization, $q = V/I$.

q^* $q^* = \frac{1}{2}\left[q_{RED} - q_{BLUE}\right]$, antisymmetric average of the circular polarization of the red and blue wings of an unresolved Zeeman split spectral line.

Q   second Stokes parameter.

σ standard error of the mean of n observations x_i;

$$\sigma^2 = \sum_{i=1}^{n} (x_i - \bar{x})^2 / n(n-1)$$

σ_i standard deviation of a single observation, $\sigma_i = \sigma\sqrt{n}$.

τ optical depth; transmission coefficient.

θ position angle (azimuth) of the direction of vibration as defined by the electric vector maximum, measured from north through east (equatorial frame of reference).

θ_o equatorial position angle of x-axis of the spectropolarimeter, i.e. the polarizing axis of the undeviated beam of the double-beam analyser.

$\odot$ scattering angle, angle between the directions of propagation of the incident and scattered wave.

ϕ position angle of the direction of vibration in an arbitrary reference frame.

U.   the third Stokes parameter.

UT   Universal Time.

V   the fourth Stokes parameter; $q = V/I$. Positive (right-hand) circular polarization occurs when the electric vector ($\underset{\sim}{E}$) has increasing Θ with time. An observer of right-handed circular polarization sees a counterclockwise rotation of $\underset{\sim}{E}$.

W   equivalent width of a spectral line.

x   micrometer reading (related to the angle of tilt, β, of the interference filter).

x_o micrometer reading for $\beta = 0$ (normal incidence); corresponds to λ_o, the longest wavelength which the filter can pass.

<div align="center">APPENDIX I</div>

MUELLER MATRICES

The most general form of light is partially elliptically polarized light; all possible states of polarization are its special cases. Such light can be described by its intensity I, degree of linear polarization p, position angle (azimuth) Θ in the equatorial co-ordinate system, and degree of circular polarization q, or by the Stokes parameters (Clarke and Grainger 1971):

$$
\begin{aligned}
I \\
Q &= I\ p\ \cos 2\Theta \\
U &= I\ p\ \sin 2\Theta \\
V &= I\ q
\end{aligned}
\tag{1}
$$

The Stokes parameters I', Q', U', V' of the light transmitted through a perfect analyser (polarizer) with the principal plane at position angle $\emptyset$ are connected with the Stokes parameters of the incident light (I, Q, U, V) by the Mueller matrix transformation equation

$$
\begin{bmatrix} I' \\ Q' \\ U' \\ V' \end{bmatrix} = \frac{1}{2}
\begin{bmatrix}
1 & \cos 2\emptyset & \sin 2\emptyset & 0 \\
\cos 2\emptyset & \cos^2 2\emptyset & \tfrac{1}{2}\sin 4\emptyset & 0 \\
\sin 2\emptyset & \tfrac{1}{2}\sin 4\emptyset & \sin^2 2\emptyset & 0 \\
0 & 0 & 0 & 0
\end{bmatrix}
\cdot
\begin{bmatrix} I \\ Q \\ U \\ V \end{bmatrix}
\tag{2}
$$

For the double-beam analyser described in the text $\emptyset$ has the values 0°, 90° for Beams 1 and 2, respectively.

The transformation equation for a perfect retarder of retardance Δ and optical axis at position angle α is

$$
\begin{bmatrix} I' \\ Q' \\ U' \\ V' \end{bmatrix} = \begin{bmatrix} 1 & 0 & 0 & 0 \\ 0 & G + H\cos 4\alpha & H\sin 4\alpha & -\sin\Delta\sin 2\alpha \\ 0 & H\sin 4\alpha & G - H\cos 4\alpha & \sin\Delta\cos 2\alpha \\ 0 & \sin\Delta\sin 2\alpha & -\sin\Delta\cos 2\alpha & \cos\Delta \end{bmatrix} \cdot \begin{bmatrix} I \\ Q \\ U \\ V \end{bmatrix} \qquad (3)
$$

where $G = \frac{1}{2}(1 + \cos\Delta)$, $H = \frac{1}{2}(1 - \cos\Delta)$.

From equations (2) and (3), the intensity of light transmitted through a retarder with the optical axis at position angle α followed by an analyser with the principal plane at position angle $\emptyset = 0^\circ$ (upper signs) or $\emptyset = 90^\circ$ (lower signs) is given by

$$
I' = \frac{1}{2}\left[I \pm Q(G + H\cos 4\alpha) \pm UH\sin 4\alpha \mp V\sin\Delta\sin 2\alpha \right] \qquad (4)
$$

For a <u>half-wave plate</u>, $\Delta = 180^\circ$, $G = 0$, $H = 1$ and

$$
I' = \frac{1}{2}(I \pm Q\cos 4\alpha \pm U\sin 4\alpha) \qquad (5)
$$

The transformation equation for two retarders in series is obtained by replacing the 4x4 matrix in equation (3) with a product of two such matrices for the two retarders. In the special case of a quarter-wave plate ($\Delta = 90^\circ$) followed by a half-wave plate, with their optical axes at position angles α_1 and α_2 respectively, and the combination followed by an analyser at $\emptyset = 0^\circ$ or 90°, then,

$$
I' = \frac{1}{2}\Big\{ I \pm \tfrac{1}{2}Q\big[\cos 4(\alpha_1 - \alpha_2) + \cos 4\alpha_2\big] \pm \tfrac{1}{2}U\big[\sin 4(\alpha_1 - \alpha_2)
$$
$$
+ \sin 4\alpha_2\big] \mp V\sin(2\alpha_1 - 4\alpha_2)\Big\} \qquad (6)
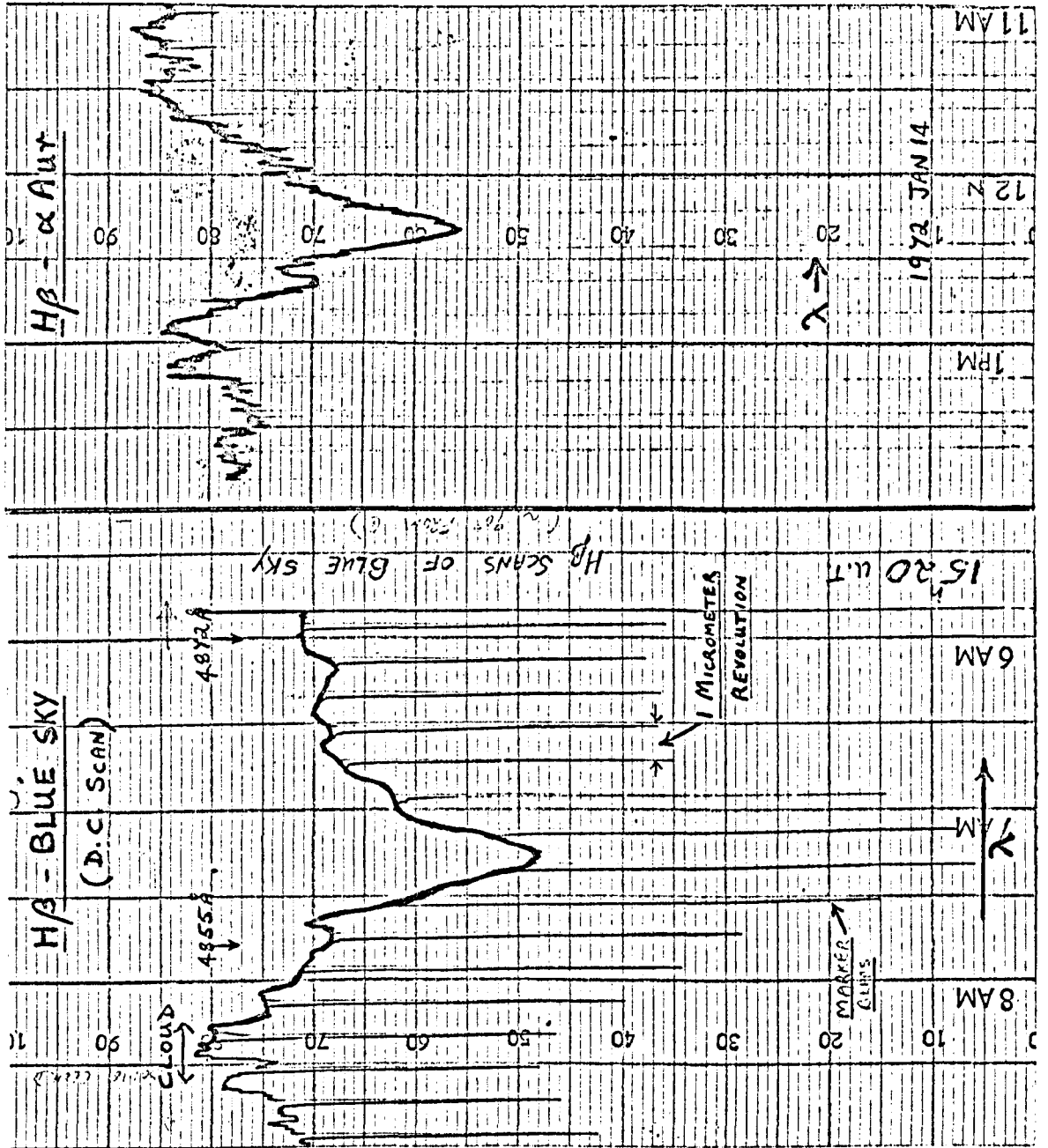$$

Finally, the matrix for a <u>rotation</u> of axes through an angle, γ, measured counterclockwise from the x-axis, and a <u>partial polarizer</u> with orthogonal intensity transmission coefficients K_1, $K_2 = \varepsilon K_1$ are respectively:
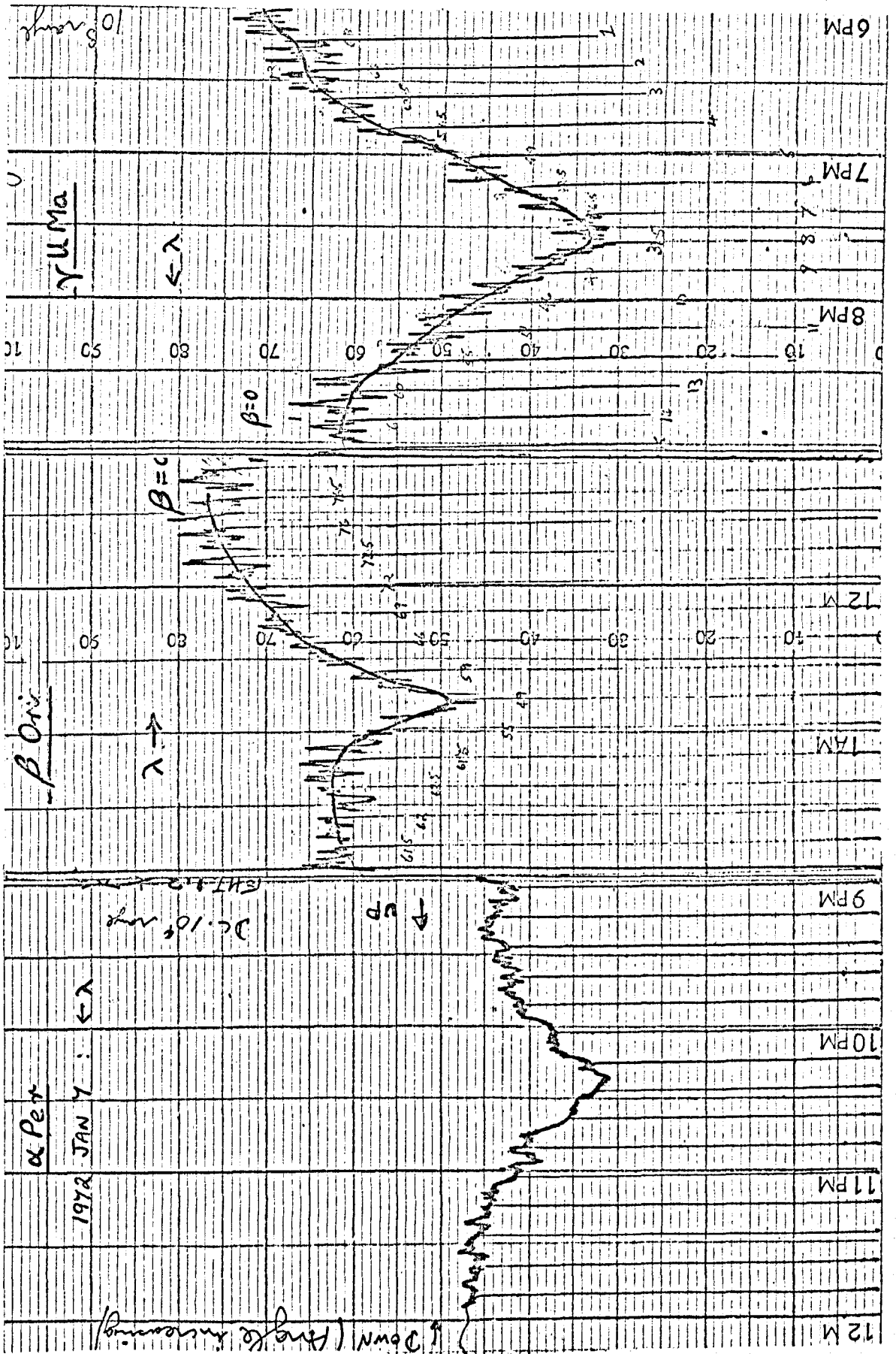
$$\begin{bmatrix} 1 & 0 & 0 & 0 \\ 0 & \cos 2\gamma & \sin 2\gamma & 0 \\ 0 & -\sin 2\gamma & \cos 2\gamma & 0 \\ 0 & 0 & 0 & 1 \end{bmatrix} \quad \text{and} \quad \frac{K_1}{2} \begin{bmatrix} 1 + \varepsilon & 1 - \varepsilon & 0 & 0 \\ 1 - \varepsilon & 1 + \varepsilon & 0 & 0 \\ 0 & 0 & 2\sqrt{\varepsilon} & 0 \\ 0 & 0 & 0 & 2\sqrt{\varepsilon} \end{bmatrix}.$$

$$(7), (8).$$

APPENDIX II

Chart-recorder Tracings of Hβ Line Profiles Obtained by Tilt-Scanning a 2.5 Å Filter

δ Ori.
(B0, m_v = 2.5) ← λ
1972 MAR 12:

ε Ori.
(B0, m_v = 1.75) ← λ
1972 MAR 12:

δ Ori. λ →
1972 MAR 5:

Same gain settings
for ε Ori and δ Ori.
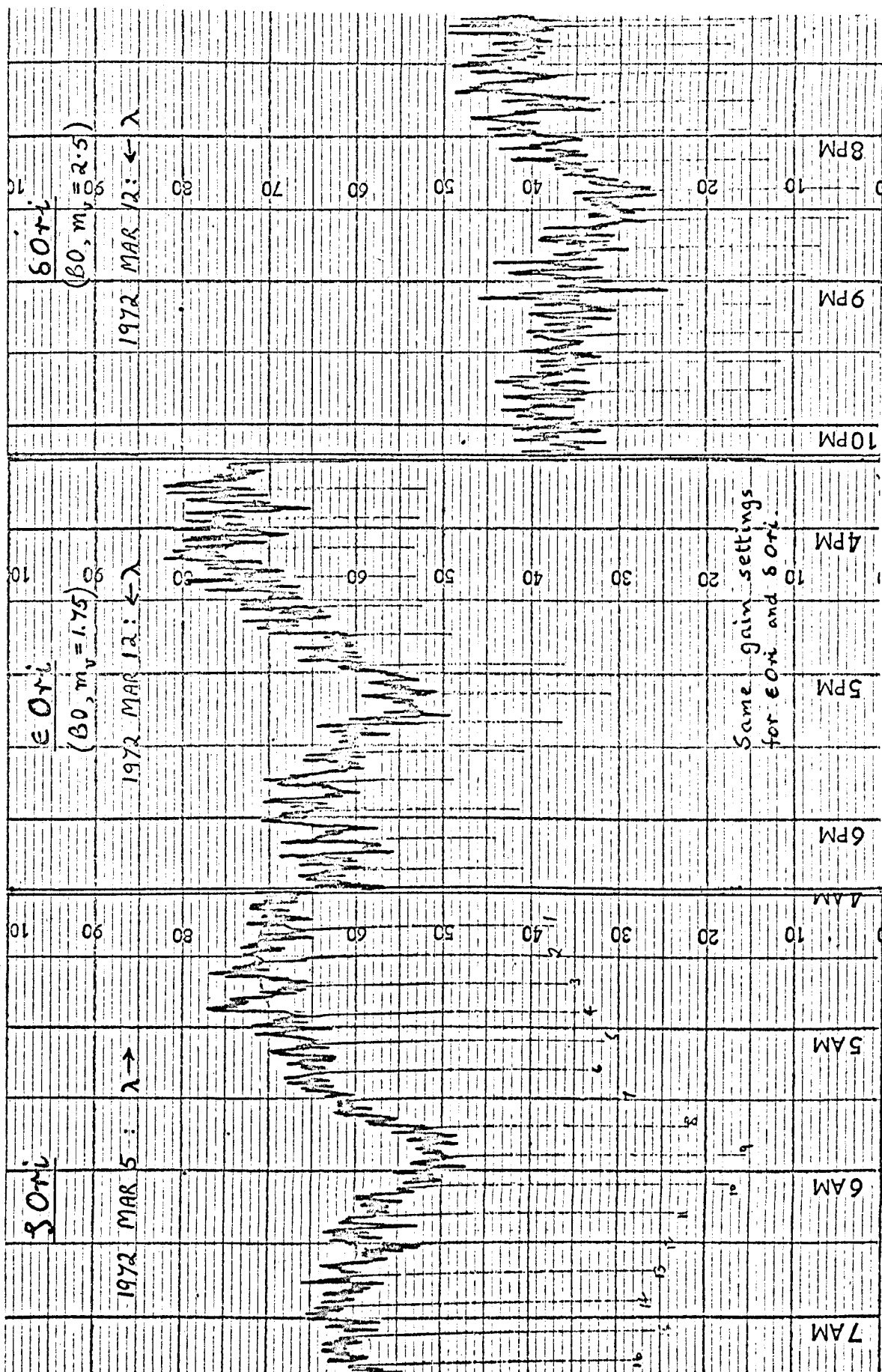
REFERENCES

A'HEARN, M. F. 1973. Astron. J. 77 : 302.

ANGEL, J. R. P. 1974. "Planets, Stars and Nebulae, studied with photo-polarimetry," ed. T. Gehrels, Univ. of Arizona Press : 54-63.

ANGEL, J. R. P., and LANDSTREET, J. D. 1970a. Ap. J. 160 : L147-L152.

———— 1970b. Ap. J. 162 : L61-L66.

ANGEL, J. R. P., McGRAW, J. T., and STOCKMAN, H. S. Jr. 1973. Ap. J. 184 : L79-L83.

AUMAN, J. R., JENSEN, O. G., and WALKER, G. A. H. 1971. Bull. A. A. S. 3 : 442.

BABCOCK, H. W. 1947. Ap. J. 105 : 105-119.

———— 1953. Ap. J. 118 : 387-396.

———— 1958. Ap. J. Suppl. 3 : 141-210.

———— 1960. "Stellar Atmospheres", ed. J. L. Greenstein, Chicago, Univ. of Chicago Press : 282-320.

———— 1962. "Astronomical Techniques", ed. W. A. Hiltner (Chicago, Univ. of Chicago Press) Ch. 5.

BAHCALL, J. N., ROSENBLUTH, M. N. and KULSRUD, R. M. 1973. Nature, 243 : 27.

BARFORD, N. C. 1967. "Experimental Measurements: Precision, Error and Truth"; Addison-Wesley Publ. Co. Ltd., London.

BECKERS, J. M. 1971. "Solar Magnetic Fields", ed. R. Howard : 3-23, Dordrecht, Holland; D. Reidel Publ. Co.

BEHR, A. 1956. Veröff. Univ.-Sternw. Göttingen 6 : (No. 114) 401-435.

———— 1959a. Zs. für Astrophys. 47 : 54-58.

———— 1959b. Nachr. Akad. Wiss. Göttingen II Math-Phys. Kl. No. 7 : 185-219 Veröff. Göttingen No. 126.

BORRA, E. F. 1972. Ph.D. thesis; Univ. of Western Ontario, Canada. Unpubl.

BORRA, E. F.   1973.   Ap. J. <u>186</u> : 959-960.

―――― 1974a.   Ap. J. <u>187</u> : 271-274.

―――― 1974b.   Ap. J. <u>188</u> : 287-290.

BORRA, E. F., and LANDSTREET, J. D.   1973.   Ap. J. <u>185</u> : L139-L143.

BORRA, E. F., LANDSTREET, J. D., and VAUGHAN Jr., A. H.   Ap.J. <u>185</u> :
    L145-L147.

BRINKMANN, R. T. · 1968.   Ap. J. <u>154</u> : 1087-1093.

CAPPS, R. W., COYNE S.J., G. V. and DYCK, H. M.   1973.   Ap. J. <u>184</u> : 173-179.

CASSINELLI, J. P. and HAISCH, B. M.   1974.   Ap. J. <u>188</u> : 101-104.

CASSINELLI, J. P. and HUMMER, D. G.   1971.   Mon. Not. R. astr. Soc. <u>154</u> :
    9-22.

CHANDRASEKHAR, S.   1946.   Ap. J. <u>103</u> : 351-370.

―――― 1950.   "Radiative Transfer".   Oxford Univ. Press (Clarendon), London
    and New York.

CHANDRASEKHAR, S. and ELBERT, D. D.   1951.   Nature <u>167</u> : 51-54.

CLARKE, D.   1973.   Astron. Astrophys. <u>24</u> : 165-170.

CLARKE, D. and GRAINGER, J. F.   1966.   Ann. Astrophys. <u>29</u> : 355-359.

―――― 1971.   "Polarized Light and Optical Measurement".   Oxford;   Pergamon
    Press.

CLARKE, D. and IBBETT, R. N.   1968.   J. Sci. Inst. (J. Phys. E.)   Ser. 2,
    Vol. 1 : 409-412.

CLARKE, D. and McLEAN, I. S.   1974a.   "Planets, Stars and Nebulae, studied
    with photopolarimetry,"   ed. T. Gehrels, Univ. of Arizona Press :
    752-761.

―――― 1974b.   Mon. Not. R. astr. Soc. <u>167</u> : 27P-30P.

―――― 1974c.   Planetary and Sp. Sci.   In press.

COLLINS II, G. W.   1970.   Ap. J. <u>159</u> : 583-591.

COULSON, K. L. 1974. "Planets, Stars and Nebulae, studied with photopolarimetry," ed. T. Gehrels, Univ. of Arizona Press : 444-471.

COYNE S.J., G. V. and KRUSZEWSKI, A. 1969. Astron. J. 74 : 528-532.

CRUVELIER, P. 1967. Ann. Astrophys. 30 : 1059-1111.

DERVIS, T. E. 1970. Astrophysics (trans. from Russian). Original Volume 6, No. 4.

EATHER, R. H. and REASONER, D. L. 1969. Applied Optics 8 : 227-242.

FESSENKOV, V. G. 1959. Astron. Zhurnal 36, 1094 (Soviet Astron. A. J. 3, 1007).

FINN, G. D. and KEMP, J. C. 1974. Mon. Not. R. astr. Soc. 167 : 375-391.

FORMAN, W., JONES, C. A. and LILLER, W. 1972. Ap. J. 177 : L103-L107.

FOSTER, L. V. 1938. J. Opt. Soc. Am. 28 : 124-126.

GEHRELS, T. 1974. "Planets, Stars and Nebulae, studied with photopolarimetry", ed. T. Gehrels, Univ. of Arizona Press.

GEHRELS, T. and TESKA, T. M. 1960. P. A. S. P. 72 : 115-122.

GRAINGER, J. F. 1962. Ph.D. Thesis - Manchester; (unpublished).

GRAINGER, J. F. and RING, J. 1962a. Nature 193 : 762.

——— 1962b. IAU Symposium No. 14 (1960), Pulkovo; The Moon, eds. Z. Kopal and Z. K. Mikhailov, Academic Press : 445-452.

——— 1963. Mon. Not. R. astr. Soc. 125 : 93-104.

HALE, G. E. 1908. Ap. J. 28 : 315-343.

HALL, J. S. 1949. Science 109 : 166-167.

HALL, J. S. and MIKESELL, A. H. 1950. Pub. U. S. Naval Obs. 17 : Part I, (7-62).

HARRINGTON, J. P. 1969. Astrophys. Letters 3 : 165-168.

HARRINGTON, J. P. and COLLINS, G. W. 1968. Ap. J. 151 : 1051-1056.

HILTNER, W. A. 1949. Science, 109 : 165.

——— 1951. The Observatory 71 : 234-237.

HILTNER, W. A. and MOOK, D. E.   1967.   "The Magnetic and Related Stars", ed. R. Cameron, Mono Book Corp., Baltimore : 123-129.

HOUTGAST, J., MINNAERT, M. and MULDERS, G. F. W.   1940.   "A Photometric Atlas of the Solar Spectrum," Utrecht.

HUNTEN, D. M.   1970.   Ap. J. 159 : 1107-1110.

HUTCHINGS, J. B.   1970.   Mon. Not. R. astr. Soc. 150 : 55-66.

JACQUINOT, P.   1954.   J. Opt. Soc. Am. 44 : 761.

JANSSEN, E. M.   1946.   Ap. J. 103 : 380.

JAMES, J. F. and STERNBERG, R. S.   1969.   "The Design of Optical Spectrometers".   Chapman and Hall, London.

JARZEBOWSKI, T.   1963.   "Stellar and Solar Magnetic Fields", ed. R. Lüst. North-Holland Publ. Co., Amsterdam.   (IAU Symp. No. 22).

JOHNSON, H. L.   1966.   Ann. Rev. Astron. Astrophys. 4 : 193.

KEMP, J. C.   1969.   J. Opt. Soc. Am. 59 : 950-954.

KEMP, J. C. and SWEDLUND, J. B.   1970.   Ap. J. 162 : L67-L68.

KEMP, J. C., SWEDLUND, J. B., LANDSTREET, J. D. and ANGEL, J. R. P.   1970. Ap. J. 161 : L77-L79.

KEMP, J. C., WOLSTENCROFT, R. D. and SWEDLUND, J. B.   1972.   Ap. J. 177 : 177-189.

KEMP, J. C., and WOLSTENCROFT, R. D.   1973a.   Ap. J. 182 : L43-L46.

——— 1973b.   Ap. J. 185 : L21-L25.

——— 1973c.   Ap. J. 179 : L33-L37.

——— 1974.   Mon. Not. R. astr. Soc. 166 : 1-18.

KRUSZWESKI, A.   1974.   "Planets, Stars and Nebulae, studied with photopolarimetry", ed. T. Gehrels, Univ. of Arizona Press : 845-857.

LANDSTREET, J. D.   1970.   Ap. J. 159 : 1001-1007.

——— 1974.   "Planets, Stars and Nebulae, studied with photopolarimetry", ed. T. Gehrels, Univ. of Arizona Press : 981-987.

LANDSTREET, J. D. and ANGEL, J. R. P. 1971. Ap. J. <u>165</u> : L71-L75.

MACLEOD, H. A. 1969. "Thin-Film Optical Filters", Adam Hilger Ltd., London.

MARTIN, P. G., ANGEL, J. R. P., and McGRAW, J. T. 1973. Bull. A. A. S. <u>5</u> : 408.

MARTIN, P. G., and ANGEL, J. R. P. 1974. Ap. J. <u>188</u> : 517.

MEABURN, J. 1970. Astrophys. and Space Sc. <u>9</u> : 206-297.

MIE, G. 1908. Ann. Physik. <u>25</u> : 377.

MOLLENAUER, L. F., DOWNIE, D., ENGSTROM, H. and GRANT, W. B. 1969. Applied Optics <u>8</u> : 661.

NIKULIN, N. S., KUVSHINOV, V. M. and SEVERNY, A. B. 1971. Ap. J. <u>170</u> : L53-L58.

NOXON, J. and GOODY, R. 1965. Atm. and Oceanic Physics, <u>1</u> : 275-281.

ÖHMAN, Y. 1934. Nature <u>134</u> : 534.

ÖHMAN, Y. 1943. Stockholms Obs. Meddelande No. 54 : 1-7.

ÖHMAN, Y. 1946. Ap. J. <u>104</u> : 460-462.

PAVLOV, V. E., TEIFEL, Ya. A. and GOLOVACHEV, V. P. 1973. Soviet Physics - Doklady, <u>17</u> : 1038-1039.

PIDGEON, C. R. and SMITH, S. D. 1964. J. Opt. Soc. Am. <u>54</u> : 1459-1466.

PRESTON, G. W. 1969. Ap. J. <u>158</u> : 243-249.

PRESTON, G. W. and STURCH, C. 1967. "The Magnetic and Related Stars", ed. R. C. Cameron, Mono Book Corp., Baltimore : 111-121.

PYPER, D. 1969. Ap. J. Suppl. <u>18</u> : 347-378.

SEN, K. K. and LEE, W. M. 1961. Publ. astr. Soc. Japan <u>13</u> : 263-275.

SERKOWSKI, K. 1962. "Adv. in Astron. and Astrophys.", <u>1</u> , ed. Z. Kopal, Academic Press, New York : 289-352.

—— 1966. Ap. J. <u>144</u> : 857-859.

—— 1968. Ap. J. <u>154</u> : 115-134.

—— 1970. Ap. J. <u>160</u> : 1083-1105.

SERKOWSKI, K. 1974a. "Planets, Stars and Nebulae, studied with photopolari-
metry", ed. T. Gehrels, Univ. of Arizona Press : 135-174.

———— 1974b. Preprint for a chapter on "Polarization Techniques" in Methods
of Experimental Physics, vol. 12.

SERKOWSKI, K. and CHOJNACKI, W. 1969. Astron. Astrophys. 1 : 442-448.

SEVERNY, A. B. 1970. Ap. J. 159 : L73-L76.

SHAKHOVSKOJ, N. M. 1962. Astr. Circular (U.S.S.R.), No. 228 : 16-17.

SHURCLIFF, W. A. 1962. "Polarized Light". Cambridge Mass., Harvard Uni-
versity Press.

SOBOLEV, V. V. 1963. "A Treatise on Radiative Transfer", (transl. S. I.
Gaposchkin), D. van Nostrand, Princeton.

STENFLO, J. O. 1971. "Solar Magnetic Fields", IAU Symp. No. 43. (Dor-
drecht; D. Reidel Publishing Co.)

STRUTT, J. W. (LORD RAYLEIGH). 1871. Phil. Mag. 41 : 107-120, 274-279.

TAMBURINI, T. and THIESSEN, G. 1961. Rendiconti delle Classe di Scienze
Fisiche, Matematiche e Naturali, Serie VIII, Vol. XXX : 492-496.

TANDBERG-HANSSEN, E. 1974. "Planets, Stars and Nebulae, studied with photo-
polarimetry", ed. T. Gehrels, Univ. of Arizona Press : 730-751.

THIESSEN, G. 1961. Astron. Abh. Hamburg, 5, No. 9 : 273.

TINBERGEN, J. 1972. Ph.D. thesis (unpublished); University of Leiden,
Holland.

———— 1973. Astron. Astrophys. 23 : 25-48.

UNDERHILL, A. B. 1960. "Early-type stars with extended atmospheres" in
STELLAR ATMOSPHERES, Ch. 10; ed. J. L. Greenstein, University of
Chicago Press.

———— 1966. "The Early Type Stars". (Dordrecht; D. Reidel Publ. Co.)

Van de HULST, H. C. 1957. "Light scattering by small particles." Wiley &
Sons, New York.

de VAUCOULEURS, G. 1967. IAU Symposium No. 30 : 91-101.

VITRICZENKO, E. A. and EFIMOV, Y. S. 1965. Izv. Crimean Astrophys. Obs.
34 : 114-117.

WOLSTENCROFT, R. D. and KEMP, J. C. 1974 preprint. Ap. J.

ZELLNER, B. H. and SERKOWSKI, K. 1972. Publ. A. S. P., 84 : 619-626.